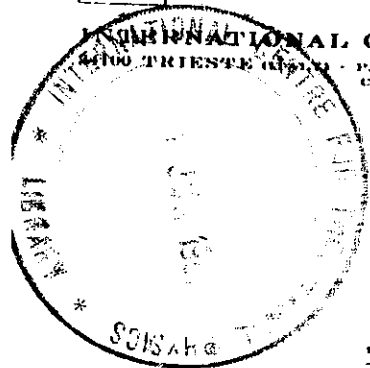




INTERNATIONAL ATOMIC ENERGY AGENCY  
UNITED NATIONS EDUCATIONAL, SCIENTIFIC AND CULTURAL ORGANIZATION



INTERNATIONAL CENTRE FOR THEORETICAL PHYSICS  
4100 TRIESTE (ITALY) - P.O. B. 589 - MIRAMARE - STRADA COSTIERA 11 - TELEPHONE: 2240-1  
CABLE: CENTRATOM - TELEX 400302-1

SMR/206-2

"SCHOOL ON POLYMER PHYSICS"

27 April - 15 May 1987

From the book:

"POLYMERS, LIQUID CRYSTALS AND LOW-DIMENSIONAL SOLIDS"

Editors

N. March

M. Tosi

"INTRODUCTION TO POLYMERIC STRUCTURE AND PROPERTIES"

by

Professor A. KELLER

University of Bristol

H.N. Wills Physics Laboratory

Bristol, U.K.

These are preliminary lecture notes, intended only for distribution to participants.  
Missing or extra copies are available in Room 231.

1

30

# Introduction to Polymeric Structure and Properties

A. Keller

## 1.1. Classification

Polymers are large molecules of a long sequence of units. The basic units are the "monomers," which are joined together by chemical bonds in the course of the chemical reaction constituting the synthesis (polymerization). The monomer itself can be anything from a simple molecule, consisting of a few atoms, to a large and complex molecule. Its nature will define the chemical identity of the polymer. In the simplest case it is one single kind of unit repeating itself in the final chain — it can also be a multiplicity of units forming more complicated repeat sequences or no repeating sequence at all (see later). The essential feature of the monomer is that it must be multifunctional, i.e., it must contain more than one potentially reactive chemical group, potential "hooks" so to speak, by which the monomer units can be joined up.

### 1.1.1. Linear Chains and Networks

#### 1.1.1.1. Linear Chains

If the monomer is bifunctional, the polymerization will lead to a linear chain molecule. This is represented schematically in Figure 1a. Here  $\times$ — $\times$  represents the monomer, where  $\times$  stands for the functional

A. Keller - Department of Physics, University of Bristol, England.

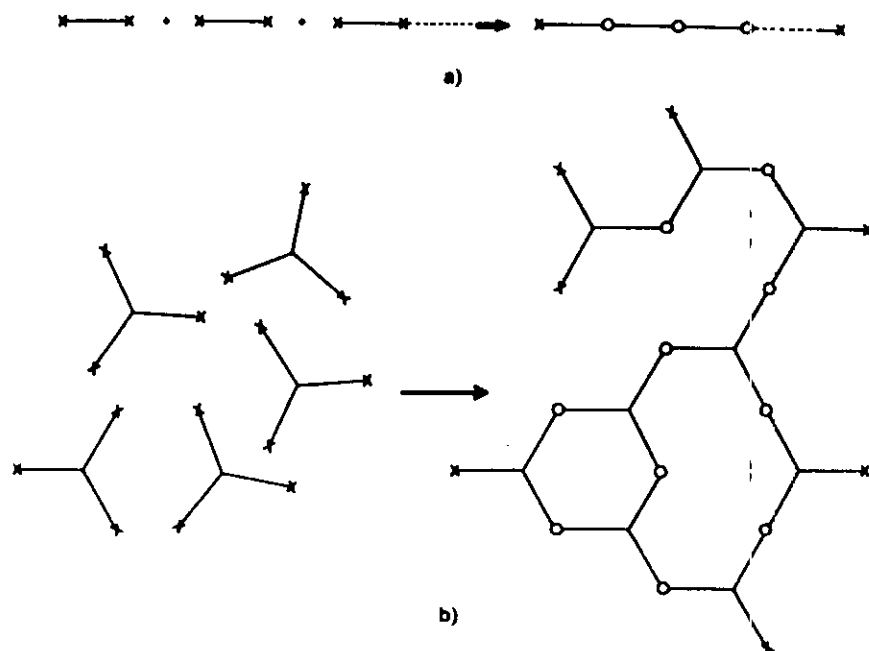


Figure 1. Polymerization scheme of (a) a bifunctional monomer leading to chains and (b) a trifunctional monomer leading to branched chains and eventually networks.

group drawn at each end, and the rest of the monomer is represented by a straight line. In the course of the polymerization reaction the monomers join up at their functional groups, the sites of combination, i.e., the newly formed chemical bonds, indicated by the open circles representing the junction sites.

#### 1.1.1.2. Networks

The polymerization of polyfunctional monomers (i.e., with more than two reactive groups) leads to networks, such as that represented schematically by Figure 1.1(b) for a trifunctional monomer.

#### 1.1.1.3. Intermediate Cases

*a. Open Trees — Branched Molecules.* Here, the branches have not yet become joined up sufficiently to form a continuous network. The stage at which the network becomes continuous is very distinct experimentally

(the so-called "gel point" in the stage of polymerization) and represents mathematically a percolation problem handled by the appropriate mathematical techniques.

*b. Linear Chains with Latent Functionalities.* In this case, two functional groups within a monomer are more reactive than the rest. These can be made to react first, leading to linear chains. Reacting some of the remaining functional groups will subsequently join these chains into a network.

Linear chain and network polymers display extremely different properties. The former are soluble and fusible, the latter insoluble and infusible (the latter in the sense that the polymer does not flow and is thus unmoldable). Linear chain materials can thus be obtained in desired shapes by molding and/or casting and can be reformed in other shapes subsequently if so desired. In the technological sphere these form the class of thermoplastic materials. Materials of network chains set in a permanent, unalterable shape in the course of the polymerization reaction; hence once polymerized, they cannot be processed further. In the technological sphere these form the class of thermosetting materials. The intermediate class in subsection b above clearly combines the characteristics of both, a salient technological example being the vulcanization of rubber, where the vulcanization corresponds to the formation of the network by linking the linear chains already present.

The present discussion, including the continuing classification below, will be confined to the linear polymers mentioned above, as these lend themselves more to physical structure studies and application of physics in general.

### 1.1.2. Periodic and Aperiodic Polymers

#### 1.1.2.1. Periodic Polymers

This category comprises polymers that consist of a single identical monomer unit repeating along the chain, or of a repeating pattern of monomer units. This class embraces the most important synthetic polymers and such biopolymers as possess structural function in the organism (e.g., cellulose, chitin, and other polysaccharides). For most people the repeating feature in question is the essence of a polymer, in fact synonymous with the concept of a polymer itself as reflected by conventional textbooks. It should be recognized nevertheless, that this is merely a limiting case of a spectrum, ranging from a strict repetition (implied by the present heading) to such an imperfect repeat pattern that for most purposes the molecule is virtually aperiodic.



The general feature of copolymers is that they combine the properties of those possessed by the homopolymers corresponding to the individual monomer species. Exactly in what way will depend on which type (1), (2), or (3) of copolymer is formed, and within each type on the gross ratio of the species, and in cases (2) and (3) on the distribution of the blocks and grafts. (The relevance of the block copolymeric nature on the crystallizability has been mentioned in the previous section.) Copolymers therefore offer a virtually limitless possibility of tailoring polymers to particular needs and are very widespread among industrial products. They are also frequent in nature (e.g., structural polysaccharides).

#### 1.1.4. Single-Component Polymers — Polymer Blends

##### 1.1.4.1. General

Copolymerization (see Section 1.1.3) is the chemist's method of tailoring polymers. There is now a rapidly developing new trend of physical tailoring, which consists of blending different polymer species that are chemically unconnected. There is a broad analogy in this respect with alloying in the metallurgical field. There is, however, a very basic difference between alloying metals (or other simple materials) and the blending of polymers, in that polymers are largely incompatible even in the liquid (molten) state. Crystallization may accompany or follow the primary liquid-liquid phase separation in cases where the components are crystallizable under the given circumstances.

The origin of the intrinsic incompatibility of polymers rests in the very small entropy of mixing, which in turn has its source in the large size of the molecules. Hence compatibility will only be achieved when the affinity between the different species is sufficiently large to provide the driving force for mutual dissolution. (Beyond stating this generality the present review will not develop the argument quantitatively.) Thus, in general, with very few exceptions, chemically different polymers will not mix. The few exceptions known to date have important applications.

Present trends in the polymer blend field can be summarized as follows:

1. Search for compatible systems: the practical activity of finding compatible systems more or less empirically; and the theoretical attempts to understand the conditions of compatibility.
2. Understanding and optimization of the phase segregation within incompatible systems: the achievement of desirable states of dispersion of phases in a controlled manner; and the study of the condition of segregation and of the particulars of the phase-segregated structures.

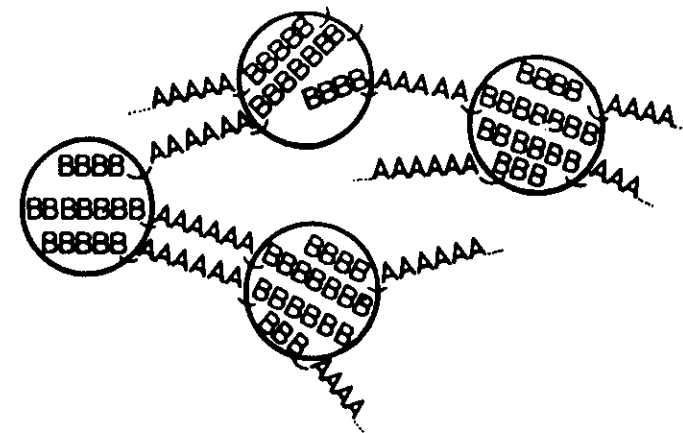


Figure 1.2. Schematic illustration of microphase segregation in the case of a triblock copolymer. Here the AAA... blocks constitute the matrix and the BBB... blocks the (in this case) spherical dispersed phase.

##### 1.1.4.2. Block Copolymers as Blends — A Special Case

The components of block copolymers (see Section 1.1.3.2 above) are usually intrinsically incompatible even in the liquid state. Thus the individual blocks will have the tendency to phase-segregate. However, since the different phases in a given chain are molecularly limited, such segregation can only occur on a microscale where the phases will remain molecularly connected. Let us consider the triblock system AAAA---ABBBB---BAAAA---A. The resulting microphase is represented schematically in Figure 1.2. Here A is the matrix and B the (in this case) spherical, dispersed phase, where the B units in the spheres come from the B block components of a number of different chains. Dependent on the ratio of A and B in the system as a whole, the microphases will be spheres (for the most disparate ratios), cylinders (less disparate ratios), or lamellae (comparable amounts of A and B). In the case of spheres and cylinders the components in larger and smaller amounts will form the matrix and the dispersed phase, respectively. Typical dimensions of microphases are in the range of a few hundred angstroms.

##### 1.1.4.3. Phase-Segregated Polymers as Composites

All phase-segregated systems, whether blends or block copolymers, are essentially composites. Their special properties arise from the nature of

the individual components and from the way they are interconnected. As polymers can be, mechanically speaking, solid (crystalline, or glassy) or liquid (or rubbery, depending on the temperature — see later) the most interesting and useful cases are those where one of the composite components is in a stiff state, the other in a compliant state (such as rubber) at the temperatures of application. Some block copolymers are specifically designed to serve this purpose (thermoelastomers: e.g., the triblock polystyrene-polybutadiene).

Having stated the broader background, the discussion will be confined to the simplest class of all, namely the linear homopolymer: Its purpose will be to provide an appreciation of the structural features within a polymeric material when confined to the above class as a model for the more complicated and specialized systems. "Structure" is to be understood in the widest generality, any discussion of which must start from the nature of the individual molecule. The chain molecules are chemical compounds so a certain amount of chemical background will therefore be invoked in what follows.

## 1.2. Main Types of Polymerization Reaction

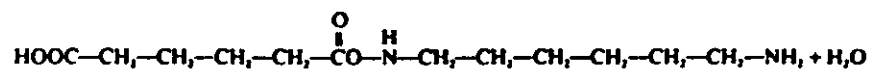
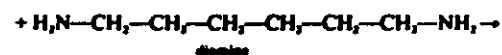
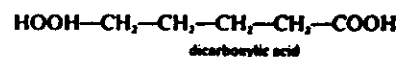
While chemistry does not lie within the scope of this review, the appreciation of an absolute minimum of the chemical reactions involved in the synthesis is deemed necessary.

There are two main routes to the synthesis of a polymer chain according to the nature of the monomer.

### 1.2.1. Condensation Polymerization

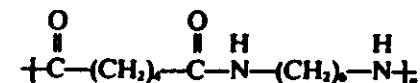
Here the functional groups are COOH and OH leading to polyesters, and COOH and NH<sub>2</sub> leading to polyamides with the splitting out of water.

As an example, let us consider the case of a technologically important polyamide, the most widely used nylon (nylon 66):



Here, the functional group of the new entity remains, as before, capable of

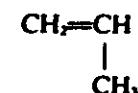
reacting with corresponding groups in other entities leading to the polymer



where  $n$  is the number of repeats (monomer units in the molecule).

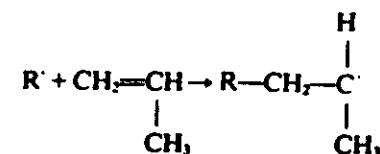
### 1.2.2. Addition Polymerization

In this case the monomer units link up without any product splitting off. This occurs by an initially unreactive electron pair becoming available for chemical bonding. For this to happen initial activation is necessary, a step termed "initiation." We illustrate this initiation and the polymerization to follow by the example of a free-radical-initiated unsaturated monomer, propylene, leading to the technologically important polymer, polypropylene: Propylene monomer,



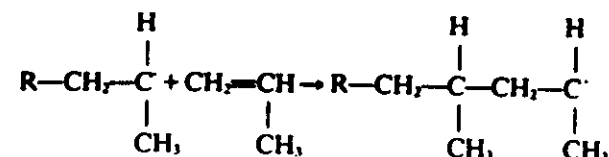
Free radical,  $\text{R}^\cdot$ , where  $\text{R}$  is a general symbol and the dot stands for an unpaired electron.

#### 1.2.2.1. Initiation Step



Here the radical becomes attached to the monomer by leaving one unpaired electron resulting from the opening of the double bond at the terminal carbon atom, which thereafter will be an active site. This can react with a still unreacted monomer and thus propagate the polymerization reaction.

#### 1.2.2.2. Propagation Step



This reaction can repeat itself many times and thus lead to the polymer. The chain, however, will not grow indefinitely even in the presence of unreacted monomer, but will become terminated in a variety of ways.

### 1.2.2.3. Termination Step

Termination can occur by the reactive chain end combining with a free radical, with an active monomer, with an active polymer, or with a reactive impurity. In all these cases polymerization ceases and a reactive center is removed from the system. In another method of termination the reactivity of a center is not removed altogether but is transferred elsewhere. This method of termination is named "chain transfer." Here, e.g., a hydrogen atom is extracted from another polymer chain, which will thus inactivate the reactive carbon atom along the growing chain. At the same time this process will activate one of the carbon atoms along another chain (or at a remote part of the same chain — termed "backbiting"), which will lead to branched chain growth. An appropriate monovalent atom of the solvent may also be extracted, thus leading to a reactive solvent atom that can then act as a free radical and initiate polymerization in itself.

For the present purposes two consequences of the nature of the polymerization reaction are noteworthy: first, it determines the nature of the end group of the final polymer chain, and second, it determines the length of the chain or, more precisely, the distribution of chain lengths in the final assembly. Both of these features will be referred to again below.

## 1.3. Imperfection Types in a Linear Homopolymer Chain

As stated earlier we shall confine ourselves to linear homopolymers for the rest of the review. It is important to realize, however, that a material consisting even of this simplest type of polymer is still not uniform. A given chain will contain various sources of imperfection and nonuniformity; also, all the chains within an assembly will not be equal with respect to these nonuniformities and imperfections. It is important to bear this in mind, and to be aware of the imperfection types when performing experiments and interpreting the results, in particular when working toward some theoretical objective. I shall use this theme as a vehicle for the introduction of some of the most important issues in polymer science.

### 1.3.1. End Groups

The ends of a chain are necessarily different from the rest, hence they represent a source of nonuniformity in themselves. The preceding section

on polymerization reactions has more or less set the scene. Accordingly, chain ends can be functionally active species as in condensation polymers (e.g., COOH, OH, or NH<sub>2</sub> groups), which given the chance could react further; or the ends can be foreign groups, such as arise in addition polymers. In the latter case, as we have seen, they can be the constituents of the initiator radicals (or ions in ionically initiated polymerization) themselves, certainly at one end of the chain, and may be the same at both ends depending on the method of termination. Different methods of termination will introduce different terminal entities, which could thus be impurity atoms, or in the case of chain transfer some constituent atom of the solvent, or simply an additional hydrogen. Alternatively it could also be a double-bonded group.

In a long chain the end group will only represent a very small fraction of the total. For many purposes therefore its influence may be totally negligible (e.g., for mechanical behavior). For some purposes, however, it may be all-important, e.g., polar end groups in the electrical properties of an otherwise insulating polymer, or if the ends initiate further chemical reactions (polymerization or degradation), say in the course of heat treatment.

### 1.3.2. Molecular Length (Weight) Distribution

A polymerization reaction as conducted in a laboratory flask or within an industrial reactor always leads to nonuniformity in chain length. (This is in contrast to nature, which can produce biopolymers where each chain is strictly of identical length.)

Finite and, as a rule, nonidentical chain lengths arise for the following reasons:

1. A thermodynamic limit of the growing chain set by the law of mass action, a limit which however is seldom, if ever, reached.
2. Kinetic limitations. Even if the end groups remain functional (condensation polymers) the chain growth will slow down as the chains get longer, and thus the reactive end groups fewer. The chain length distribution at any stage is then determined by statistics and may be predictable mathematically.
3. By the competing effects of initiation, propagation, and termination rates in cases where such pertain. Again, knowledge of the individual rate constants may enable the final length distribution to be predictable.

Ideally one would like to know the full molecular weight distribution. Indeed there are methods for achieving this. Molecular weight distribution can be characterized by averages, which are often invoked both for

theoretical and practical considerations. Often such averages can be determined directly by experiment without knowledge of the actual distribution. Two averages are particularly important:

Number average: 
$$M_n = \frac{\sum n_x M_x}{\sum n_x}$$

Weight average: 
$$M_w = \frac{\sum n_x M_x^2}{\sum n_x M_x}$$

where  $M_x$  is the molecular weight of a molecule corresponding to a degree of polymerization  $x$  (i.e., consisting of  $x$  monomer units of molecular weight  $M_0$ , thus  $M_x = xM_0$ ) and  $n_x$  is the number of such molecules.

For many purposes the width of the distribution is characterized by  $M_w/M_n$ . For a homopolymer this ratio is of course equal to unity. For a random distribution resulting, e.g., from the statistically determined combination of diacid and diamine, as in the above-quoted example of nylon 66, this ratio is ideally two. Many industrial processes (e.g., for polyethylene) result in distributions that are much broader and can have  $M_w/M_n$  values of approximately 15. In synthetic polymers  $M_w/M_n$  values of about 1.1 are usually considered as corresponding to very sharp distributions and are taken as a good approximation for a uniform (homodisperse) polymer and, as a rule, are quite difficult to obtain.

### 1.3.3. Isomerism

A chain, which is totally uniform as regards chemical constitution and has a well-defined molecular weight (or forms an assembly of uniform chains all of the same molecular weight), is still not fully characterized in view of the possibility of isomeric differences and isomeric imperfections. Exactly which kind of isomerism needs to be taken into account will depend on the polymer in question. In what follows some common and important types of isomerism will be listed briefly.

#### 1.3.3.1. Branches

The possibility of branching has been raised previously as one consequence of chain-transfer reactions. Thus, a chain of given molecular weight can be straight or branched with a variety of branch distributions, e.g.,



This form of isomerism is particularly important in the case of polyethylene, where the different technological products differ with respect to branching.

#### 1.3.3.2. Isomerism of Unsaturated Polymers (Polyenes)

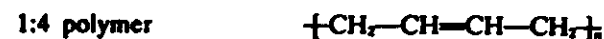
This important class of polymers comprises the conventional elastomers (rubbers). Here, two kinds of isomerism are important and widespread.

1. The monomer contains more than one double bond, where only one is used for polymerization to form a linear molecule. Isomerism arises according to which is used. An example is butadiene:

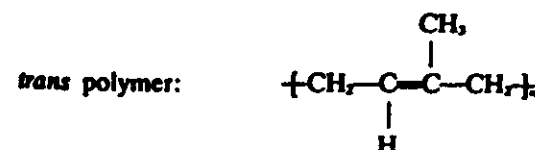
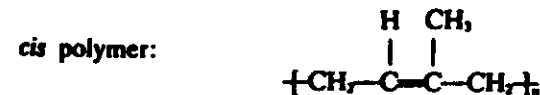
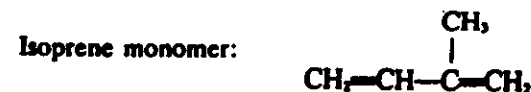


where (1), (2), etc., number the C atoms.

Polymerization may occur either via (1), (4) or (1), (2) C atom:



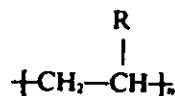
2. *Cis-trans* isomerism. This kind of isomerism based on the absence of free rotation around double bonds, well known in basic organic chemistry, has drastic consequences for poly(isoprene), the basic constituent of two important natural compounds:



The *cis* polymer is natural rubber, the *trans* polymer is guttapercha. Guttapercha is a hard solid at room temperature as opposed to the familiar behavior of rubber. The difference rests in the better crystallizing ability (higher melting point) of guttapercha, which (if the above formulas are drawn out sterically) has the straighter chain conformation.

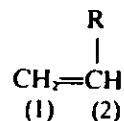
### 1.3.3.3. Isomerism in Polyolefins

Polyolefins have the general formula

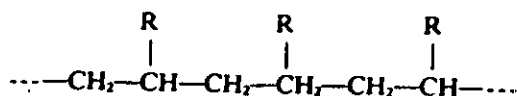


where R can be a variety of chemical groups. (In the case of polypropylene quoted earlier R is CH<sub>3</sub>.) Two kinds of isomerism will be mentioned, the second of which is of utmost importance.

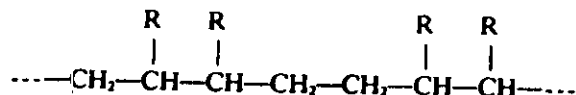
a. *Head-to-Tail and Head-to-Head Isomerism.* Let us consider the monomer



where (1) and (2) again label the C atoms. In the head-to-tail polymer carbon (1) links up with carbon (2) in the course of polymerization, leading to a chain such as



In the head-to-head polymer the carbons link as (1) to (1) and (2) to (2), leading to a chain such as

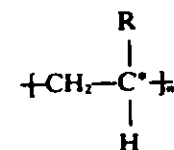


The head-to-tail sequence is the one which occurs far the most frequently and is thus considered "normal" for polyolefins. Nevertheless, "faulty" higher-energy sequences can occur along a given, otherwise head-

to-tail chain with much lower frequency, more exactly dependent on the type of substituent R and on the conditions of polymerization.

b. *Stereoisomerism.* This very important type of isomerism relies on the presence of an asymmetric carbon atom (to be denoted C\*). It is known from basic chemistry that if all the four carbon valences link up with different groups (sterically the carbon is at the center of a tetrahedron, where the four substituents are at the vertices of the tetrahedron), two stereochemically different conformations arise from the otherwise identical constituents, which are sterically mirror images of each other. In simple organic compounds the two correspond to the *d*- and *l*-configurations rotating the plane of plane-polarized light in the right and left directions, respectively.

In a polyolefin the tertiary carbon atom is asymmetric



because it links to R, H, and to the chain, portions on its right and left (as drawn in the formula above), which in general are nonequivalent, hence the tetrahedra of which C\* is the center can be of two different kinds that are mirror images of each other. The same applies to each consecutive C\* atom along the chain. Which of the two configurations pertains is determined during the polymerization reactions, when the new monomer attaches itself to the growing chain. In general there is no control over which of the two forms occurs, and hence the sequence of *d*- and *l*-configurations will be mixed, determined by random chance.

However, special catalyst systems (Ziegler-Natta catalysts) enable the controlled formation of steric isomers. In this way it is possible to obtain chains where each consecutive C\* atom gives rise to identical (i.e., *d*- or *l*-) conformation. The consequences of this can be most readily visualized as follows. Consider the C-C chain stretched out completely (disregarding whether the substituents R sterically permit this or not). Then all the C-C atoms will lie in a plane forming a zigzag corresponding to the tetrahedral angle. The substituents R and H will then lie above or below this plane as determined by the tetrahedral geometry (Figure 1.3). The two conformations *d* and *l* will then differ in as far as R lies above or below this plane. If all C\* atoms are stereochemically equivalent the Rs will all be on the same side. Such a polymer has been termed "isotactic" by Natta (see Figure 1.3a). In the random sequence the Rs will be above and below the C-C plane in a haphazard fashion. Such a polymer is termed "atactic" (see Figure 1.3c).



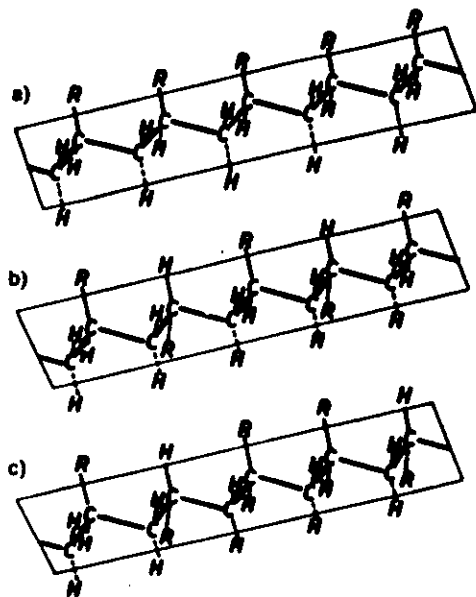


Figure 1.3. Representation of (a) an isotactic, (b) a syndiotactic and (c) an atactic polyolefin (after Natta<sup>11</sup>).

Of course, other types of regularities can also be envisaged; the next simplest one is the *ddl*--- alternating sequence. In the above representation the Rs will be alternately above and below the C-C plane (Figure 1.3b). Such a polymer is termed "syndiotactic."

The kind and degree of stereochemical regularity is termed "tacticity" and is an important parameter in the characterization of the chain with far-reaching technological consequences. The latter arises from the fact that regular sequences (isotactic, syndiotactic) can crystallize while the atactic cannot. (Polypropylene owes its commercial usefulness to the fact that it can be obtained in the isotactic form.)

Control of tacticity (by means of appropriate catalysts in the course of polymerization) and the determination of the kind and degree of tacticity that pertains to a particular product (carried out by NMR techniques) is a most important activity both academically and technologically.

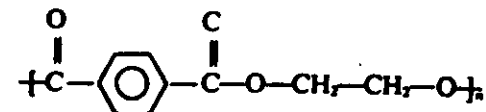
## 1.4. Formulas of Some Important Polymers

A minimum appreciation of what the real polymers actually are is clearly required for any discussion of polymeric structure. The chemical formulas of some important synthetic materials will be listed below.

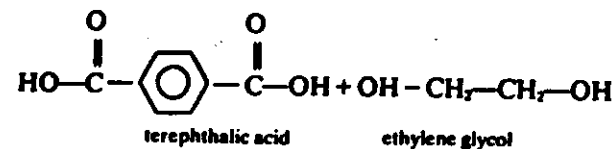
### 1.4.1. Condensation Polymers

#### 1.4.1.1. Polyesters

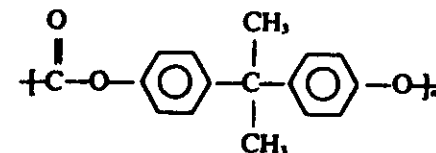
a. *Polyethylene Terephthalate* (Trade names: Terylene, Dacron (fibers), Melinex, Mylar (films))



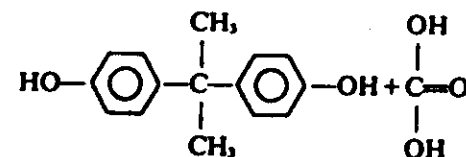
arising from



b. *Polycarbonate* (Trade name: e.g., Lexan)

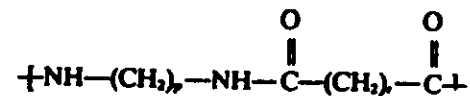


arising from

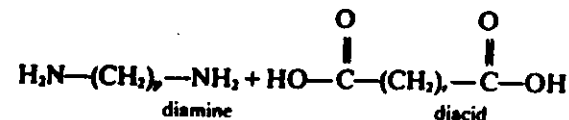


#### 1.4.1.2. Polyamides (Trade name: nylons)

a. *From Diacid and Diamine*

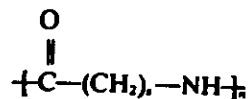


arising from

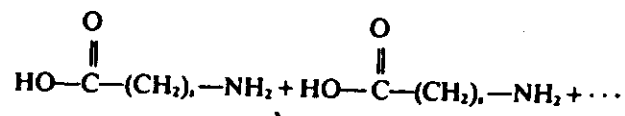


where  $p$  and  $r + 2$  signify the total number of C atoms in the amine and acid components, respectively. The most common nylons (trade name) of this type are nylon 66 and 610.

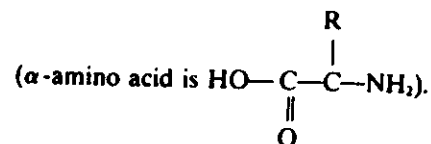
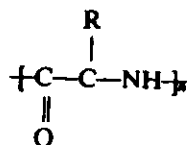
b. From  $\omega$ -Amino Acids



arising from



c. From  $\alpha$ -Amino Acids. These are the polypeptides and proteins, the basic constituents of living matter



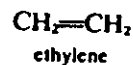
Here R is one of the 21 different organic groups defining the naturally occurring  $\alpha$  amino acids. In the so-called sequential polypeptides the Rs are all alike. With a few exceptions these are synthetic laboratory products. In the naturally occurring proteins the Rs along a given molecule are different, and in general do not form a repeating sequence. The enormous potential number of combinations of Rs is the source of the very large variety of proteins and of their specificity.

## 1.4.2. Addition Polymers

### 1.4.2.1. Polyethylene (Trade name: Polythene)



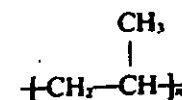
arising from



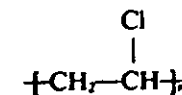
### 1.4.2.2. Polyolefins



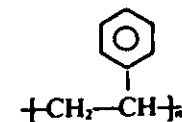
Important representatives:  
Polypropylene (PP)



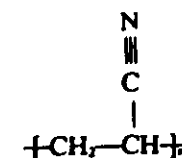
The technological product is in the isotactic form.  
Polyvinylchloride (PVC)



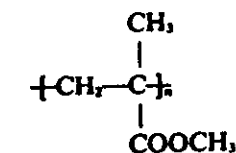
The technological product has some preponderance of syndiotacticity but is otherwise atactic.  
Polystyrene (PS)



The technological product is atactic.  
Polyacrylonitrile (PAN; trade names: Orlon, Acrylan)

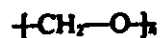


The technological product is largely atactic.  
Polymethylmethacrylate (PMMA; trade name: Perspex)



The technological product is atactic.

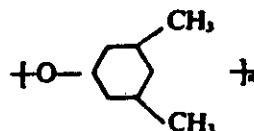
**Polyoxymethylene** (Trade name: Delrin)



**Polyoxyethylene** (Trade name: Polyox)



**Polyphenylene Oxide**



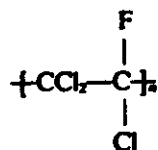
This is compatible with polystyrene and is being used as a blend component.

#### 1.4.2.4. Fluoropolymers

**Tetrafluoroethylene** (Trade names: Teflon, Fluon)

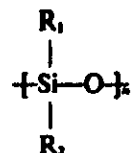


**Trichlorofluoroethylene**



#### 1.4.2.5. Inorganic Polymers

The silicon-based ones are the most important: General formula:



Here R<sub>1</sub>, R<sub>2</sub> can be a variety of organic groups.

### 1.5. Melting Range of Polymers; Specialty Materials

For structural purposes a polymeric material needs to retain its shape and support load. This it can only do in the solid state, the upper temperature limit of which is determined by the melting point. The melting range has been one of the principal considerations in the design of polymeric materials, its rise to increasingly higher temperatures being one of the main objectives. When listing polymers in order of melting points  $T_m$  we shall not only provide additional information, but shall also add to our list new polymeric materials, and through them introduce new polymeric properties associated with these materials, which are in the forefront of current research interests.

First, it must be stated that as polymers do not melt sharply (more about this later) but over a temperature range, it is more appropriate to refer to a melting range rather than a melting point, at least for practical characterization. The  $T_m$  values to be quoted are representative temperature figures within this melting range.

#### 1.5.1. Conventional Polymers

##### 1.5.1.1. Polyethylene

There are two classes: low density and high density:

1. Low-density polyethylene (LDP).  $T_m \sim 100^\circ\text{C}$ . An important technical drawback is that it becomes unusable at the temperature of boiling water. It is very tough and pliable and has the familiar waxy feel.
2. High-density polyethylene (HDP).  $T_m \sim 135^\circ\text{C}$ . It clearly overcomes the handicap of LDP. Also it is much more rigid.

A few words on the origin of the differences between LDP and HDP are in order. LDP, historically the first, is obtained by polymerization at high temperature and pressure where frequent internal chain transfer takes place ("backbiting") within the same chain. The result is branching within the chain. The branches reduce the crystallizability of the molecule leading to smaller and less perfect crystals, which are responsible for the properties listed under (1). In contrast, HDP consists of completely linear chains that can crystallize with greater facility, and hence gives rise to larger and more perfect crystals, and more of them, accounting for the increase in  $T_m$  and rigidity. The absence of branches arises from the fact that, thanks to the use of Ziegler-Natta catalysts (mentioned earlier), polymerization can be conducted at low (room) temperature and pressure when side reactions during chain growth are minimized. It is noteworthy that here, there being

no asymmetric carbon atom, the question of tacticity does not arise; nevertheless the Ziegler-Natta catalyst has a profound effect for the reasons just stated.

### 1.5.1.2. Others

Polypropylene (isotactic):  $T_m \sim 170^\circ\text{C}$ .

Technological polyesters and polyamides:  $T_m \sim 220\text{--}280^\circ\text{C}$ .

Polytetrafluoroethylene:  $T_m \sim 320^\circ\text{C}$ .

The last entry represents the upper limit for common polymers. Clearly many users require the withstanding of higher temperatures. This prompted the current research toward high-temperature polymers.

## 1.5.2. Specialty Materials

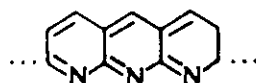
### 1.5.2.1. High-Temperature Polymers

The common underlying principle is that the chains have to be rigid, which is best obtained through the linking-up of aromatic monomers.

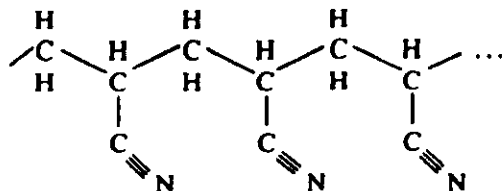
A chemically simple example is the unfusible polyphenylene



which degrades above  $530^\circ\text{C}$  without melting. A compound of the kind

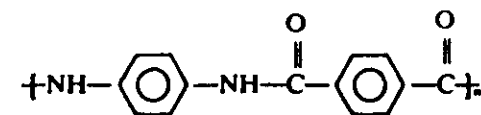


with  $T_m > 900^\circ\text{C}$  is obtained by heating polyacrylonitrile which, drawn out with appropriate valence angles, is



On further graphitization this gives rise to the much-publicized carbon fiber, which is essentially a "polycrystalline" form of one-dimensional graphite, an important specialty product of exceptional properties.

The aromatic analogue of nylons of types 66 and 610 is the recent Kevlar (trade name).



(note the aromatic rings instead of  $(\text{CH}_2)_n$  sequences), which is an exceptionally strong and stiff fiber. In common with many other polyaromatic chains of its class it is totally unfusible and can only be dissolved (which is necessary for processing) in very special and corrosive solvents. The solutions thus formed can be liquid crystals.

### 1.5.2.2. Liquid-Crystal Polymers

Kevlar is one example of a new class of polymeric materials that can be obtained as liquid crystals. The underlying science is still in its infancy. Here only a few comments will be made as regards classification.

The liquid crystals are usually the results of rigid chains or chain portions, a property assured by the multiple aromatic grouping. If the full main chain is liquid-crystal forming, the chain is usually so stiff that it will not fuse in any sense and, as Kevlar, becomes a liquid crystal through appropriate solvents (lyotropic). If the chain is a copolymer with both flexible and rigid groupings, the corresponding material may fuse and pass into the liquid-crystal state in that way (thermotropic). In another class of compounds the main chain may be totally flexible so that it can exist normally in the isotropic molten phase, but it is the appropriate side groups that form liquid crystals.

### 1.5.2.3. Conducting Polymers

Although conducting polymers deserve a chapter of their own, they will only be mentioned here because polymers in this class usually have very stiff chains and thus also possess high-temperature stability; in fact, they do not melt. It is owing to this last fact that they are mostly unprocessable, a deficiency that obstructs practical utilization. For instance, the totally untractable polyparaphenylene becomes conducting on appropriate doping, say with  $\text{AsF}_5$ .

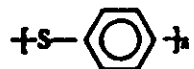
Currently, the fully conjugated polyacetylene



has attracted much attention, becoming again conducting on suitable

doping with donor molecules. Again unfusible and insoluble, it is only available as formed during the polymerization itself, which is a rather ill-defined fibrous web. While an obvious candidate for technological exploitation (to replace metals!) and for fundamental studies of one-dimensional conductivity, this unfavorable texture and its untractability presently bar progress.

As a quite recent announcement the compound



may overcome some of the difficulties. It is processable and is said to become conducting after oxidizing in the presence of  $\text{As}_2\text{F}_5$ .

The inorganic polymer referred to as  $(\text{SN})_x$ , probably with the formula



is highly conducting along the chain direction. (It clearly does not satisfy the normal rules of valency and is thus supposed to have delocalized electrons along the chain.) Quite exceptionally for polymers, it can be obtained as macroscopic single crystals in the form of needles in the course of polymerization itself, and is thus eminently suitable for structure and conductivity studies. It is a truly one-dimensional pseudometal. Again, quite exceptionally and extraordinarily, it is superconducting below 0.3 K.

The discussion of the conductivity itself is beyond the scope of this review.

## 1.6. The Physical State

Beyond the classification according to chemical constitution adopted so far, polymers can be classified and/or characterized according to their physical state. The two broadest categories are: "amorphous" and "crystalline." We shall see that this classification is not hard and fast, as most "crystalline" polymers also contain an amorphous component, and also there are gradations of order within the crystalline component. Nevertheless, as a broadly adopted criterion a polymer is termed "crystalline" when recognizable Bragg reflection can be identified in its X-ray diffraction patterns, otherwise it is classified as amorphous. At this stage it is important to recognize that a given polymeric sample may be amorphous either because although intrinsically crystallizable, it was not given the chance to crystallize, or because it is intrinsically uncrystallizable *per se*. The former will, of course, be the case with all polymers above their crystalline melting point, and in such crystallizable polymers that have

been quenched from the melt into the glassy state where crystallization is unmeasurably slow (see later). Amorphous polymers of this class may be converted into crystalline polymers by appropriate heat treatment. Amorphous polymers, termed above "intrinsically uncrystallizable," can exist only in the amorphous state, fluid or rigid (glassy, see below), by virtue of their chemically (including stereochemically) irregular constitution, which prevents them from forming a crystal lattice.

Obviously, structural features are expected mainly in crystalline polymers. For this reason the latter will be treated comprehensively in the following chapters devoted essentially to structural aspects. However, as most crystalline polymers also possess a certain amount of amorphous material, a very brief survey of the amorphous state is required for an appreciation of what is to follow. This will be accommodated under the present heading.

### 1.6.1. Résumé of the Amorphous State

#### 1.6.1.1. The Random Coil — A Reminder

A brief mention will be made of the random coil concept, which is well known to be the abstraction of a flexible molecule adopted as a model in macromolecular physics. A given flexible macromolecular chain owes its flexibility to the fact that there is rotation around the main chain bonds. If this rotation is sufficiently free and the chain is sufficiently long, the path of an isolated chain can be described by a three-dimensional random walk. A random walk is known to be characterized by the mean-square end-to-end distance  $\bar{r}^2$  given by

$$\bar{r}^2 = nl^2 \quad (1.1)$$

where  $n$  denotes the number of links of length  $l$ , and the links are freely jointed.

The "links" are neither the main chain bonds nor the monomer units, but the minimum length of chain in terms of which a chain can be described by equation (1.1) on the basis that they are totally freely jointed. They are termed "statistical segments," and the corresponding  $n$  value is the number of such segments. Of course the chain cannot cross its own path, but this "excluded volume" problem can be ignored for the present. It should suffice to say that an isolated flexible chain can be regarded as a random coil and can be readily defined mathematically as such. This random coil is the most probable state to which the system will tend to return if perturbed externally (entropy elasticity).

### 1.6.1.2. Structure of Amorphous Polymeric Matter

By definition, there should be no structure in the amorphous state other than the statistical short-range ordering required by local packing considerations. This situation is familiar from simple liquids and glasses. The analogous situation in polymers corresponds to amorphous material consisting of chains in their random configuration, as defined above for an isolated chain, with the addition that in the condensed state the chains are freely interpenetrating. The consequence of the latter will be that the expansion due to self-exclusion in the case of the isolated chain is compensated by the effect of mutual exclusion between different chains, the net result being for each chain an ideal random configuration as if excluded volume effects were absent. This is the so-called  $\Theta$ -condition, commonly realizable in dilute solutions and postulated by Flory to pertain also to the amorphous state. Short-range order in the sense pertaining to a liquid should still exist, and is in principle describable and experimentally accessible by radial distribution functions derived from diffraction patterns.

However, as in simple liquids and glasses, the possibility of larger structural units (supermolecular structures, crystal precursors, etc.) has arisen also in polymers and the existence or otherwise of such ordering has been subject to much debate. Experimental evidence quoted in favor of the latter includes nodular structures seen in the electron microscope, X-ray scattering effects at small angles and, most undeniably, changes in the properties of amorphous materials (glasses) on heat treatment. (If the structure is ideally random, clearly there should be nothing to change.)

The decisive evidence, however, in favor of Flory's totally random model is claimed to have emerged from recent neutron scattering experiments. The essentials of the method, to be referred to again in connection with crystalline material, are as follows. The aim is to characterize the configuration of a chain in an environment of chains of its own kind. This is achieved by neutron scattering with the aid of labeled probe molecules, which are distinct as regards scattering of neutrons. Such suitable probe molecules are polymers containing deuterium as opposed to hydrogen. If these are mixed in small quantities with the main mass of amorphous material, the latter will be like a dilute solution of the deuterium containing polymer as solute within a proton containing polymer as solvent. Here the neutrons will "see," so to speak, the solute molecules. Then the size (radius of gyration) and finer details, depending on the angular range of the scattering explored, can be obtained from low-angle neutron scattering patterns. The general result that has emerged from studies on PMMA and PS is that the molecule in the molten and glassy state (see below) is in the random configuration corresponding to the  $\Theta$ -state. This fully agrees with Flory's predictions and seems to disclaim the existence of larger-scale organizations. For most people this is where the subject stands.

Nevertheless, all the claims for larger-scale structures cannot be ignored even if some are undoubtedly influenced by artefacts. We have to distinguish between the ideal amorphous state undoubtedly realized by suitably chosen materials and samples, and materials and samples that are conventionally regarded as amorphous, but where the amorphous state is not fully achieved. The latter may arise in materials that are intrinsically crystallizable, in contrast to materials that are not (atactic PS and PMMA are of the latter kind). In the former, experiment may detect residual or incipient crystallinity, which can be important for the sample in question but is irrelevant or even misleading when relating to the true nature of the amorphous state. Some of the arguments in the literature may arise from a failure to recognize this distinction.

### 1.6.1.3. The Five States of Amorphous Matter

The consistency of amorphous polymers is greatly affected by temperature. This is most readily expressible in terms of a mechanical property. Following Tobolsky we shall take the modulus of atactic polystyrene (a typical amorphous polymer) as measured after 10 s loading (as polymers are viscoelastic materials, the modulus is time-dependent), and examine its behavior as a function of temperature (Figure 1.4).

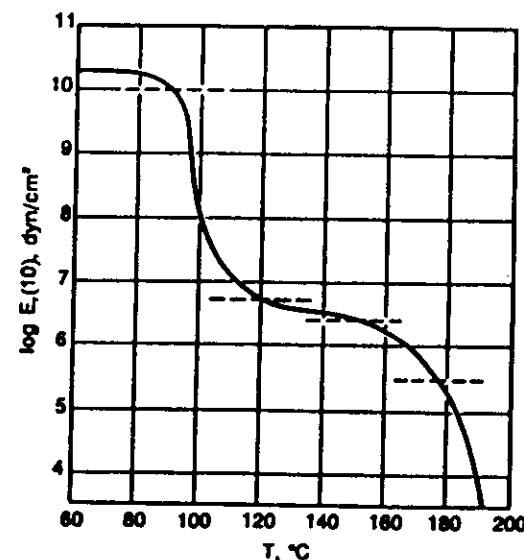


Figure 1.4. Five regions of viscoelastic behavior of an amorphous polymer after 10 s loading showing modulus ( $E(10)$ ) vs temperature in the case of polystyrene (after Tobolsky<sup>27</sup>).

We identify the following five regimes with increasing temperature:

- I. Modulus  $\sim 10^{10}$  dyn cm $^{-2}$ . The material here is a glass, rigid, and stiff.
- II. The modulus drops sharply from  $10^{10}$  dyn cm $^{-2}$  to about  $10^8$  dyn cm $^{-2}$ . This is in the range of the "glass transition" usually characterized by a single temperature, the glass transition temperature  $T_g$ .
- III. Modulus  $\sim 10^8$  dyn cm $^{-2}$  varying only little with temperature. This low-modulus region is associated with very high and (on an appropriate time scale) recoverable extensibility. This regime corresponds to the "rubbery" state.
- IV. The modulus drops again significantly with temperature from  $10^8$  dyn cm $^{-2}$  to about  $10^5$  dyn cm $^{-2}$ . Here we have a combination of rubbery behavior with viscous flow.
- V. Modulus less than  $10^5$  dyn cm $^{-2}$ , becoming increasingly undefinable on the time scale of the measurement. Here we proceed to a viscous liquid, the truly molten polymer.

Regimes I-V are readily interpreted in molecular terms. Little need be said about the glass. Here the main chains are rigid, their motion frozen in; the modulus measures the extension and deformation of covalent bonds in common with glasses from simpler substances. Regime III is unique to polymers. In this regime rotational motion around the main chain bonds is taking place and the chain is thus capable of changing its conformation by thermal motion without, however, any noticeable displacement (on an appropriate time scale) of its center of gravity (micro-Brownian motion). On external loading this micro-Brownian motion is biased and the chain will stretch out without net displacement of the center of gravity. On removal of the load the chain will retract to its random configuration, the restoring force thus being entropic (the basis of rubber elasticity), hence the high elastic extensibility coupled with low modulus, which is the characteristic of rubbers. In Regime V the center of gravity of the whole molecule is shifting in the course of thermal motion (macro-Brownian motion). On external loading this motion is biased resulting in true flow, the property of polymer melts. Regimes II and IV are the appropriate transition regions, where Regime II ( $T_g$ ) is the most dramatic, corresponding to the onset of rotation around the valence bonds of the main chain.

#### 1.6.2. The Usefulness of Polymers in Terms of Their Physical State

For structural purposes a polymer needs to retain its shape and support the load required. In the light of the foregoing we can now broadly identify the circumstances when this pertains and also classify the polymers

in daily use (and thus most readily available also for scientific investigation, and conversely, most in demand for such investigations) accordingly.

It follows that a noncrystalline polymer satisfies the above criterion only up to and including Regime III and, if rigidity is required, only in Regime I, i.e., in the form of a glass. This means that if glassy properties are required  $T_g$  must be above the temperature of intended application. Where  $T_g$  is much above, say, room temperature, intrinsically uncrystallizable atactic polymers will be glassy over a temperature range relevant to everyday use and can thus be useful commercial products, important examples being PMMA and PS. Being glasses they are also transparent, but at the same time, while rigid, they are brittle to varying extents.

If the temperature of application is above  $T_g$  or, conversely,  $T_g$  is below, say, room temperature, amorphous polymers can be useful as elastomers, like the familiar rubbers (Regime III). Unsaturated polymers possessing the highest chain flexibility are the most suitable in this mode of application (*cis* polyisoprene, polybutadiene, see Section 1.3.3.2). Nevertheless, even such materials are not suitable as technological rubbers because on protracted loading bodily displacement of chains will occur and the extension will not be fully recoverable (they will "creep"). This is prevented by permanently linking the individual chains with chemical bonds, thus forming a loose network, where the individual network elements still display the entropy elastic properties characteristic of rubbers. The above unsaturated polymers provide opportunities for the introduction of such chemical cross-links by activating very few of the double bonds along a given chain (vulcanization).

If the chain is not to be cross-linked, then for use above  $T_g$  the polymer must be crystalline to serve as a viable structural material. This applies to all those polymers, excluding those used as rubbers, where  $T_g$  is below the ambient temperature.

It is a fact that a common polymer is only semicrystalline, i.e., it will contain both amorphous and crystalline regions (more of this later). As such it combines the characteristics of crystalline and amorphous matter. As amorphous polymeric matter can exist in the form of either a glass or a rubber, this distinction will also apply to cases where it is in combination with crystals. Above  $T_g$  the amorphous component is, of course, in a rubbery consistency and the corresponding semicrystalline solid will display the properties of a stiff and strong crystalline material coupled with the elasticity and toughness of rubbers, more precisely dependent on the ratio and on the nature of connectedness of the two components. This is the consistency in which most crystalline polymers find practical application. Such a material can be considered as a rubber reinforced with crystals (in fact, the crystals also act as the (physical) cross-links preventing creep), or as a crystalline solid plasticized with a rubbery component. Polyethylene

is a widespread example of this class as a whole, LPE being more like the former and HDP like the latter. Nevertheless, even when the amorphous component is in the glassy state crystallinity still adds to stiffness and strength, but now the material, while stiff and strong, will be more brittle, i.e., it will support little strain.

In the case of crystalline materials the ultimate limit of applicability is determined by the melting point of the crystals  $T_m$ . The melting ranges of crystalline polymers have already been listed and discussed earlier. More on the physics of melting will be presented later.

It will be apparent that  $T_m$  and  $T_g$  are the most important characteristics of polymers determining their use. It is noteworthy that when a polymer can exist either in the crystalline state, or in the amorphous state, or in both states,  $T_m$  is always significantly higher than  $T_g$ .



# Crystallinity and Kinetics of Crystallization

A. Keller

## 2.1. Basic Classifications

### 2.1.1. Generalities

Crystallinity implies three-dimensional periodicity. In this respect we have to distinguish between crystallinity of periodic and aperiodic polymeric molecules. This distinction has already been implied in the introductory sections above; it is fundamental and self-evident yet, surprisingly, not usually pointed out even in basic texts.

#### 2.1.1.1. Periodic Molecules

In the case of periodic molecules the inherent periodicity of the molecule itself represents one direction in the crystal lattice. As stated earlier, this direction is a particularly important one because it corresponds to the direction of the covalently bonded chain. It is implicit that in order for this intrinsic periodicity to be utilized for the building up of a lattice, the chain direction must be uniquely defined (whether the chain is straight or helical is then a further question; see later). The parallel association of an assembly of chains with well-defined registry along their length then defines the full three-dimensional lattice (Figure 2.1a). The chains them-

---

A. Keller · Department of Physics, University of Bristol, England.

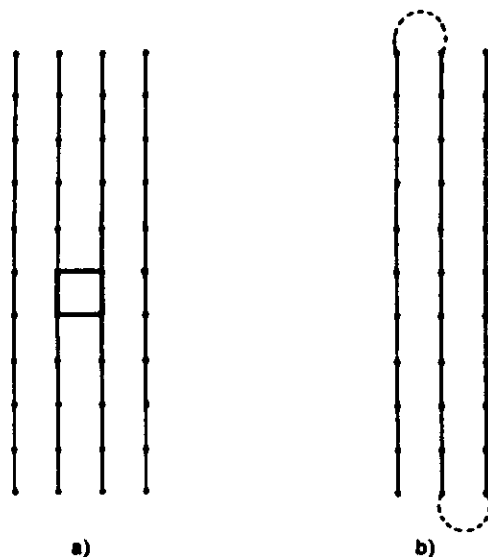


Figure 2.1. Concept of a lattice from parallel periodic chains, dots representing geometric repeating units. (a) Schematic illustration of the meaning of the unit cell (one drawn boldly). (b) Chain folding to form the lattice. In both cases the representation is two-dimensional.

selves need not be of uniform length provided they contain a sufficient number of repeats.

#### 2.1.1.2. Aperiodic Molecules

For aperiodic molecules to form a crystal lattice the molecules must be strictly equal, both as regards sequence of monomeric constituents and chain length. This is satisfied by the all-important globular proteins. These molecules assume a complex convoluted configuration so as to satisfy the requirements of delicate interactions between different monomeric units along the *same* chain. (Much of the biological function is related to these interactions.) The overall configuration will therefore be a globular coil of specific internal structure, all exactly the same for each molecule. It is these coils themselves which pack in a regularly repeating fashion to form the crystal lattice (Figure 2.2). It is noteworthy that this lattice bears no relation to the chain direction. The momentous achievements of crystal structure analysis of globular proteins (hemoglobin, enzymes, etc.) consist of the determination of the internal structure of the globule, not of the determination of the arrangement of the globules, i.e., the lattice, which in fact is usually trivial.

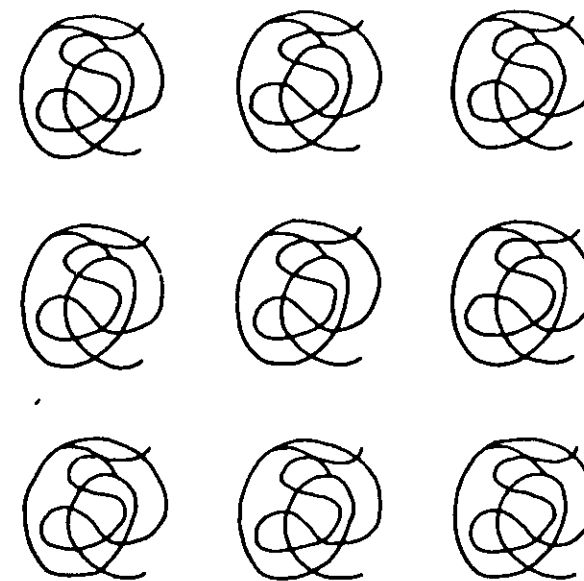


Figure 2.2. Schematic representation of a lattice from globular (protein) molecules. Here each molecule, although aperiodic, is strictly identical. The convoluted chain path is the "protein folding."

#### 2.1.1.3. Chain Folding: An Aside

The folding of chains features frequently in the subject of crystallinity of chain molecules. It is important to realize (it is in fact self-evident, although nowhere explicitly stated) that it has a different meaning in the fields of periodic and aperiodic molecules.

In the case of periodic molecules folding is one way in which the one-dimensional periodicity of the chains achieves a periodicity in a second dimension, thus leading to a sheet. Consequently, as sketched in Figure 2.1b, the folding itself contributes to the building up of a lattice.

In the case of aperiodic molecules, globular proteins in particular, the term "folding" refers to the establishment of the convoluted globular structure of the coil. Here the fold is at some specified localities of the chain, so as to satisfy some specific intramolecular interaction. This is the "protein folding," which accordingly does not contribute to the building up of the lattice *per se*.

In what follows we shall confine ourselves to the crystalline state associated with periodic molecules.

### 2.1.2. Sources of Lattice Imperfections in Polymers

Crystal imperfections represent a major facet of the physics of the solid state. Lattices are not, as a rule, ideally perfect but contain imperfections such as point defects and dislocations. This is also true for polymer crystal lattices. However, the lattices of polymer crystals contain defects over and above the conventional defects of the solid state in simpler substances and these are usually more significant. These additional defects arise from the chemical (including stereochemical) imperfections within the chain itself. In what follows we shall briefly review all those chemical imperfection types discussed in a previous section that could be the source of potential lattice imperfections:

- a. End groups. As noted already all chains have ends. The chain lengths are nonuniform, so these ends cannot be in register throughout the lattice and hence cannot be part of the lattice periodicity.
- b. Chemical irregularities along the main chain. These irregularities are either accidental, due to a "wrong" step in the polymerization reaction (e.g., a double bond in polyethylene), or deliberate, as in the case of a random copolymer.
- c. Stereochemical irregularity, i.e., nonuniform tacticity.
- d. Irregularly placed side groups — branches. As in category (b), these can be either accidental (e.g., branches in low-density polyethylene), or deliberate, as achieved by copolymerization (such as in the case of currently frequently used ethylene-propylene, or ethylene-butylene copolymers).

The above chain imperfections will impair crystal perfection in two ways: (1) they may become incorporated into the lattice, formed by the dominant periodic component of the chain, giving rise to lattice defects of various kinds, and (2) they may become ejected from the crystals into the amorphous regions, which will limit the size of the crystals that can develop. Whether (1) or (2) occurs is the subject of long-standing debates. There is not likely to be a unique answer as this will depend on the system in question and on the mode of crystallization. In the latter respect, in particular, it will depend on whether the crystallization is slow enough for the imperfect chain portion to become ejected from the growing crystal, if indeed this is thermodynamically favored.

In "real life" there are always some unavoidable chain imperfections of the kind listed above under (a)–(d). Such imperfections are often deliberately created in attempts to chemically tailor molecules, a trend of ever-increasing topicality.

If there is an excessive number of irregularities along the chain, the

existence of crystallinity proper (as evidenced by well-recognizable X-ray reflections) becomes questionable and we enter the gray area of when a polymer is to be regarded as still crystalline or as being amorphous. There are two categories of such a high level of crystal imperfections, or incipient states of ordering (depending on the end of the ordering spectrum from which the issue is approached):

- i. The lattice is in principle more or less perfect, but the crystals are so small that they do not give rise to sharp diffraction effects. PVC of normal commercial use, while largely atactic yet possessing a certain amount of crystal-forming syndiotacticity, may well be an example.
- ii. The lattice itself is not a completely regularly repeating assembly of the basic motive but incorporates systematic departures. This includes the much quoted and argued concept of paracrystallinity [R. Hosemann and S. N. Bagchi, *Direct Analysis of Diffraction by Matter*, North-Holland Publ. Co., Amsterdam (1962)], where the mean position of one motive with respect to the next does not correspond to that of an exact lattice repeat. A possible example is commercial PAN.

Finally, if chain irregularities exceed a certain proportion, the molecule becomes uncrystallizable and the corresponding material will be amorphous on any standard.

Having introduced all the above imperfection types, we shall now confine ourselves to the ideal lattice of ideally periodic molecules.

### 2.1.3. Modes of Crystallization

There are essentially three basic modes by which crystallinity can develop in a polymer.

1. *Concurrent with polymerization.* Here the crystallinity develops in the course of the polymerization reaction itself. As the chains grow in the course of the reaction, under appropriate circumstances the system becomes supercooled and the growing chains precipitate in the form of crystals (taking the frequent example that polymerization starts in solution) while the chains continue growing. The resulting product is the so-called "nascent polymer." Many widespread technological polymers are obtained in this form (polyethylene, polypropylene). In very special instances a macroscopic monomer crystal can be converted into a macroscopic polymer crystal by polymerization in the solid state (see later).
2. *Orientation-induced crystallization.* In this case, if long chains are aligned first while in the amorphous state they can be induced to

crystallize under conditions (temperature) where normally they would not. This includes the historically most important case of stretching-induced crystallization of rubber (detected by X-ray diffraction in 1925).

3. *Crystallization from the completely random state.* Here a random system, stationary melt or solution, is being supercooled sufficiently for it to pass into the crystalline state.

It is to be noted that (1) and (2) are typically "polymeric" phenomena without counterparts in the crystallization of simple substances. Case (3) is the equivalent of the normal supercooling-induced crystallization in simple atomic or low-molecular-weight materials. However, even here the long-chain nature of the molecule gives rise to many intriguing and novel effects. While some of them are necessarily much more complicated than in simpler substances, this need not always be the case: namely the one-dimensional periodicity intrinsic to the basic building units can represent a simplification when compared to the truly three-dimensional processes in simpler materials. Some references to this point will be made later.

In what follows we shall be largely concerned with case (3). Case (2) will have a smaller, but nevertheless decisive part to play, while only brief reference will be made to case (1) in the rest of this review.

## 2.2. Crystal Structure

Traditionally, the principal purpose of crystallographic research is the determination of the crystal structure. Knowledge of the crystal structure requires identification of the repeating entity, the unit cell, which is traditionally followed by determination of the cell content in atomic detail. Even if in later trends of macromolecular crystallography this sequence is often reversed (see further below), we shall proceed with the unit cell first.

### 2.2.1. The Unit Cell

The essentials have already been implied by the foregoing and are illustrated in Figure 2.1. Accordingly, the repeating unit does not involve the molecule as a whole but merely its repeating constituents. Thus one of the unit cell dimensions (usually denoted by  $c$ ) corresponds to the repeat unit *along* the chain, while the other two cell edges ( $a$  and  $b$ ) correspond to lateral repeat distances between different chains in equivalent positions (see Figure 2.3 for PE). Thus along one direction the lattice periodicity is defined by valence bonds in contrast to that along the other directions, where it corresponds to distances between otherwise unconnected atoms.

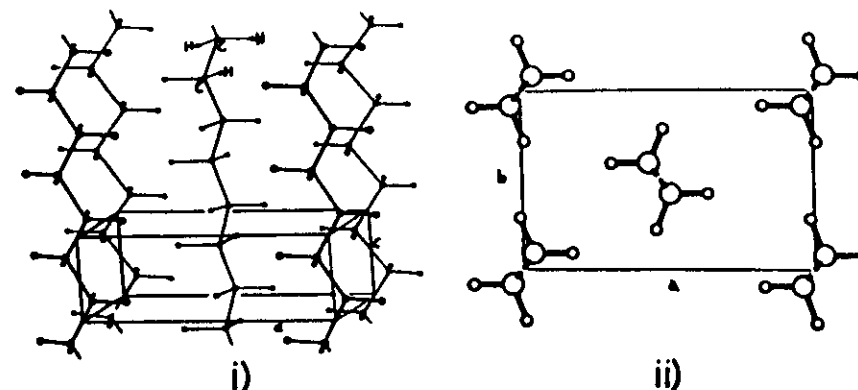


Figure 2.3. The unit cell of polyethylene. (i) Perspective view. (ii) View along the chain direction ( $c$  axis) (after Bunn<sup>29</sup>).

In view of this last emphasized feature the issue of crystal-structure determination is subdivided into two facets:

1. *Chain conformation*, corresponding to the shape and path taken up by the individual chain directly responsible for the geometric periodicity.
2. *Chain packing*, corresponding to the mode of packing of the different, but parallel, chains which is related to their lateral separation.

Clearly chain conformation is the more important of the two as it is an intrinsic property of the chain molecule. The above subdivision makes the crystal-structure issue of a long-chain molecule distinct from that of simple substances, say metals or small molecules, where the different directions are not as fundamentally different physically because they all correspond to distances between unconnected entities.

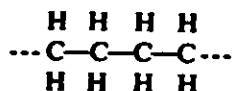
In what follows we shall treat (1) and (2) in turn.

### 2.2.2. Chain Conformations

The determination of chain conformations is one of the principal activities in structural polymer science. It can be done in two ways: (1) by analysis of diffraction patterns (X-ray or electron), and (2) by *a priori* predictions from the chemical formula, or most productively by a combination of (1) and (2). Method (2) in particular can again be pursued in two ways: (a) by building space-filling models with which the sterically impossible or unfavorable clashes can usually be spotted, and (b) by calculation,

the so-called conformational analysis, by which the energetically most favorable conformation can be determined, provided sufficiently realistic parameters (bond lengths, bond angles, atomic radii) and potential functions are used. In what follows some basic results will be quoted using the example of the simplest of all carbon chains.

Let us consider the simplest hydrocarbon chain, i.e., that corresponding to polyethylene:



where each C atom is at the center of a tetrahedron with its four valences leading to the four vertexes. Suppose full rotation around each C—C bond is possible and we wish to find the energetically most favorable configuration arising from these rotations.

Let us select any one C—C bond and regard it as vertical to the plane of the paper, so that we are looking along the bond. For any one of the two overlapping carbon atoms we shall then see the three remaining valences (lines connecting the center of the tetrahedron to the three apexes of one of its faces) at  $120^\circ$  to each other. Figure 2.4 shows an arrangement for the ethane molecule, where the three valences that belong to the upper carbon are denoted by solid lines, those that belong to the lower carbon are denoted by dashed lines, and the bold central circle corresponds to the two overlapping carbon atoms. All rotation angles are possible, so the three solid and dashed lines in Figure 2.4 could assume any rotational relation with respect to each other. It turns out that the particular arrangement in Figure 2.4 where the solid and dashed lines are at maximum angular separation in the presented projection is energetically the most favorable. This result is the principle of "staggered bonds," which expresses the fact that substituents, of adjacent carbon atoms are trying to avoid each other as much as possible.

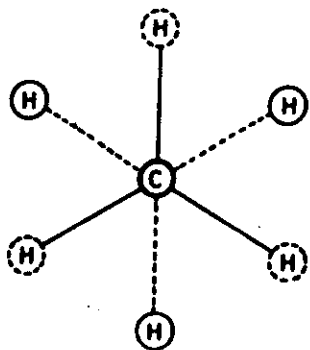


Figure 2.4. Illustration of the staggered bond principle in the case of an ethane molecule. View along the C—C bond.

In alkanes there are three possible such staggered positions, as is apparent from Figure 2.5. One of them is termed trans (T) and, as will be apparent, ensures that the main-chain carbon atoms all lie in one plane within which the C—C bonds form a zigzag line. The other two conformations in Figure 2.5 are termed gauche (G), distinguished by  $G^+$  and  $G^-$ . Here the C—C bonds will not lie in a single plane but will describe a convoluted path. Calculation reveals that for a simple  $\text{CH}_2$  chain (hydrocarbons, polyethylene) the T conformation is energetically the most favorable. There are energy minima also for the other two staggered positions  $G^+$  and  $G^-$ , as shown by the function of potential energy  $V$  vs angle of rotation  $\phi$ , but these are not as deep as for the *trans* state (Figure 2.6).

When replacing the H atoms by other constituents, which will necessarily all be bulkier than H, these may clash to varying extents. In order to minimize this clash there will be rotation around the C—C bonds away from the *trans* position which, if always in the same sense in a given chain, will transform the planar zigzag into a helical path. This can occur to different degrees according to the substituents.

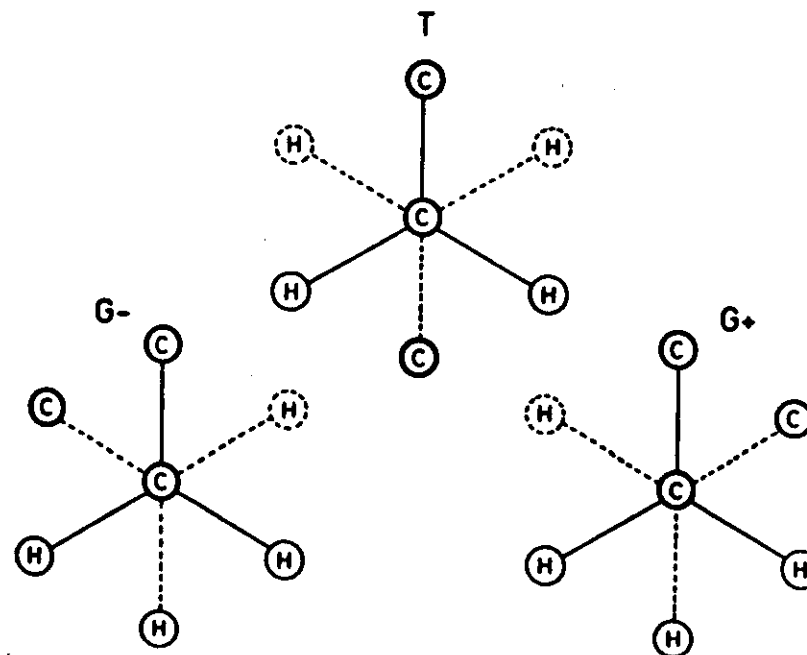


Figure 2.5. Three staggered bond configurations in the case of an alkane chain: T is the all-planar *trans* configuration,  $G^+$  and  $G^-$  are the two *gauche* configurations.

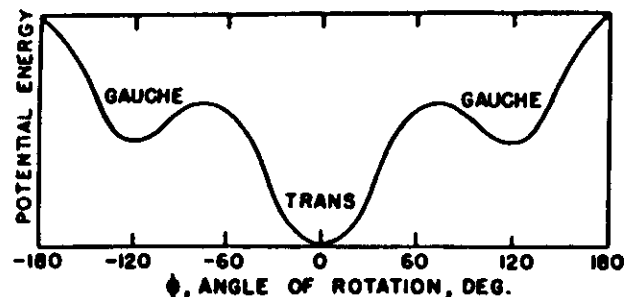


Figure 2.6. Potential energy as a function of rotation around a C—C bond. The deepest central minimum corresponds to the *T* state and the two smaller minima at  $-120^\circ$  and  $+120^\circ$  correspond to the two *G* states in Figure 2.5.

In PTFE each H atom is replaced by an F (fluorine) atom causing a rotation around the C—C bonds. This rotation is only slight, yet essentially within the trans trough of the potential surface, even if displaced from  $\phi = 0^\circ$  (or  $180^\circ$ ). The result will be a slowly winding helix, which at room temperature is a  $1_3$  helix (13 repeat units in 1 turn of the helix; see Figure 2.7).

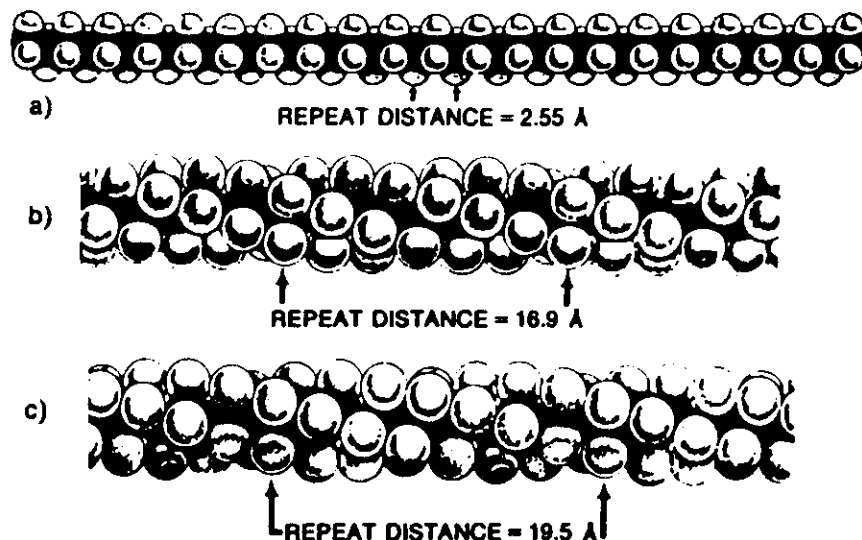


Figure 2.7. Space-filling models showing (a) the planar zigzag of polyethylene, and (b), (c) two slowly winding helical conformations of polytetrafluoroethylene. Dark balls represent carbon atoms and white balls the hydrogens in (a) and the fluorines in (b) and (c) (after Geil<sup>10</sup>).

In an isotactic polyolefin every second C atom will possess a more or less bulky constituent other than H, and when considering the chain stretched out in a planar zigzag (*T* configuration) they will all lie on the same side with respect to the plane of the zigzag, as shown in Figure 1.3. If these substituents are  $\text{CH}_3$  (polypropylene) or larger, they will clash in this all-*T* configuration, consecutive bonds requiring a rotation around every second bond by  $120^\circ$ , i.e., into one of the *G* troughs. The most favorable conformation along a given chain will therefore be  $\text{TG}^+\text{TG}^+\text{---}$  or  $\text{TG}^-\text{TG}^-$ . This will define a  $3_1$  helix (3 monomer repeats in 1 turn of the helix). This  $3_1$  helix with near variants (such as the  $7_1$  helix) is the standard chain formation for polyolefin (Figure 2.8), first predicted from models by Bunn [C. W. Bunn, *Proc. R. Soc. London, Ser. A* 180, 67 (1942)] before isotactic polymers were available, later abundantly verified on the actual systems by Natta and Corradini [G. Natta and P. Corradini, *Nuovo Cimento* 15, Suppl. No. 1, 68 (1960)]. (It should be stated that while the above comments appear in all textbooks and are essentially correct, latest experimental findings and subsequent calculations reveal also conformations other than the  $3_1$  helix as being of low energy, which under certain circumstances can determine the behavior of the system. The causes and consequences of these alternatives have not yet been fully evaluated. Even so they point to the extreme caution required as regards the *uniqueness* of the predicting power of conformational analysis.)

### 2.2.3. Chain Packing

#### 2.2.3.1. Geometric Considerations

Provided there are no specific interactions between chains but only van der Waals forces, the packing of long-chain molecules is most readily envisaged with reference to the packing of cylinders. Circular cylinders, of course, pack in regular hexagonal arrays. Chains with helical conformations are in fact close approximations to circularly cylindrical rods and many of them indeed pack hexagonally (e.g., isotactic polystyrene). Packing other than regular hexagonal can still be profitably considered in the same terms because even here the packing can be usually recognized as pseudohexagonal.

As an example let us consider polyethylene. The unit cell projection along the chain directly reveals the pseudohexagonal nature of the chain packing (Figure 2.3). The cross-sectional view of the all-*T* planar zigzag is approximately an ellipse, and the particular packing in Figures 2.3 and 2.9 corresponds to the optimum packing of ellipses [A. I. Kitaigorodsky, *Organic Chemical Crystallography*, Consultants Bureau, New York (1961)].

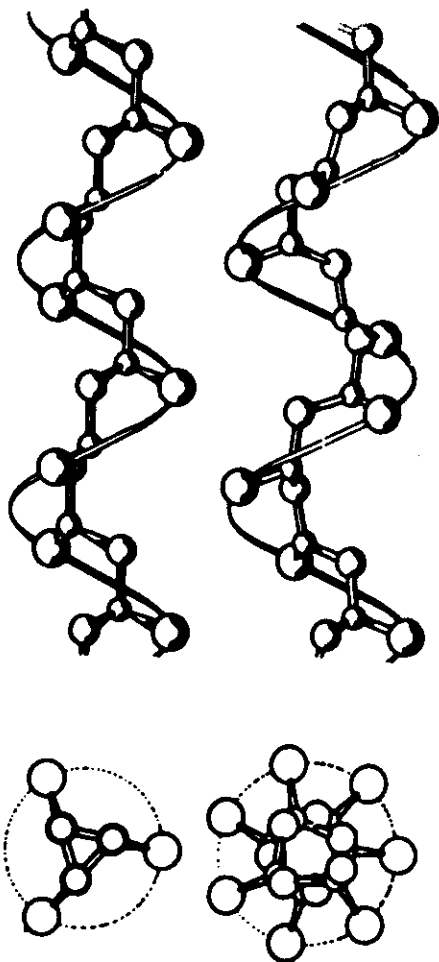


Figure 2.8. Two polyolefin chain conformations based on TG sequences. Left: 3, helix (an example is polypropylene); right: 7, helix (an example is poly-4-methyl-pentane). Top and bottom diagrams represent views perpendicular and parallel to the helical axes, respectively (after Natta<sup>49</sup>).

Looking at the packing problem in the above way is not only simple, but can be helpful when considering changes in packing caused by physical and/or chemical circumstances.

Let us examine thermal expansion. It is general knowledge with all paraffinoid substances (paraffins, fatty acids, polyethylene) that on increasing the temperature the orthorhombic lattice of Figure 2.3 will change

toward becoming truly hexagonal, a state that, depending on the materials or other circumstances, may only be approximately or actually attained (rotary phase in paraffins). The reasons for this will be evident if we remember that the chain, or segments of it, will perform increasing thermal vibrations around the chain axis and will lead to an overall circular envelope, the packing of which will approach that of hexagonal rods (Figure 2.9).

The same happens under the influence of chemical imperfections such as side branches (copolymers, low-density polyethylene) and occasional cross-links (e.g., those that can be introduced by irradiation). Whatever the description in detailed molecular and atomic terms, such imperfections reduce the overall ellipticity of the chain cross-section in the sense of Figure 2.9 with the result that the system will approach hexagonal packing.

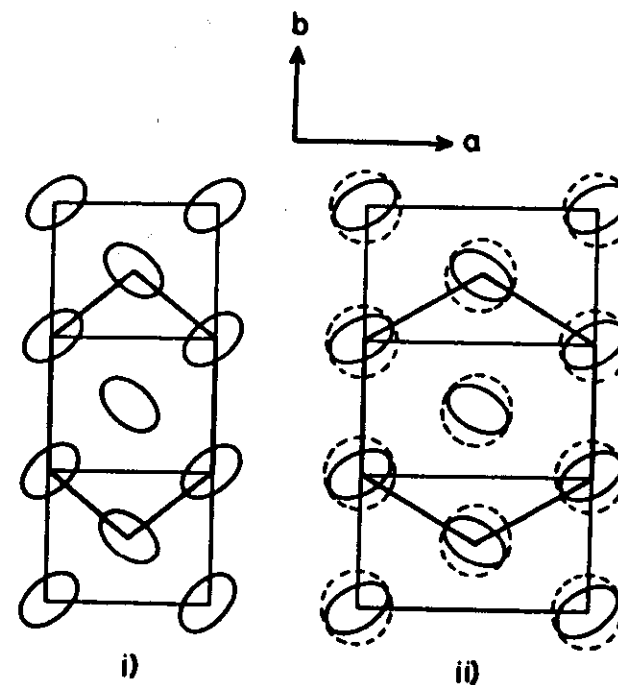


Figure 2.9. Schematic illustration of pseudo-hexagonal packing of chain molecules with elliptical cross section (i), which changes toward regular hexagonal packing (ii), on increasing thermal vibration so causing expansion along the  $a$  direction. The respective hexagons are drawn by solid lines. (The lattice with the given dimensions does not correspond to any particular polymer.)

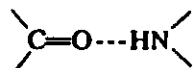
### 2.2.3.2. A Note on Crystal Polymorphism in Polymers

Polymorphism is a widespread occurrence among crystalline polymers. With very few exceptions the polymorphic structures differ as regards mode of chain packing but not chain conformation. This follows from the fact that chain packing is determined by interchain forces, which in general are not only much weaker than the intrachain forces but also much less specific. As a result there will be a number of ways in which chains can pack with only comparatively small differences in stability, i.e., corresponding to only comparatively shallow potential wells with only slight differences between them, leading to the possibility of several crystal structures. In simple substances differences in crystal structure usually have a profound effect on the material. This is generally not so with polymers. Although possibly interesting for the crystallographer, the unspecific nature of chain packing and the small energetic differences associated with the different polymorphs, as well as differences in crystal structure are usually not of primary significance for polymeric behavior. (This assertion may need to be qualified when specific forces between chains are operating (see below), especially when the effect of polarity on electric properties is involved as, e.g., in the case of the piezoelectric polyvinylidene fluoride.)

### 2.2.3.3. Specific Interchain Interactions

In the above discussion on chain packing only geometric packing factors were considered without the specific forces between the chains, for which polyethylene and the most common polyolefins are appropriate examples. In polymers containing polar groups the interchain interactions can be more specific. Such groups could be ions (in polyelectrolytes they form ion bridges between chains), dipoles, and whatever are capable of forming hydrogen bonds. Below we shall consider examples from the last-mentioned category.

Important examples of hydrogen bonding are found in polyamides. Here hydrogen bonds form between the carbonyl and the amine groups belonging to adjacent chains



where  $\cdots$  denotes the hydrogen bond. In such polymers the adjacent chains will occupy positions so as to satisfy these interactions. In favorable instances hydrogen bonding between all groups capable of such bonding can be achieved, in which case the mutual arrangement of the chains can be obtained virtually by inspection. This will be illustrated by two examples: nylon 66 and nylon 6.

The arrangement in nylon 66 is shown by Figure 2.10, where all hydrogen bonds are seen to be formed. As the  $\uparrow$  and  $\downarrow$  directions are equivalent, any parallel chain can hydrogen-bond with its neighbors. This is not so with nylon 6 where the chain direction has polarity, hence directions  $\uparrow \neq \downarrow$ . Nevertheless, it is seen from Figure 2.10(b) that hydrogen bonding can be fully satisfied if and only if alternate chains point up and down, i.e., the arrangement is  $\uparrow \downarrow \uparrow \downarrow \cdots$ .

As in both cases the chains are planar zigzags, the hydrogen-bonded structures are sheets. The rest of the chain-packing problem will then be confined to the mode of packing of these sheets. As there are no specific forces between the hydrogen-bonded sheets the optimum sheet packing is not very distinct from other packing possibilities. It follows that the different, energetically very similar modes of sheet packing form a source of polymorphism in polyamides. This again exemplifies the theme already stated in connection with the packing of individual chains and polymorphism, namely the less specific the interactions, the more difficult it is to predict or to determine the corresponding packing geometry. On the other hand, the distinction between the various possibilities (polymorphism) is correspondingly less significant for the behavior of the system as a whole.

We wish to mention that the presence of strongly interacting groups, if closely spaced along the chain, can affect not only the chain packing but even the configuration of a given chain itself. This is the situation with polypeptides, where hydrogen bonds can form internally within a chain leading to the famous Pauling  $\alpha$ -helix, one of the starting points of modern structural molecular biology.

### 2.2.4. Crystal Structure Determination

For the kind of chain molecules under discussion, crystal structures are usually determined from X-ray fiber diffraction patterns. These correspond to single-crystal rotation patterns with the chain (fiber) axis as axis of rotation. These diffraction patterns display layer lines perpendicular to the fiber axis. The layer-line periodicity, directly read off the patterns, corresponds to the geometric periodicity along the chain. In a straight zigzag chain this will be the monomer periodicity (or a higher order of it in the case of systematic absences). If the chain is helical or has some convoluted conformation the geometric repeat will be correspondingly different, but as long as the staggered-bond principle holds (i.e., only T and G configurations apply) the conformational possibilities will be finite. Hence the actual chain conformation, the most important structure feature, is usually directly identified (by model building, simple geometric calculations, or even by inspection) from the layer-line periodicity.



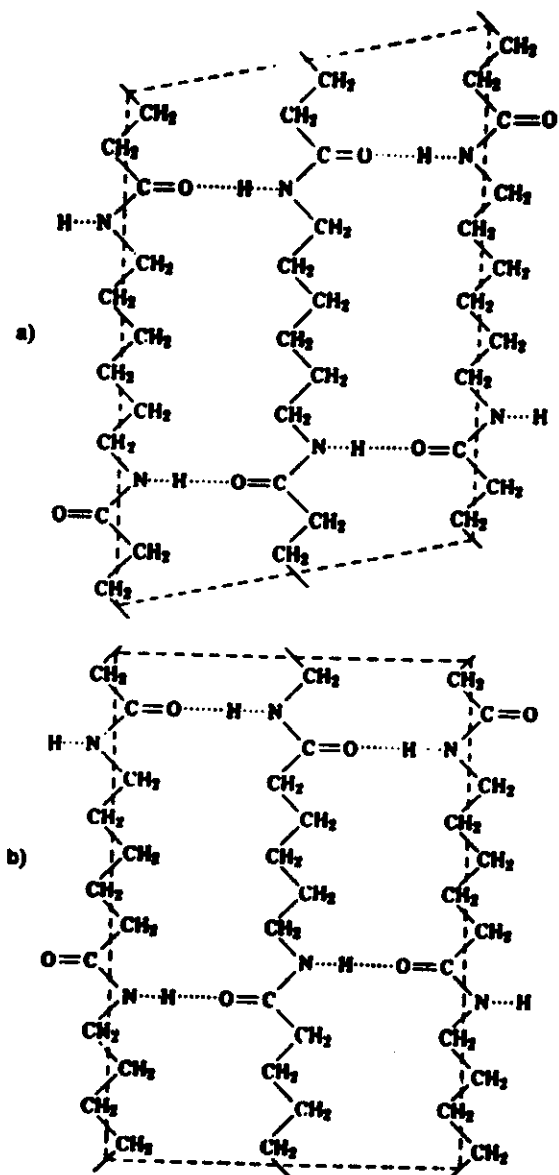


Figure 2.10. Examples of sheet formation in nylons via establishment of hydrogen bonds between chains: (a) nylon 66 and (b) nylon 6.

For more complicated chains, as in the case of many biopolymers, the Fourier transform method is particularly useful, namely the chain itself often has a readily recognizable, highly structured transform (the diffraction, which would be produced by a single chain, or a parallel array of uncorrelated chains) and the reflections actually correspond to the sampling of this transform by the interference function due to the full three-dimensional crystal lattice. The Fourier transform of some conjectured chain conformation can be readily calculated and then, after cylindrical averaging in the case of fibers, compared with the diffraction pattern; or conversely, certain typical chain conformations have readily recognizable fingerprints (arrangements of strong reflections or absences) in the diffraction patterns.

The trend toward hexagonal packing can be a useful guide for the determination of chain packing. Regular hexagonal packing is readily recognized where the strongest reflections on the equator (0 layer line) correspond to that of the hexagonally close-packed planes. If the structure is pseudohexagonal there will be two or three such strong reflections instead of one (e.g., 110 and 200 in polyethylene). This is the origin of the characteristic prominent single ring (hexagonal) or doublet ring (orthorhombic, etc.) in the unoriented (i.e., powder-type) diffraction patterns of most simple synthetic polymers.

### 2.3. Degree of Crystallinity

As stated earlier, materials consisting of long-chain molecules are in general not fully crystalline and contain a not-inappreciable amount of amorphous constituent. A most self-evident manifestation of this is the fact that, say, a piece of plastic such as polyethylene, while displaying clearly defined X-ray reflections, does not have properties like that of a conventional crystalline solid but behaves to some extent like an amorphous rubber or glass. If crystallinity is only partial, then clearly knowledge of the "degree of crystallinity" is required.

#### 2.3.1. The Principle of the Determination

For a quantitative determination of the degree of crystallinity, often referred to as the "amorphous-crystalline ratio," the following general method is usually adopted. A property that is crystallinity-sensitive is chosen. If its dependence on crystallinity is known for a polymer, it can serve as an indicator of the degree of crystallinity for any given sample of that polymer. Such properties fall broadly within three classes: thermodynamic, diffraction-based, and spectroscopic.

### 2.3.2. Methods of Determination

#### 2.3.2.1. Thermodynamic

a. *Specific Volume  $v$  or Density  $\rho$ .* If the degree of crystallinity is denoted by  $\chi_c$ , then

$$\chi_c = \frac{v_s - v}{v_s - v_c} = \frac{\rho - \rho_s}{\rho_c - \rho_s} \quad (2.1)$$

where  $v$  and  $\rho$  refer to the relevant property of the sample under examination,  $v_s$  and  $\rho_s$  to that of the purely crystalline state, and  $v_c$  and  $\rho_c$  to that of the purely amorphous state. If the crystal structure (i.e., at least the unit cell dimensions and the number of chains within this cell) is known,  $v_c$  or  $\rho_c$  are also known quantities. The determination of  $v_s$  or  $\rho_s$  can present a problem if the polymer is unobtainable in a fully amorphous state at the temperature at which  $\chi_c$  is required (usually ambient temperature), which is frequently the case. In this situation  $v_s$  must be extrapolated from its value in the melt assuming knowledge of its thermal expansion coefficient in the molten state. This is a long extrapolation with all the related uncertainties, not to speak of the inherent assumption that  $v_s(T)$  is a linear function over the temperature range concerned. Hence for this method,  $v_c$  is the limiting factor to the accuracy that can be attained, in addition to such apparently trivial, but by no means easily avoidable problems as the influence of voids (which can be submicroscopic) on the measurements.

b. *Heat of Fusion ( $\Delta H$ ).* Here  $\chi_c = \Delta H / \Delta H_c$ , where  $\Delta H$  is the heat of fusion of the sample under consideration and  $\Delta H_c$  that of the fully crystalline material;  $\Delta H_c$  is the basic limitation in view of the fact that a fully crystalline material is not generally available. Therefore in this case  $\Delta H_c$  has to be obtained theoretically and/or by extrapolation from the behavior of shorter chain oligomers (e.g., paraffins as oligomers for polyethylene).

#### 2.3.2.2. Diffraction Methods

These essentially rely on the assessment of the ratio of the amorphous to the crystalline scattering intensities in the X-ray diffraction patterns of random specimens. The technical problems encountered mainly pertain to the separation of crystalline reflections from amorphous halos in the usual case where they overlap to some extent. Problems of principle comprise the issues of how far out one needs to go in reciprocal space (scattering angle) for the information to be meaningful and of how small a crystal is still a crystal (i.e., how broad a reflection still counts as a Bragg reflection).

#### 2.3.2.3. Spectroscopic Methods

a. *Infrared Spectroscopy.* Certain features in the infrared spectrum are sensitive to the configuration and/or packing of the chains in the crystal and can thus serve for the assessment of crystallinity. These features fall into two categories.

The first kind relies on the observations that certain adsorption bands appear in the crystalline state and disappear on melting, and are accordingly then classified as "crystalline" bands. Similarly, "amorphous" bands can also be identified by their disappearance, or at least reduction, on crystallization. The intensity of such bands can then be used as a measure of the degree of crystallinity. In the first place this may only be a purely empirical exercise, which at a later stage may or may not acquire theoretical foundation.

The second class of spectral features relies on the fact that in a crystal structure containing symmetrywise nonequivalent neighbor chains, such chains can vibrate inphase or antiphase while in the crystalline state corresponding to two adsorption bands at slightly different frequencies. The result will be doublets in the spectrum. This distinction disappears in the amorphous phase where only a singlet will be seen. The evaluation of such doublets, where they exist, provides a theoretically well-founded method for the measurement of amorphous-crystalline ratios.

b. *NMR Spectroscopy (Broad Line).* This method does not measure crystallinity but mobility, and can be used for crystallinity determinations only as far as mobility can be equated with the amorphous phase and immobility with the crystalline phase. It relies on the fact that in the immobile (crystal) phase the external magnetic field will be locally modified by the magnetic moments of the neighboring nuclei (protons), and differently so by the different neighbors, with the result that the resonance envelope will be broad. In the mobile (amorphous) regions there will be an averaging out of the effect of neighboring nuclei and the resonance peak will be sharp. The method then consists of measuring the ratios of the sharp and broad resonance peaks. It should be noted that this method is sensitive to small amounts of mobile material.

### 2.3.3. An Appreciation of the Different Methods

There exists much literature concerned with the correct absolute value of crystallinity and with the comparison of results obtained by different methods, including claims for agreement and disagreement. The first point to be appreciated is that the different methods are measuring different properties, and therefore even if correctly measured and interpreted (some of the potential uncertainties have already been noted), they need not

necessarily give exactly identical numerical results. It therefore follows that the measurement and definition of any absolute value of the crystallinity is problematic. Even if it were possible to obtain a reliable unique absolute value this would still be of questionable significance *per se* because, as will be apparent below, materials possessing the same degree of crystallinity as determined by one particular method can still have grossly different properties depending on the route along which the particular degree of crystallinity was attained. This is because this route affects the crystalline fine structure, i.e., the morphology, of which much more will be said below.

More meaningful than the absolute values themselves are the comparative differences between different samples as regards degree of crystallinity and, in particular, changes within the same sample produced by, say, certain treatments. In this respect the different methods should at least indicate the same trends, which they generally do.

One of the most straightforward applications of comparative crystallinity measurements on a given sample is that which records the development of crystallinity as a function of time. This serves to determine the rates of crystallization, and in general represents the basis for the study of crystallization kinetics.

## 2.4. Kinetics of Crystallization

### 2.4.1. Rates of Crystallization

The kinetics of crystallization is important in technological applications as it determines, e.g., the rate of solidification of a molded object during cooling or that of a thread emerging from a spinnerette. It is also important, of course, for the fundamental understanding of crystallization.

The basic investigations consist of measuring  $\chi_c$  as a function of time at preselected constant temperatures. In what follows we shall take the specific volume as an indicator of crystallinity. This can be most readily measured with a dilatometer. We express the results in terms of  $v_c - v_a = \Delta v$  as a function of time at a given temperature  $T$ . These lead to sigmoidal curves, such as that drawn schematically in Figure 2.11. The rate  $R$  can then be defined either as the steepest slope at the inflection point, or as the half-time of the full volume change  $\Delta v_{\max}$ .

In general, the curve of  $R$  vs  $T$  will be bell-shaped, such as that in Figure 2.12, because the rate will be zero at the melting point  $T_m$  (in fact, it will not assume a measurable value until well below  $T_m$ , i.e., polymer crystallization only starts at considerable supercooling) and will become vanishingly slow again at the glass transition  $T_g$ . In between  $T_m$  and  $T_g$  there will necessarily be a maximum at some temperature  $T_{\max}$ . This

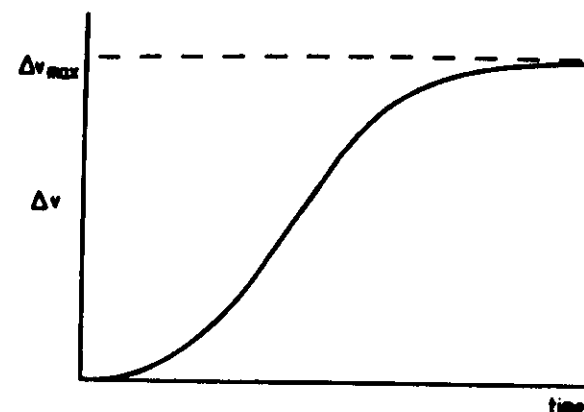


Figure 2.11. A schematic crystallization isotherm obtained in the study of crystallization kinetics. In this instance volume change  $\Delta v$  is plotted against time.

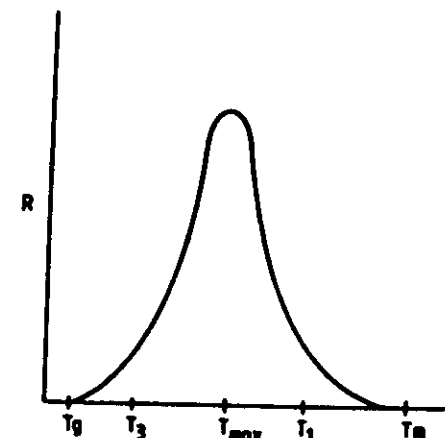


Figure 2.12. A typical curve representing rate of crystallization  $R$  as a function of crystallization temperature  $T$ .

maximum is due to two opposing effects: the increasing thermodynamic driving force with increasing supercooling  $\Delta T$  ( $\Delta T = T_m - T$ ) and the decreasing mobility at the correspondingly lower temperature.

The different crystallizable polymers differ as regards the magnitude of the maximum in the  $R$  vs  $T$  curve. In practice one may place them in two groups: those where  $R_{\max}$  is sufficiently low so that a normal sample can be cooled through  $T_{\max}$  without crystallization setting in, and those which cannot. The former group can be obtained in an amorphous state, hence in the glassy state, and if so required can be crystallized at temperatures below  $T_{\max}$ . PET, polycarbonates, and isotactic polystyrene are examples. In fact crystallization rates in the latter two cases are so slow

that prolonged holding at  $T_{max}$  is required to achieve any crystallization at all. This is why polycarbonates, though crystallizable, are or can be used in the glassy amorphous state and are mostly used as glasses by virtue of being transparent in this state, while owing to their particular chemical constitution they possess a high  $T_g$  (180 °C).

#### 2.4.2. The $\chi_c$ vs $t$ Curves

It is most important to realize that  $\Delta v_{max}$  does not correspond to full crystallinity, i.e., to  $\chi_c = 1$ . It corresponds to the maximum  $\chi_c$  achievable at that particular temperature  $T$ , which is  $< 1$ . Thus the kinetically fully crystallized material is not fully crystalline (which reflects the fact that complete crystallinity is not normally achievable).

We shall therefore define the kinetic crystallinity  $\chi'_c$  in the form

$$\chi'_c = \frac{v_0 - v_t}{v_0 - v_\infty}$$

where the subscripts of  $v$  refer to the time elapsed after the sample has attained the intended crystallization temperature. It follows that  $\chi'_c$  at  $t = \infty$ , denoted  $\chi'_{c\infty}$ , is always less than unity.

Next we consider the  $\Delta v$  vs  $t$  curves as a function of  $T$ . When these curves can be obtained over the full range of crystallization temperatures, the resulting situation corresponds to that sketched diagrammatically in Figure 2.13. Three  $T$  values are represented with  $T_1 > T_2 > T_3$ , where  $T_2$  corresponds to  $T_{max}$ . It is noteworthy that  $\chi'_{c\infty}$  depends on  $T$  for values of  $T$  below  $T_{max}$ . In particular  $\chi'_{c\infty}$  (the maximum value for  $\Delta v$ ) becomes

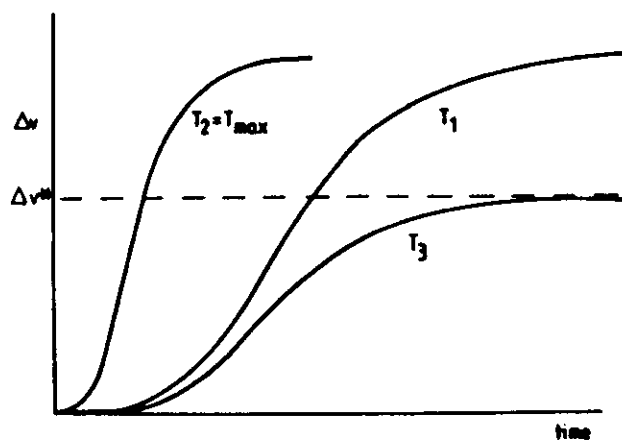


Figure 2.13. Crystallization isotherms corresponding to crystallization temperatures at the high-temperature side  $T_1$ , low-temperature side  $T_3$ , and maximum region in Figure 2.12.

increasingly smaller with decreasing temperature. This means that the maximum achievable crystallinity at these temperatures will be lower even if, kinetically defined, the sample is fully crystallized.

#### 2.4.3. Morphological vs True Crystallinity

When a polymer melt crystallizes, spherical crystal aggregates nucleate and grow (so-called spherulites; more about this later!). At each stage of growth the sample volume will be partitioned between the spherulites and the unaltered melt, the fraction of spherulite-filled volume becoming increasingly larger with time. When all the spherulite-free amorphous volume is consumed, the crystallization (primary, see later) comes to an end. At this stage  $\Delta v_{max}$  is attained, hence  $\chi'_c = \chi'_{c\infty} = 1$ . Here the sample is fully crystallized and in morphological terms fully spherulitic. We can say that the sample is *morphologically* (but not truly) fully crystalline. Thus the  $\Delta v$  vs  $t$  curves record the development of morphological crystallinity.

It follows from the fact that  $\chi'_{c\infty}$  can be different for different temperatures of crystallization (e.g., for  $T_2$  and  $T_3$  in Figure 2.13) that in absolute terms the degree of crystallinity of the spherulites themselves must be different for the two different crystallization temperatures. (Thus spherulites formed at the lower temperature  $T_3$  are *less* crystalline.)

Accordingly, the properties of polymers can show a twofold dependence on crystallinity: a dependence on the degree of morphological crystallinity and on the degree of true crystallinity. Conversely, it follows that a single (true) crystallinity value does not fully characterize the crystalline state of a sample.

The last statement will be illustrated schematically as follows. Let us consider again Figure 2.13 and take the development of crystallinity corresponding to  $\Delta v^*$ . We see that along curve  $T_3$  this corresponds to  $\Delta v_{max}$ , hence to  $\chi'_{c\infty}$ , i.e., to the morphologically fully crystallized sample, while along curve  $T_1$  the crystallization is far from complete. If we compare sections of the two samples under the microscope we see images such as in Figure 2.14a and b corresponding to  $\Delta v^*$  along curves  $T_1$  and  $T_3$ , respectively. Figure 2.14a is meant to represent isolated spherulites within an amorphous matrix, while in Figure 2.14b the spherulites are all impinging and no untransformed material is left. Clearly, the two morphologies are very different, a difference reflected by the physical properties. Yet the absolute crystallinity as defined by equation (2.1) will be identical. Conversely, identical morphological crystallinities (i.e., fractional spherulite occupancy) attained along the different isotherms will correspond to different true crystallinities; the properties here again will be largely different. (The above significant exposition does not feature in the conventional literature; it is based on unpublished researches by the author.)

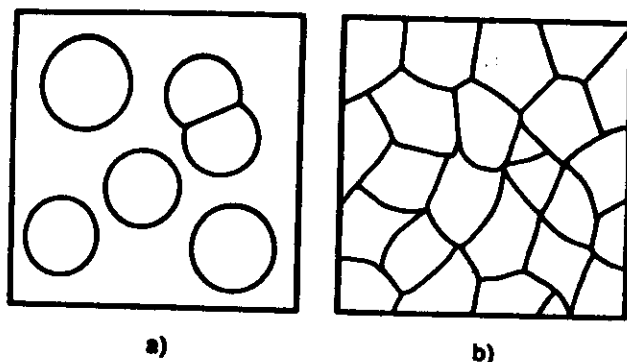


Figure 2.14. Schematic representation of two stages in the course of crystallization. (a) Spherulites are largely isolated within an untransformed amorphous matrix. (b) Sample is fully pervaded by spherulites. Such a sample is fully crystallized and corresponds to the stage  $\Delta v_{\infty}$  in Figure 2.11, or to  $\Delta v^*$  along curve  $T$ , in Figure 2.13.

#### 2.4.4. Primary and Secondary Crystallization

The  $\Delta v$  vs  $t$  curves do not often level off smoothly but can take one of the two courses shown in Figure 2.15. This behavior is the consequence of secondary crystallization following the initial primary crystallization discussed earlier. In Figure 2.15a the first plateau signifies the termination of the primary crystallization, and the second plateau that of the secondary crystallization. In this case the rates of the two processes are sufficiently disparate for them to appear separately in the  $\Delta v$  vs  $t$  curve. If both processes occur at comparable rates, i.e., the primary process is still in progress when the effect of the secondary process becomes significant, their

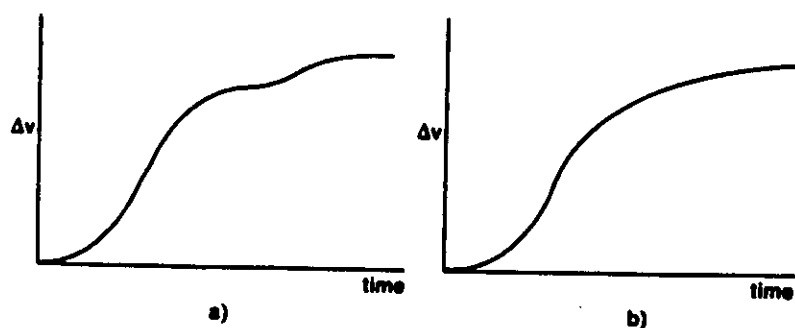


Figure 2.15. Crystallization isotherms with two different manifestations of secondary crystallization.

resultant effect will merge and curves such as those in Figure 2.15b will result.

In structural terms, secondary crystallization represents the increase in the true degree of crystallinity of the spherulites (which themselves are the products of the primary crystallization). Thus the spherulites improve their crystallinity with time! If this improvement is slow compared to the growth of the spherulites themselves, we have the behavior demonstrated in Figure 2.15a, otherwise that in Figure 2.15b. This is an important illustration of the many-stranded relation between crystallinity and crystalline texture. Of the fine structural features underlying this effect more will be said later.

#### 2.4.5. Textures

The overall process of crystallization consists of two separate processes: (1) nucleation of new crystals and (2) growth of crystals already present. The overall crystallization rates, as in Figure 2.12, result from the compounding of these two separate processes. The rate of each of the separate processes (1) and (2) has a maximum with temperature (the maxima for the two do not coincide, that for (1) being at lower temperatures). For a given crystallization temperature, the comparative rates of the two processes and the number of nuclei present to begin with determine the overall scale of the resulting crystal entities within the final polycrystalline material. This feature is termed *crystal texture* as opposed to crystal structure on the molecular level.

Nucleation itself can be of two types: (1) predetermined and (2) spontaneously forming.

1. The predetermined nuclei are heterogeneities, the effect often being referred to as heterogeneous nucleation. In polymers there can be a further subdivision: extraneous heterogeneities (catalyst residues, impurities, etc.) and residual crystal fragments of the polymer itself giving rise to so-called "self-seeding." This latter mode of nucleation is unique to polymers and arises from the fact that, for a variety of reasons to be dealt with later, polymers have a broad melting range. The last crystal fragments to melt may be present in such a small proportion that they are undetectable in what otherwise appears to be a homogeneous melt, and may even be in a superheated form above the conventionally identified melting range. These will serve as nuclei for crystallization on cooling.
2. Spontaneously forming nuclei in principle result from spontaneous fluctuations that exceed the critical nucleus size. It is often termed *sporadic nucleation* or *homogeneous nucleation*.

In general, large numbers of nuclei lead to a fine-grained texture and few nuclei to a coarse-grained texture. This is true for all polycrystalline materials. In addition, with polymers we have a two-tiered texture. The texture as determined by primary nucleation in the above sense relates not to single-crystal grains (as in metals or rocks, etc.) but to the spherulites. As we shall see, these spherulites are not single crystals but are themselves crystal aggregates, hence possess a texture. The fact that the spherulites themselves can possess different degrees of crystallinity relates to differences in their texture; in particular, the increase in crystallinity on secondary crystallization relates to the coarsening of this spherulite texture, more of which later.

It is a general feature of all polycrystalline materials that the macroscopic (e.g., mechanical) properties are highly texture-dependent. Coarsely textured materials are generally stiffer (high modulus) but more brittle (support lower strain before fracture), and conversely for the finer-scale texture. This is true also for polymers, with the important addition that it applies to textures on both levels, the spherulitic and intraspherulitic. In fact, we shall see that there can be more than two levels. The existence of such texture hierarchies is a unique feature of macromolecular substances and becomes extremely intricate with biological materials.

In general, the crystallization of polymer melts is practically always induced by predetermined nuclei. Extraneous heterogeneities (mostly catalyst residues) can virtually never be avoided. For this reason the temperature regime of homogeneous nucleation (except for some very specialized experiments) cannot be reached because crystal (spherulite) growth emanating from these predetermined centers pervades the whole sample, hence completes the primary crystallization, before temperatures low enough for homogeneous nucleation to occur at appreciable rates are attained in the course of cooling. The predetermined nature of the nucleation is usually apparent from the fact that the spherulites are all of equal size, signifying that growth started from given centers simultaneously. This is not to say that sporadic nucleation cannot be observed, i.e., spherulites continually appear in the still untransformed portion of the material, giving rise to a final texture of widely differing spherulite sizes. However, there is evidence that even in this latter case nucleation starts from predetermined centers where the nucleating efficiency of these centers is different, resulting in a sporadic emergence of new spherulites. The latter is to be envisaged as a reservoir of predetermined nuclei, the nuclei having a range of incubation periods, the predetermined nature of the centers only becoming apparent when the exhaustion of the reservoir can be observed before the primary crystallization is complete. A more rigorous understanding of all these nucleation phenomena has yet to be achieved.

## 2.4.6. Analytical Treatment of Crystallization Kinetics

### 2.4.6.1. Analysis in Terms of Expanding Spheres (the Avrami Equation)

The recognition that crystallization of polymers is represented on a macroscopic scale by nucleation and growth of spherulites leads to a simple mathematical description of isotherms, such as that in Figure 2.13. This relies on the calculation of the volume fraction as yet uncovered (i.e., the amorphous fraction) by the newly forming and growing spherulites at any particular time of crystallization. The information required initially is the rate of volumetric spherulite growth (alternatively, this can be obtained from the experimental isotherms using the theory to be outlined below).

Let us first consider the growth rates. An important basic fact is that, at a given temperature, spherulites are observed to grow at a constant linear velocity, and are thus characterizable by a single radial growth rate  $\dot{r}$  in the mathematical treatment.

As regards the formation (nucleation) rate, the usual treatments embody the two alternatives discussed in the preceding section: (1) the spherulite centers are predetermined (heterogeneous nucleation) and (2) new spherulites form at a constant rate within the still untransformed material (sporadic nucleation).

In treating dimensionality and shape, the spherulites in three-dimensional samples are regarded as spheres. Two-dimensional samples (thin films) can also be important for basic laboratory studies under the microscope, in which case the spherulites are considered as disks. Other shapes and their combination with different dimensionalities also feature in the literature. It will be shown that except for special, restricted conditions of application, the formulas derived for these are erroneous.

The treatment of expanding spheres and circles to be outlined below is usually referred to as the *Avrami treatment*, although it has been applied in several instances prior to Avrami, notably as far back as Poisson.

Consider spherical bodies 1, 2, ...,  $n$  of volume  $V_1, V_2, \dots, V_n$  in some state of expansion before they impinge, with total volume  $V$ . The probability  $p_i$  that a randomly chosen point  $P$  lies outside  $V_i$  is given by

$$p_i = 1 - V_i/V$$

The probability  $p$  that the point lies simultaneously outside bodies 1, 2, ...,  $n$  is expressed by

$$p = p_1 p_2 \cdots p_n = \prod_{i=1}^n (1 - V_i/V) \quad \text{or} \quad \ln p = \sum_{i=1}^n \ln(1 - V_i/V)$$

Since  $V_i \ll V$ , powers of  $V_i/V$  higher than the first can be neglected in the expansion of  $\ln p$ , hence

$$\ln p = - \sum_{i=1}^{\infty} (V_i/V) = \delta \bar{V} \quad \text{or} \quad p = e^{-\delta \bar{V}}$$

where  $\delta = n/V$ , the number of entities per unit volume or the nucleus density, and  $\bar{V} = \sum V_i/n$ , the mean volume of entities present.

An expression for  $p$  is also given by the volume fraction of material not engulfed by the "bodies," namely the volume fraction of the remaining nonspherulitic (hence totally amorphous) material. Thus

$$p = 1 - \chi'_c = e^{-\delta \bar{V}} \quad (2.2)$$

The main problem beyond this simple geometric derivation is how to treat the situation when different bodies abut. Avrami does it in a very elaborate way. However, this situation can be treated very simply (essentially going back to Poisson, but revived by U.R. Evans [*Trans. Faraday Soc.* 41, 365 (1945)] for the treatment of the spread of rust on a metal surface) by considering two potentially overlapping spherical bodies, as presented in Figure 2.16, where 1 and 2 refer to the unobstructed spheres. If a point  $P$  is situated within either of the unobstructed spheres, then it will lie within the overlapping composite body as well. If it is outside the unobstructed spheres (point  $P'$ ) it will also be outside them when they abut (see Figure 2.16) as long as neither body outgrows the boundaries of the other in the hypothetical absence of overlap. Thus we can assume that  $P'$  lies in the nonspherulitic material irrespective of overlap. Accordingly, equation (2.2) will still hold.

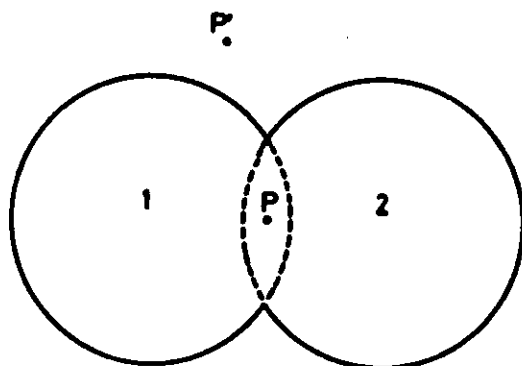


Figure 2.16. Effect of spherulite overlap as referred to in the derivation of the Avrami equation.

The exponent in equation (2.2) can be expressed as a function of time  $t$  (see standard textbooks on polymers embracing crystallization) in the form

$$1 - \chi'_c = e^{-Kt^n} \quad (2.3)$$

where  $n$  and  $K$  are constants,  $n$  depending on the dimensionality (two- or three-dimensional growth) and on the type of nucleation and  $K$  including the parameters relevant to the rate of growth, rate of nucleation, and number of nuclei. This is shown more explicitly in Table 2.1.

Equation (2.3) usually provides a good description of the observed  $\Delta v$ , or  $1 - \chi'_c$ , the kinetic amorphous fraction into which  $\Delta v$  is readily converted, as  $t$  varies (Figures 2.11 and 2.13) with appropriate constants. The constants can then be determined by plotting  $\ln(1 - \chi'_c)$  against  $\ln t$ , which usually yields a straight line of slope  $n$  and intercept  $K$ . Hence the nature of the nucleation (predetermined or sporadic) and the growth and nucleation rates, respectively, can be assessed. These quantities can be observed directly under the optical microscope in suitably prepared specimens, and agreement with those derived from the  $\Delta v$  vs  $t$  curves via equation (2.3) can be checked.

In a number of cases correspondence between the kinetic isotherms and the measurements on the microscopic image was sufficiently encouraging to provide confidence when employing the above method of kinetic analysis, which is used extensively as a consequence. Nevertheless a few reservations, not to be found in textbooks, may be appropriate.

#### 2.4.6.2. Limitations of the Avrami Analysis

Measurements giving  $\chi'_c$  as a function of  $t$  (particularly via  $v$  or  $\rho$ ) can be very simple and the result is always informative *per se* as regards the rate of crystallization. Possession of these isotherms then naturally invites evaluation via equation (2.3), hence the widespread popularity and frequent misuse of the Avrami analysis.

Table 2.1. Parameters in the Avrami Equation (2.3)\*

Dimensionality	Constants	Predetermined nuclei	Sporadic nucleation
Two dimensional (circles)	$n$ $K$	2 $\pi r^2 g$	3 $\frac{1}{2} \pi k r^2$
Three dimensional (spheres)	$n$ $K$	3 $\frac{4}{3} \pi r^3 g$	4 $\frac{1}{4} \pi k r^3$

\* The number of nuclei per unit volume or area is denoted by  $g$ , the rate of radial growth by  $r$ , and the rate of nucleation by  $k$ .

Table 2.1 is confined to circles (disks in the case of two-dimensional, i.e., thin, samples) and spheres. Textbooks often give more extensive tables for other geometries too. These can be misleading or outright erroneous. The assumption underlying the derivation was that point  $P'$  remains outside the body irrespective of whether the growth of body 1 (see Figure 2.16) is being obstructed or not. For spherical objects growing at a constant rate, this is obviously true (sphere 1 in Figure 2.16 could never outgrow sphere 2). It will not, however, be generally true for disks in any arbitrary orientation within a three-dimensional specimen or, as often quoted, for arbitrarily oriented rods growing longitudinally. For both these cases this will only hold if they are all parallel (which is satisfied for the two-dimensional case in Table 2.1) but not otherwise. For other, more complex shapes (such as sheaves) sometimes quoted, the above condition relating to  $P'$  will never hold, hence the Avrami treatment for these situations will be invalid.

Even for spheres, the above treatment is confined to primary crystallization only, i.e., when the spherulites do not subsequently change their crystallinity. Although a treatment for the inclusion of secondary crystallization exists, this is not normally noted in most published works and would in any case be very difficult to incorporate in actual practice, thus removing much of the simplicity, and hence the attraction of the method. By the simple considerations featuring in Table 2.1 integral  $n$  values are expected. Early works indeed have claimed such values, usually the value 3. However, subsequent accumulated experience has shown that nonintegral  $n$ s can be just as frequent. Lack of attention to secondary crystallization may well be responsible for these departures.

Finally, whatever information may be correctly obtained by the Avrami-type analysis it will leave unanswered the basic questions regarding the intimate fine structure of the crystallization. For this a direct attack on the structure is required.

## 2.5. Spherulites

Spherulites represent the highest level in the morphological hierarchy of a crystalline polymer. In the previous sections we treated crystallization in terms of formation and growth of spherulites readily identifiable in the optical microscope, and defined the resulting texture in terms of these spherulites. In this respect, spherulites are analogous to the grains in, say, a polycrystalline metal with the fundamental difference, however, that they themselves are not single crystals but a particular type of aggregate of crystals. A spherulite is usually defined as a birefringent object with spherical (circular in thin layers of material) symmetry (Figure 2.17). The

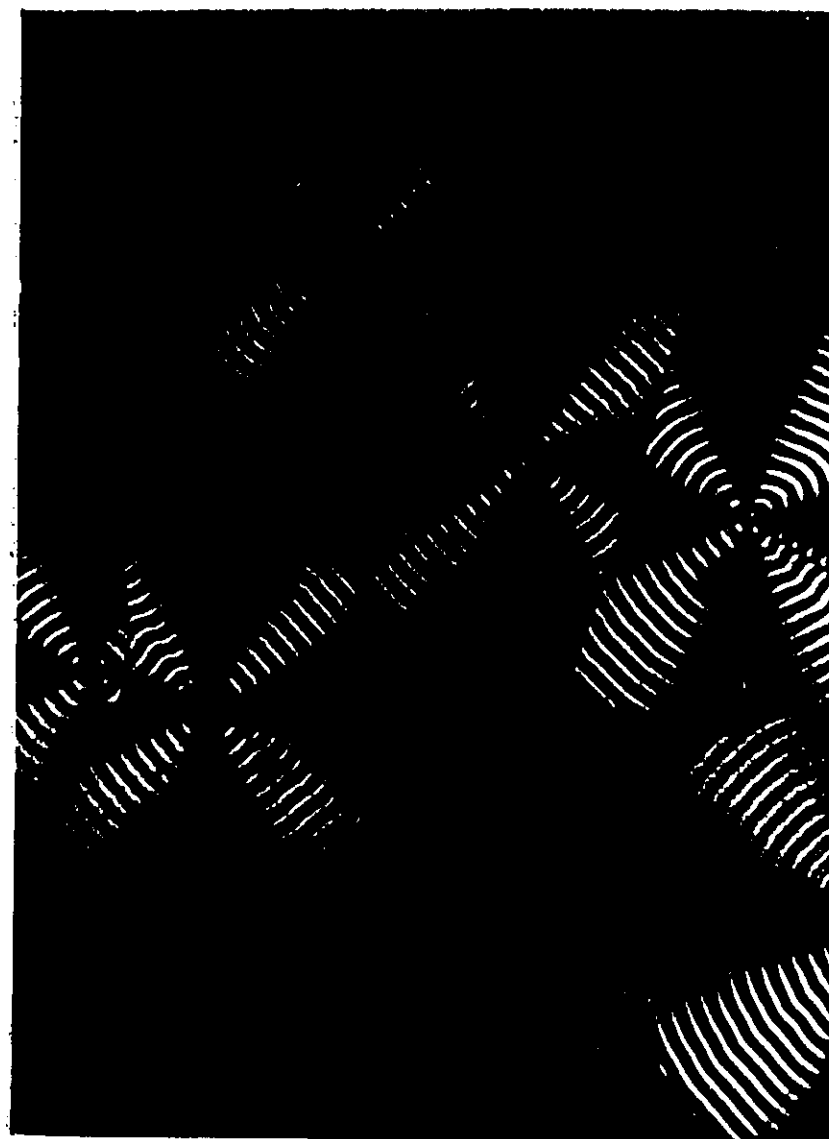


Figure 2.17. Photomicrograph of a particular spherulitic sample displaying spherulites in the process of impingement during growth. The spherulites are banded, corresponding to rotation of a biaxial crystal (Figure 2.20). The polymer is poly ( $\beta$ -hydroxybutyrate). Crossed polaroids (Barham *et al.*<sup>1977</sup>).



developed objects themselves are spheres (or circles in thin layers) as long as they are isolated. When they abut, they acquire polygonal outlines (see the examples in Figure 2.17), the internal spherical symmetry nevertheless being maintained.

In what follows we shall discuss the optical properties, and following this, the morphology.

### 2.5.1. Optical Properties of Spherulites

The optical characteristics are the foremost features of spherulites via which they are normally identified. Two principal features are usually observed when viewed between crossed polaroids in parallel light, and are readily visible in Figure 2.17: a dark Maltese cross and concentric dark banding. The former is practically always present and in fact forms part of the definition of spherulites, while the latter is usually, but not necessarily, associated with it.

#### 2.5.1.1. The Maltese Cross

The Maltese cross is parallel to the polarizer and analyzer directions, as in Figure 2.18. It arises from the spherically (or circularly) symmetrical arrangement of the index ellipsoid, which in turn corresponds to the anisotropic entity (crystal) constituting the spherulite as shown by Figure 2.18. The origin of the cross should be apparent: it is due to extinction arising wherever a transmission direction coincides with the direction of the polarizer or analyzer. The transmission directions themselves corres-

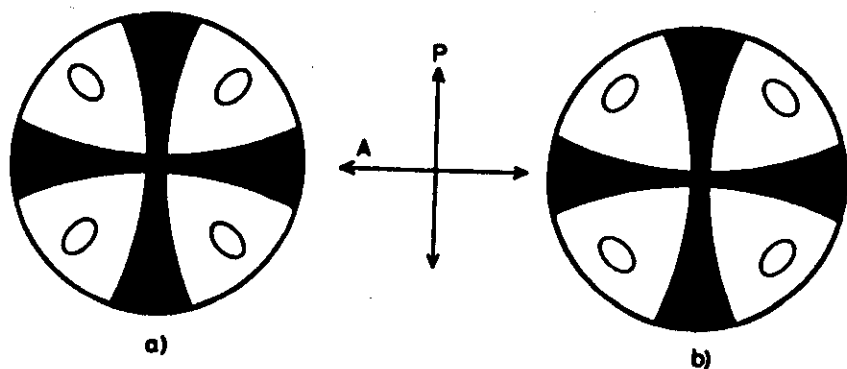


Figure 2.18. Illustration of the origin of the Maltese extinction cross in spherulites. Small ellipses represent appropriate sections of the index ellipsoids of the optically anisotropic constituents. (a) Direction of slow vibration is radial. (b) Direction of fast vibration is radial. P and A denote polarizer and analyzer directions.

pond to the long or short axes of the elliptical projections (in a plane perpendicular to the direction of viewing) of the index ellipsoids (Figure 2.18).

#### 2.5.1.2. Concentric Banding

This banding represents a periodicity in the orientation of the index ellipsoid (hence that of the underlying crystal) along any given spherulite radius, the periodically varying orientations along different radii being in phase at any given radial distance throughout the whole spherulite. The black bands arise through an optic axis becoming periodically parallel to the direction of viewing, when the birefringence is zero, hence complete extinction will arise at the corresponding locality. This implies that the birefringent units are rotated around a radial direction (while being simultaneously displaced radially) so that an optic axis is perpendicular to this radial direction. (This is usually the case but not always. An optic axis can also lie at an angle to the axis of rotation, in which case more complex periodic extinction effects result in the microscopic image.) If the crystal is uniaxial the dark bands will be equidistant (Figure 2.19). If the crystal is biaxial and the rotation axis (the spherulite radius) is normal to the optic axial plane, the banding will be constituted by two sets of nonequidistant

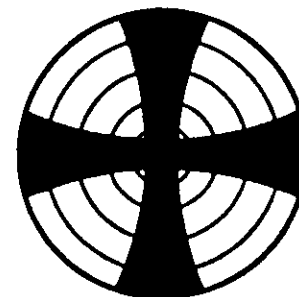


Figure 2.19. Sketch of banded spherulite with banding due to helicoidally varying orientation of a uniaxial crystal with optic axial direction perpendicular to the spherulite radius, which is the rotation axis.

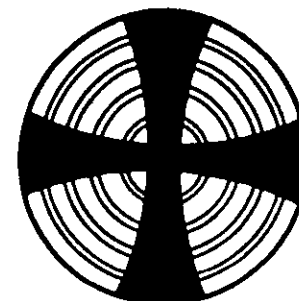


Figure 2.20. Sketch of banded spherulite with banding due to helicoidally varying orientation of a biaxial crystal with optic axial plane normal to the spherulite radius, which is the rotation axis. Alternating band spacings reflect the inequality of optic axial angles, narrow and wide spacings corresponding to acute and obtuse angles, respectively.

rings, where the relative ring separations correspond to the ratio of the optic axial angles (see textbooks on crystal optics; Figure 2.17). The micrograph in Figure 2.17 corresponds to such a situation.

The ultimate reason for the helicoidal arrangement of the index ellipsoids and of the underlying crystals, giving rise to the above concentric bandings, is not known and represents one of the major outstanding problems in polymer crystallization and beyond that in crystal growth. In the latter context it is most important to realize that the phenomenon is not confined to polymers. Virtually any crystallizable substance can display the effect. In fact, it was first identified in silicate minerals late in the 19th century followed by extensive studies of the phenomena in a descriptive manner, but virtually forgotten thereafter. While in small molecular substances the effect is regarded rather as a curiosity, in high polymers it is typical. Impurities are believed to be a requirement for both spherulites and the associated helicoidal crystal arrangements within them. As polymers are never absolutely pure (e.g., distribution of molecular lengths, lack of perfect tacticity, etc.) they are clearly candidates for this kind of crystal growth on that score. This is clearly a fruitful area for further research, but no clear direction of research is evident.

### 2.5.2. Morphology of Spherulites

The crystal texture and the underlying growth of a spherulite are always fibrous. Morphologically therefore they need to be visualized as a radiating array of fibrous crystals, which through appropriate branching will fill out spherical space. It follows that there must be a central discontinuity. The center could be a heterogeneity that nucleates fibrous crystals, which will thus grow out from it radially. Such uncoordinated radial growth does occur under certain circumstances and the resulting entity will display the Maltese cross, even if not the concentric bands. Such objects (Figure 2.21) nevertheless are not typical spherulites.

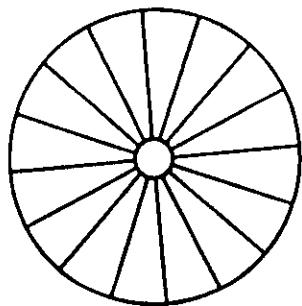


Figure 2.21. Sketch of a spherulite nucleated by heterogeneity. The radially growing fibrils are uncoordinated.

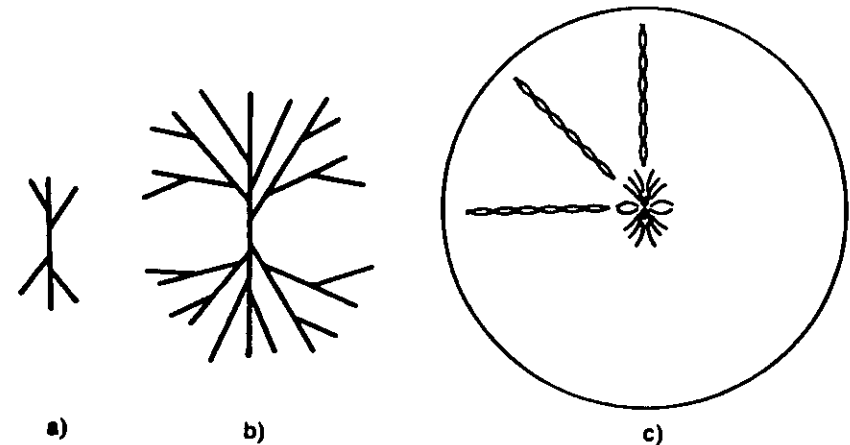


Figure 2.22. Development of a typical spherulite from a single-crystal nucleus: (a) branching fibrillar parent crystal; (b) developing sheaf; (c) final spherulite with sheaf-like origin recognizable in the center.

Typical spherulites develop through sheaving crystal growth of a single fibrous parent crystal, represented in two dimensions by Figure 2.22 (without any attempt to incorporate helicoidal winding in stages (a) and (b) of the sketch). When developed sufficiently, the sheaf will take on approximately spherical (circular in two dimensions) outlines. The first essential point to note is that here each point within the spherulite is generically related to the initial fiber situated in the center, hence also to all other fibers in the spherulite. Such a spherulite could therefore be regarded generically (even if not geometrically) as a single crystal, as opposed to the type of growth in Figure 2.21 where the different fibers are uncoordinated. The second point to note is the characteristic shape of the central discontinuity, namely double-leaf-shaped (or a corresponding three-dimensional form), by which this type of spherulitic growth is readily identified. If this double leaf is small compared to the final spherulite, it will hardly impair the spherical symmetry of the latter. If it is large it may even make unrecognizable the spherical symmetry, as manifest by the Maltese extinction cross. Whether the former or the latter applies, depends on the scale of the fibrosity relative to the final spherulite size, where the latter in turn depends on the nucleation density.

The above distinction leads to two types of definition of spherulitic structure:

1. Polarizing optical definition: This is the historical definition quoted at the commencement of this section and relies on an identifiable Maltese cross.

## 2. Morphological definition: This is based on the sheaf development, as in Figure 2.22.

It is noteworthy that a sample can be "spherulitic" by (2) without displaying the optical effects in (1) (e.g., the sheaves have not been given the chance to develop into spheres). This is often a source of confusion in the literature as to whether a given sample crystallizes in a spherulitic or some other mode. Definition (2) is more general and appropriate, even if historically the subject owes its existence to definition (1) by which the spherulitic crystallization was first identified.

If we superpose helicoidal windings onto the fibrils, as in Figure 2.22c, three-dimensional space filling creates additional topological problems so far unsolved. (One is tempted to compare this situation with droplets of cholesteric liquid crystals formed by appropriate simple substances, which display both a Maltese cross and periodic banding, the origin of the latter being fully understood. However, liquid crystal drops are low-energy equilibrium shapes (without any internal fibrous texture) while crystalline spherulites result from a particular mode of fibrous crystal growth, the resulting entities being far from equilibrium. Hence the topological arguments for the liquid-crystal case cannot be simply transferred.)

As regards the origin of spherulitic growth a particular quantifiable scheme is finding widespread acceptance, according to which fibrous growth develops due to impurities causing constitutional supercooling, analogous to cellular growth in metals [H. D. Keith and F. J. Padden, *J. Appl. Phys.* 34, 2406 (1963)]. To this should be added a noncrystallographic branching scheme (for which there is no *a priori* reason, even less so for the helicoidal winding when the latter is present). One advantage of the scheme, however, is that it defines the scale of the fibrosity in terms of assessable parameters, namely the diffusion coefficient of the crystallizing molecule  $D$  and the linear growth rate  $G$ . Accordingly, the scale of the fibrosity should be defined by  $D/G$ . There are differing views and experimental results regarding the appropriateness of the ratio  $D/G$  for characterizing the intraspherulitic texture. The most recent fine structure results [D. C. Bassett and A. M. Hodge, *Proc. R. Soc. London, Ser. A* 377, 25, 39, and 61 (1981)] in fact explicitly refute the expected correspondence between  $D/G$  and the dimension of the relevant structure element, with corresponding implications for the underlying theoretical scheme.

### 2.5.3. The Fine Structure of Spherulites

Spherulites are highly organized crystal aggregates and are so compact that they do not yield readily to a direct attack on their finer architecture. In particular, questions as to both the basic crystal units constituting them

and their mode of space filling are not readily answered by their continued direct examination. However, in polymers, we know through an indirect approach (see later) that the basic crystalline entities constituting the spherulite are ribbonlike lamellae (see, e.g., Figure 3.19 in the next chapter). It is very plausible therefore to visualize a radial entity within a spherulite as a continuous helicoidally twisting ribbon sprouting branches so as to occupy spherical space, as implied by Figure 2.22. However, such a continuous helicoidal path along a given ribbon has not yet been followed through morphologically (examinations are necessarily confined to fracture surfaces, usually etched so as to provide a relief); this deficiency is to be contrasted with the unassailable polarizing optical evidence of a continuous and periodic orientation variation of the index ellipsoid. There are running disputes in the literature on the explicit morphological realization of these orientation variations owing to the above-mentioned missing morphological information.

Whatever the explanation for spherulites and the banding within them, it must have general validity for crystallization and cannot be restricted to polymers alone. For polymers certainly, some specific features need considering, such as the lamellar ribbon-shaped basic crystal entity, and the fact that (as observed by micro-X-ray work not to be elaborated here) the overall direction of the chain molecules is perpendicular to the spherulite radius.

Even though so many features about spherulites are unknown, their study has served many useful purposes toward understanding and describing polymer crystallization. Thus their number in a given sample is an indicator of nucleation in polymer melts and their rate of radial growth ( $G$ , which as noted earlier is a constant at a given temperature) provides a measure of crystal growth, both of these quantities having served a useful purpose in the analyses presented in Section 2.4.6. In addition,  $G$  can be measured as a function of supercooling  $\Delta T$ : it has been found that

$$G \propto e^{-Q/\Delta T} \quad (2.4)$$

where  $Q$  is a constant to be specified later. This relation suggests that the growth-rate-determining factor is secondary (i.e., surface) nucleation along the growing crystal front, a long-standing observation the significance of which will become apparent later.



446

# The Basic Crystal Unit

A. Keller

## 3.1. Single-Crystal Lamella

Historically, the basic crystal entity was observed on crystallization from solution, primarily because in the dilute system the basic entities could be obtained in isolation, in contrast to crystallization from the melt, where the individual crystal entities are intimately interlocked and thus escape identification by straightforward inspection. It has taken many years of subsequent development until the same entities, which were already familiar from solution crystallization, could be identified also in the bulk melt-crystallized product where they are usually components of more complex aggregates (such as sheaves or spherulites).

### 3.1.1. Discovery and Description

The polymer, polyethylene in the first instance, was dissolved in hot solvent and then precipitated by cooling. The crystalline precipitate formed a turbid suspension where the suspended particles could be examined by optical (phase or interference contrast) and electron microscopy after sedimentation on suitable support. The particles proved to be lamellae with well-defined crystallographic facets usually forming lozenges or various truncated versions of them (Figure 3.14, more exactly depending on the crystallization temperature. The crystal increases its overall thickness via the familiar spiral terrace screw dislocation growth mechanism. The thickness of the individual layers, as readily assessed in the micrographs

---

A. Keller · Department of Physics, University of Bristol, England.

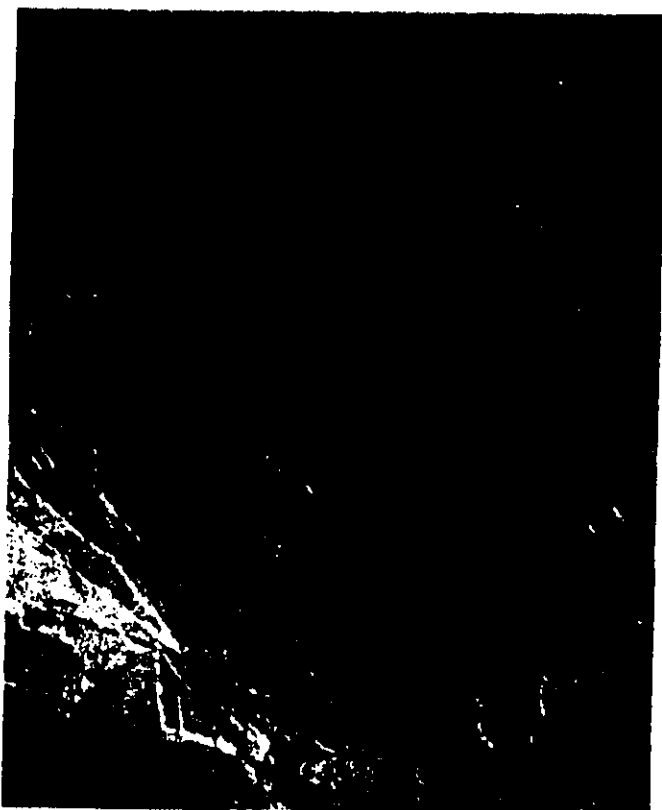
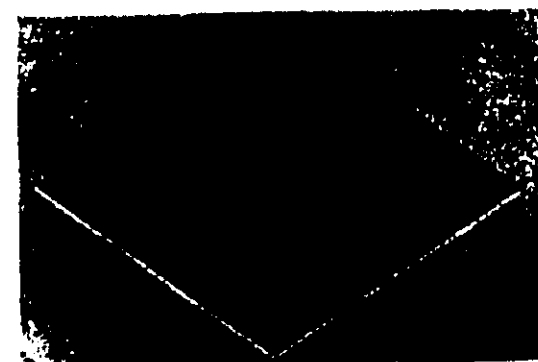


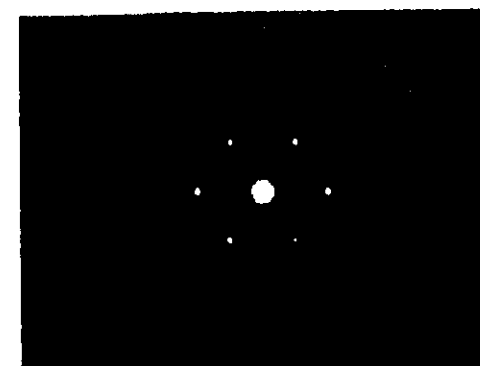
Figure 3.1. Electron micrograph of a typical solution-grown single crystal of polyethylene (after Keller<sup>10</sup>).

themselves by the shadow length of suitably metal-shadowed specimens, was in the 100 Å range.

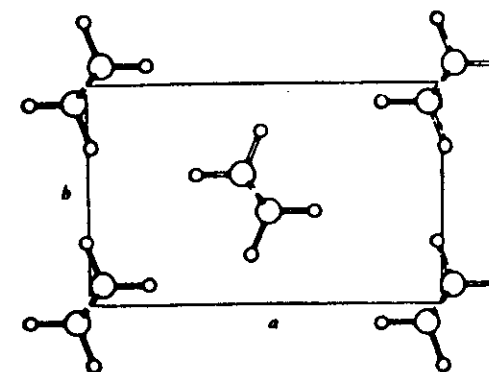
Electron diffraction confirmed the single-crystal nature of the object (Figure 3.2) and identified the lattice orientation with respect to external morphology (Figure 3.2a, c). It is seen from Figure 3.2c that the chains (the  $c$  direction) are perpendicular to the lamellar plane: in some instances they can also lie at a specific large angle (around  $60^\circ$ ) to the lamellar surface. The prism faces of the lamellae can also be readily assigned; for the specific case of polyethylene in Figure 3.2 this is {110}. While the present illustration is for polyethylene, the situation is analogous for all other flexible polymers, namely the crystals are lamellae, which for different



a)



b)



c)

Figure 3.2. (a) Electron micrograph of a monolayer crystal of polyethylene (after Keller and Organ). (b) Corresponding electron diffraction pattern (after Keller and Organ). (c) Lattice orientation with unit cell in  $c$  projection corresponding to (a) and (b). It follows that the chain direction is perpendicular to the lamellar surface.

polymers will follow different external habit patterns with the chain direction always perpendicular (or at a specified large angle) to the lamellar surface.

### 3.1.2. The Chain-Folding Model

At this point it should be noted that the chains are long, say  $10^3$ – $10^4$  Å, and are of nonuniform length in a given material. The following problem arises: how can such chains be perpendicular to layers the thickness of which ( $\sim 10^2$  Å) is much less than the length of the chains, and be of uniform thickness? The answer is that the chains must fold back on themselves at regular intervals (as illustrated in Figure 3.3), the lattice register within the crystal, i.e., between the fold stems, being retained (as mentioned earlier in connection with Figure 2.1b). This is the argument on which the existence of chain folding is based. It is a nonmathematical commonsense argument, altogether convincing and irrefutable in its essentials. Any arguments about it (and, as we shall see, there are many) relate to the nature of the folding (see later) and not to its existence! (There are unfortunately several misleading popularizations to do with these controversies of which the reader is duly forewarned.) In particular, the neatness of the folding and the strictly adjacent deposition of the stems as expressed in Figure 3.3 are subject to debate. Nevertheless the representation in Figure 3.3 will be used in order to develop more readily some of the arguments to follow.

It is worth recalling the total unexpectedness of the developments just outlined. The findings are unexpected because (1) the basic crystal units

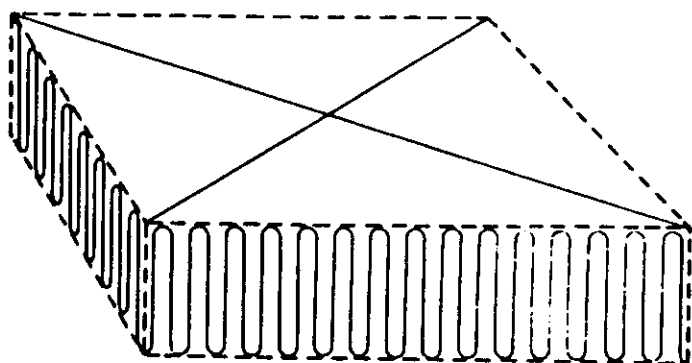


Figure 3.3. Schematic illustration of a chain-folded crystal structure to account for evidence in Figure 3.2.

turned out to be lamellae instead of fibrils, which might have been anticipated from long chains, and (2) the chains are along the shortest (not the longest!) crystal direction, a fact that leads directly to the model of chain folding.

Let us consider the unprecedented situation these crystals create in the study of crystals in general. In such a situation we have an external habit feature, the lamellar thickness  $l$ , which corresponds to a molecular structure feature, the fold length. Hence the descriptive study of external shape and size (morphology) and that of internal fine structure on a molecular level (traditional "crystal structure analysis") merge into a more generalized investigation of the total crystal structure.

The fold length  $l$ , as we have seen, has both morphological and molecular significance so we shall concentrate on its measurement, behavior, and interpretation in what follows.

### 3.1.3. Fold Length $l$

Various questions arise: Is the fold length invariant or variable? In either case what are the factors determining it? How is chain folding to be accounted for in terms of molecular behavior? First, however, we must clarify the methods of measuring  $l$ .

#### 3.1.3.1. Methods of Measurement

There are essentially three methods:

1. Electron Microscopy (EM). This technique relies on the measurement of the shadow length of appropriately metal-shadowed samples on the electron micrographs themselves.
2. Small-Angle X-Ray Diffraction (SAX). The crystals that precipitate as a suspension can be sedimented into coherent macroscopic sheets, so-called mats, which contain the lamellae in an overall parallel orientation. Such a mat of layers acts as a one-dimensional grating to X-rays falling on it edgewise, giving rise to X-ray diffraction maxima in accordance with Bragg's law ( $l = \lambda / 2 \sin \theta$ , where  $\lambda$  is wavelength and  $2\theta$  scattering angle). As the layer periodicity is large (100 Å and more) the diffraction angle is small, hence the diffraction maxima are observed at small angles requiring appropriate collimation techniques. This is the most widely used method, the lamellar thickness thus obtained often referred to as "long spacing."

<sup>1</sup> It should be noted that chain folding is superposed onto the primary chain conformation. For instance, if the primary conformation is helical, such as in polyolefins (Figure 2.8), then the whole helical chain itself folds.

3. Low-Frequency Raman Spectroscopy (referred to as LAM, longitudinal accordion (or acoustic) mode). This method is comparatively recent and has its origin in the longitudinal accordion-type vibration of the straight stems with nodes in the center and antinodes at the lamellae surfaces (Figure 3.4). If the vibrating stems are approximated by straight rigid rods, the fundamental Raman frequency  $\nu$  is given by

$$\nu = \frac{1}{2l} \sqrt{\frac{E}{\rho}} \quad \text{hence} \quad l = \frac{1}{2\nu} \sqrt{\frac{E}{\rho}} \quad (3.1)$$

where  $E$  is the modulus (force constant in molecular terms) and  $\rho$  the density. While more elaborate expressions than the simple approximation of equation (3.1) have been derived, this equation describes adequately what is required for most purposes. It follows that for large  $l$ ,  $\nu$  will assume very small wave numbers, hence very high degree of monochromatization is required in the experimentation so as to detect peaks close to the exciting frequency.

### 3.1.3.2. Comparison of Methods

1. EM. Advantages: qualitatively, it shows in real space what the entities actually are, all-important information not directly obtainable by

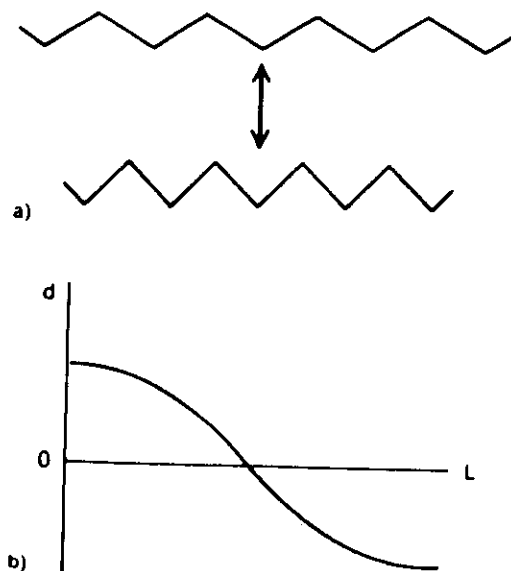


Figure 3.4. Origin of the low-frequency longitudinal accordion-type Raman band (LAM). (a) Accordion-type vibration of the chain. (b) Corresponding longitudinal total displacement ( $d$ ) along the vibrating chain with origin at  $L = 0$ .

### 3 • The Basic Crystal Unit

any other method (e.g., without EM we would never know that we have lamellae!), and quantitatively, it measures the layer thickness directly and at the localities of potential interest. One disadvantage is that information derived pertains to a very small fraction of the material and thus may not be representative; also accuracy is limited.

2. SAX and 3. LAM. An advantage is that the information is representative of the whole or of large portions of the sample, and can thus be used for systematic quantitative work and hence to lay the foundation for theories. A disadvantage is that these methods are not self-contained but require EM [method (1) above] for knowledge of what the units are which actually produce the SAX and LAM effects. Hence the message is clear: the combination of *all* techniques is essential!

There are various distinctions between SAX and LAM. SAX relies on interference effects due to a periodic structure, hence on the existence of a periodicity (in addition to the existence of the layers as such). Such a periodicity is produced by the regular stacking of lamellae, which accordingly is a prerequisite for the application of SAX, at least in the present simplest form utilizing Bragg's law. In contrast, LAM relies only on the existence of the individual layers as such. This can be important, e.g., in cases where we have a mixture of lamellar thicknesses. Here complicated, smoothed-out interference effects result by SAX, while the LAM effect may remain clear, giving rise to separate Raman peaks corresponding to each lamellar thickness in the mixture.

SAX gives the total interlayer periodicity (stem plus fold; plus interlayer gap, if any) while LAM is expected to depend primarily on the stem length only. Hence in LAM we have a potential tool to distinguish between crystal core and fold surface — a topical issue (see later). However, efforts in this direction have encountered considerable difficulties, insofar as LAM, by equation (3.1), usually gives the same value for  $l$  as does SAX by Bragg's law. At present this is an open problem, which invites further in-depth theoretical considerations.

SAX (and recently LAM) effects in the form of discrete peaks have been observed also in melt-crystallized bulk polymers even when lamellae could not be directly, or at least readily, observed by EM. By analogy with solution-grown crystals, such effects are nevertheless being interpreted in terms of lamellar thickness and fold length. Indeed, such "jumps" in the argumentation proved to be justified in most cases when bulk samples became accessible to EM experimentation through later improvement in techniques. Even so a certain caution is advised in the indiscriminate identification of SAX maxima and LAM peaks with lamellar thickness in the absence of explicit EM evidence. Examples prompting this statement exist, but will not be elaborated here.



While applying methods (1)–(3) above, it was observed that the fold length  $l$  is not invariant but is affected by the temperature of crystallization  $T_c$ , and by the temperature of heat treatment subsequent to crystallization, i.e., heat annealing  $T_A$ , where  $T_A > T_c$ .

a. *Temperature of Crystallization.* At the first level of experimentation  $l$  vs  $T_c$  curves, such as those in Figure 3.5, were obtained with polyethylene. Accordingly higher  $T_c$  values yield higher values of  $l$ , increasingly so toward higher  $T_c$ . Figure 3.5 shows two curves, one from a poorer solvent (octane) the other from a better solvent. The identical  $l$  values for different  $T_c$  values along the two curves, i.e., the horizontal shift of the two curves by an approximately constant factor, means that it is not the absolute  $T_c$  but the supercooling  $\Delta T = T_m^0 - T_c$  that is the factor determining  $l$  (where  $T_m^0$  is the dissolution point of the infinitely extended chain crystal or the melting point for melt crystallization). For a poorer solvent  $T_m^0$  is higher, hence the same  $T_c$  corresponds to smaller  $\Delta T$ .

The following important additional observation should be added to the findings expressed by Figure 3.5. If  $T_c$  (or  $\Delta T$ ) is being changed during crystal growth, the crystal continues to grow with an altered  $l$  appropriate to the new  $T_c$ , or  $\Delta T$ , as expressed by Figure 3.5. Morphologically, this will be apparent by a step in the crystal lamella concentric with the crystal boundaries, where the crystal has become thinner or thicker according to whether  $\Delta T$  has been decreased or increased, respectively. This means that the fold length is only affected by  $\Delta T$  but remains unaffected by the thickness of the substrate onto which the molecule deposits.

Curves such as those in Figure 3.5 have formed the basis of all theories until recently. In subsequent developments, suitable choice of polymers (other than polyethylene, e.g., isotactic polystyrene) have enabled higher

values of  $\Delta T$  to be attained for such  $l$  vs  $T_c$  studies. The results now extending over a much wider range of  $T_c$  (hence  $\Delta T$ ) values are expressed schematically by Figure 3.6, which can be taken as the general  $l$  vs  $T_c$  relationship as known today. It is characterized by the same behavior as in Figure 3.5 for comparatively small supercoolings (high  $T_c$ ) followed by a horizontal plateau at high  $\Delta T$  (low  $T_c$ ), i.e., at high values of  $\Delta T$   $l$  becomes insensitive to the temperature of crystallization.

The last feature was not included in the original formulation of the crystallization theories. Subsequent adaptation of theories to incorporate the horizontal portion of the  $l$  vs  $T_c$  curves is a subject of topical interest (see later).

b. *The Annealing Phenomenon ( $T_A$ ).* First we make the following observation: When a crystal is heated beyond  $T_c$ , the temperature of its formation, it thickens irreversibly ( $l$  increases according to all methods of assessment) without any change in the overall lattice, in particular the chain orientation.

Subsequent interpretation leads to the inescapable fact that the chains have refolded in order to give rise to a new increased fold length, represented schematically (with the provisos expressed in connection with Figure 3.3) by Figure 3.7.

This extraordinary chain-refolding effect underlies all annealing behavior of crystalline polymers, including heat treatment in technological practice. It raises many questions and touches on many issues (not to be treated further in the present review), including the mechanism of refolding; the kinetics of refolding; the issue of chain mobility, particularly in the

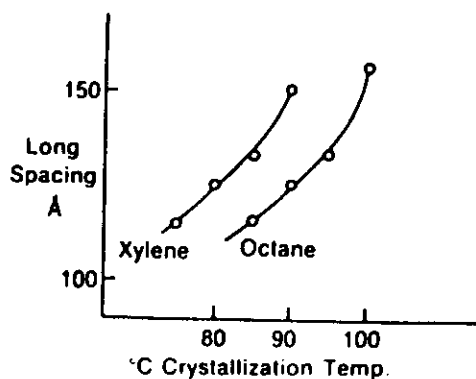


Figure 3.5. Crystal thickness ("long spacing" as measured by small-angle X-ray diffraction) as a function of crystallization temperature in polyethylene single crystals grown from two different solvents (xylene, octane) (after Kawai and Keller<sup>11</sup>).

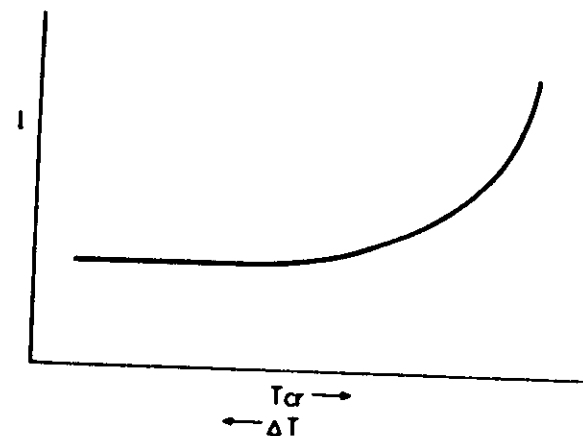


Figure 3.6. Fold length vs crystallization temperature over a very large range of supercoolings ( $\Delta T$ ) in case of crystallizations from solution (a combination of behavior observed for polyethylene and isotactic polystyrene).

solid state; the issue of full or partial melting followed by recrystallization, as opposed to pure solid-state transformation with the chain threading through the crystal.

The range of  $l$  values achievable by refolding can be very large: from the initial  $\sim 100$  Å it can attain several thousand angstroms, particularly when hydrostatic pressure is applied. For polyethylene, the normally realized upper limit by standard heat treatments on a laboratory time scale is approximately 600 Å.

c. *Isothermal Thickening.* It was recognized early that under certain circumstances a crystal can thicken even while it is growing isothermally, i.e., crystals form with a particular  $l$ , and then this  $l$  increases while the edges of the crystal are continuing to grow and incorporate more, still uncrystallized material. Thus older crystals, or crystal portions, will be thicker than the younger ones in such isothermally crystallized material. So far this effect has only been observed in melt crystallization, and I personally believe this is a consequence of the fact that here  $T_\alpha$  (absolute) is higher than in the case of crystallization from solution. This phenomenon has a very important role in current developments, both as regards knowledge of what is the primary  $l$  value of the crystal as formed, and as regards the detailed fold structure of the crystal still unaffected by subsequent refolding. Further, isothermal thickening is the principal source of "secondary crystallization," i.e., the perfectioning of the crystals during crystallization, a concept that has featured in the earlier chapter dealing with crystallization kinetics.

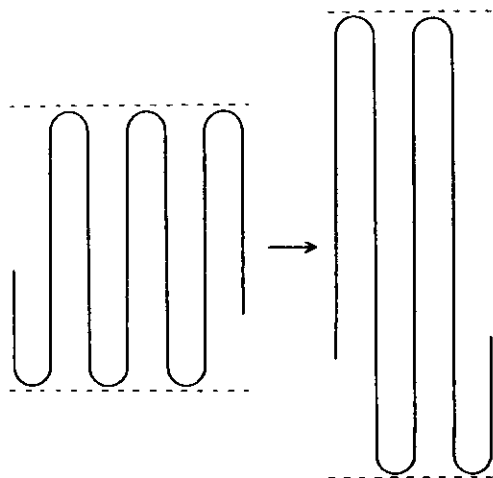


Figure 3.7. Schematic illustration of chain refolding to yield greater fold length as induced by heat annealing of single crystals.

### 3.2. Theories of Chain Folding

A theory with any claim of validity would have to provide answers to the following questions: (1) Why chain folding? (2) Why uniform fold length? (3) Why the observed dependence of  $l$  on  $\Delta T$  as expressed by Figure 3.5 (when the theories were first postulated the full  $l$  vs  $T_c$  dependence in Figure 3.6 was not yet known) together with the observation that  $l$  remains uninfluenced by a preexisting substrate? (4) Why the observed irreversible fold-length increase on annealing?

Initially theories were pursued along two lines:

- I. *Equilibrium Approach.* In this approach, the crystallization occurs by chain folding because the folded chain corresponds to the state of lowest free energy and hence is thermodynamically in the stablest form. Hence reversibility of  $l$  with temperature would be expected, but was never observed. Even if excuses for the latter were found, this class of theories, while not actually disproved, never made their mark on the subject and are at present only of historical interest.
- II. *Kinetic Approach.* Here it is the fully extended chain crystal that has the lowest free energy. Nevertheless the chains crystallize by folding because in this way crystallization is most rapid. Thus chain folding is due to kinetic reasons, and the resulting crystals are not in their stablest state but will tend toward it whenever they have a chance, e.g., on subsequent heating. The latter immediately explains the trend toward high  $l$  values on heat annealing. From now on we shall be concerned with this class of theories only.

#### 3.2.1. Framework of the Kinetic Theories

##### 3.2.1.1. The Basic Scheme

First we invoke the basic fact that  $l$  is not influenced by a preexisting substrate. This means that as long as we are only concerned with accounting for  $l$ , we can ignore primary nucleation and consider crystal growth only, i.e., we consider the deposition of chains along a preexisting substrate of any thickness. For simplicity one may take this thickness as infinite.

We shall therefore consider the deposition of a chain along an infinitely thick crystal face of the polymer. In the first stage the chain is regarded as infinitely long (so that chain ends will not matter) and the system as dilute, so that a given chain can deposit unimpeded by others. Further, and this is most important, it should be remembered that the

system is supercooled, ( $T_c < T_m^0$ ). Pictorially the deposition is represented by Figure 3.8, and the reaction path by Figure 3.9 where  $\phi$  is the free energy and  $n$  the number of depositing chain atoms.

Now let us consider deposition of the first straight stem  $P-Q$ . This will be associated with an increase in  $\phi$  due to the creation of new surfaces. (For simplicity the pathway  $P-Q$ , etc., is drawn as a straight line in Figure 3.9; the finer-scale representation, embodying discontinuities corresponding to the deposition of successive individual chain members, is ignored.) Thus the continuing deposition of this straight segment will lead to an increasingly less stable state. If at some point  $Q$  the chain happens to fold back on itself (such as  $Q-R$ ), for which there is a finite statistical

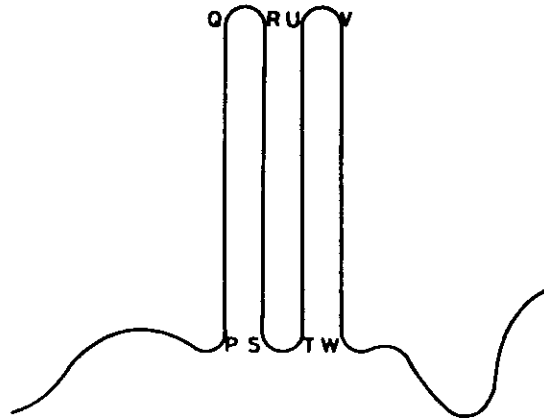


Figure 3.8. Folding scheme of a chain depositing along a crystal face of infinite thickness (not shown).

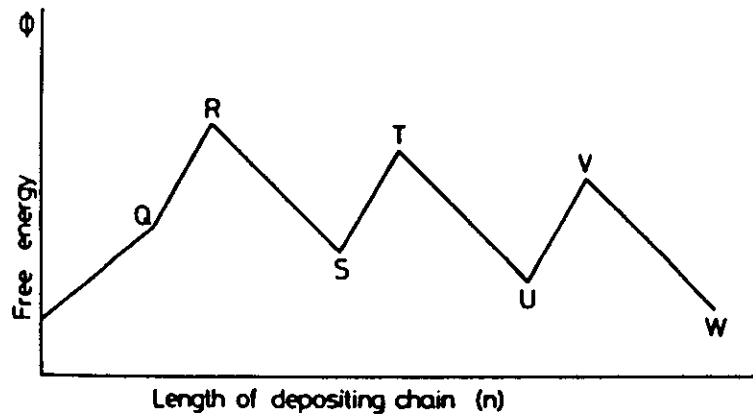


Figure 3.9. Free-energy pathway corresponding to chain deposition in Figure 3.8.

probability,  $\phi$  increases sharply ( $Q-R$  in Figure 3.9). However, after completion of the fold, continuing deposition  $R-S$  will cover up newly created surface while creating more crystal. Consequently  $\phi$  decreases. Further deposition would create new surface again, hence raise  $\phi$ , but if the chain subsequently folds ( $S-T$ ) then after a sharp initial rise ( $S-T$  in Figure 3.9)  $\phi$  will drop again during continuing deposition ( $T-U$ ), and so on. As long as  $\phi$  decreases successively for stages  $Q, S, U, W$ , etc., continuing folding will increase the stability of the new chain-folded patch along the preexisting crystal face until it becomes a stable critical nucleus with  $\phi$  lower than in the starting state, and the crystal will be capable of continuing growth. (It is noteworthy that the critical nucleus just mentioned corresponds to a secondary growth nucleus along a completely smooth crystal face in growth theories of conventional crystals.)

It will be seen that a plausible model is provided to explain why folding occurs in the first place. The next question is why this should lead to a predominant fold length. In broad outlines this can be seen as follows:

If  $P-Q$  (hence the first segment) is long, namely  $l$  is large, there is a high increase in  $\phi$ , hence the attachment probability of such a segment will decrease with its length. However, once the chain folds over there will be a larger decrease in  $\phi$  on steps  $R-S, T-U$ , etc., for a long initial segment  $P-Q$ , hence the detachment probability of such a longer folded-over segment will be lower. For a shorter initial length  $l$  (short  $P-Q$ ) the probability of the first-segment attachment will be higher, but so will be the probability of detachment after the chain has folded over ( $R-S, T-U$ , etc.). With two opposing trends there will exist a most probable fold length ( $l^*$ ) optimizing the resultant of the corresponding attachment and detachment rates. The purpose of the detailed theories is to calculate this value of  $l^*$ .

Mathematically, the first steps of this process are as follows: Consider each stem as a prism-shaped box of length  $l$ , width  $a$ , and thickness  $b$  (Figure 3.10). Let the side surface energy be  $\sigma$ , the end surface energy (that of the fold surface) be  $\sigma_e$ , where  $\sigma \ll \sigma_e$ , and suppose  $\Delta f$  is the change of free energy involved in creating unit volume of crystal. The net free-energy change  $\Delta\phi$  on depositing the first segment  $l$  is then given by

$$\Delta\phi = 2b\sigma l + 2ab\sigma_e - abl\Delta f \quad (3.2)$$

where the first two terms on the right-hand side represent the work involved in creating the new side and end surfaces, respectively, while the third term is the free-energy change in creating the corresponding volume of crystal. Clearly, the formation of surfaces increases the free energy of the system while the formation of a volume of crystal (in the supercooled state) decreases it. For a ribbon to become stable the volume term (namely  $abl\Delta f$ ) must exceed the sum of the surface terms.

Now side surface is produced by the first segment only; subsequent segments cover up as much surface as they have produced. Thus continuing segment deposition will create new end surface only, plus new crystal. The limiting condition for segment deposition to proceed is that the newly formed lattice must at least compensate for the creation of the new end surface, i.e.,

$$abl_{\min}\Delta f = 2ab\sigma_e$$

hence

$$l_{\min} = 2\sigma_e/\Delta f \quad (3.3)$$

where  $l_{\min}$  is the lowest stable stem length.

Conditions for stability are represented schematically in Figure 3.11, where the spikes in Figure 3.9 have been smoothed out and the lines connect points Q, S, U, V, etc. For  $l = l_{\min}$  there is no gain in stability as  $n$  increases, i.e., as the crystal grows, consequently there will be no driving force for growth. In the case  $l < l_{\min}$  continuous growth will increase the free energy of the system, hence growth will not occur *a fortiori*. It follows that, for finite growth rate,  $l$  must be larger than the critical length ( $l_{\min}$ ).

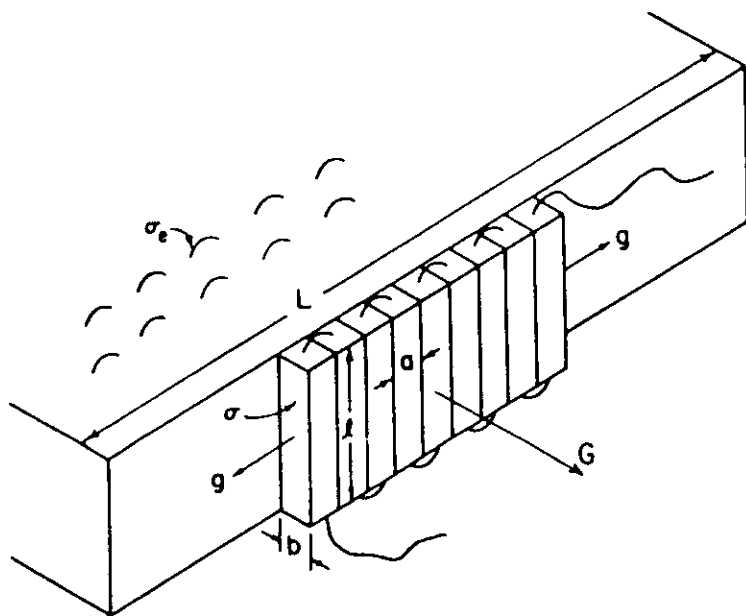


Figure 3.10. Crystal strip depositing along the prism face of a crystal with spreading rate  $g$  resulting in an advance rate  $G$  of the crystal face (after Hoffman *et al.*<sup>(10)</sup>).

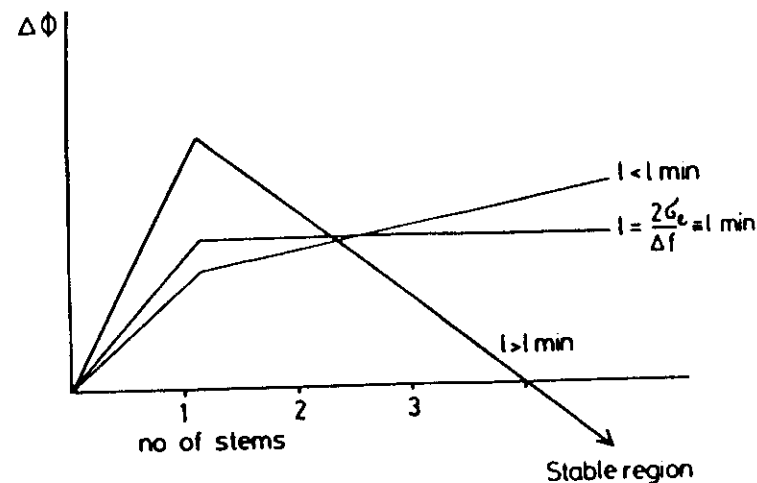


Figure 3.11. Simplified free energy pathway for chain deposition showing existence of a limiting lowest fold length ( $l_{\min}$ ).

Next we derive an expression for  $\Delta f$ . By definition  $\Delta f = \Delta H - T\Delta S$ , where  $\Delta H$  is heat of fusion and  $\Delta S$  entropy of fusion. In case of equilibrium (i.e., at the melting or dissolution point  $T_m^0$ )  $\Delta f = 0$ , hence  $\Delta S = \Delta H/T_m^0$ . If  $\Delta S$  is assumed to remain unchanged for a particular supercooling corresponding to  $T < T_m^0$  we have

$$\Delta f = \frac{\Delta H \cdot \Delta T}{T_m^0} \quad (3.4)$$

where  $\Delta T = T_m^0 - T$ .

If expression (3.4) is inserted into (3.3) for  $l_{\min}$ , we derive

$$l_{\min} = \frac{2\sigma_e T_m^0}{\Delta H \cdot \Delta T} \quad (3.5)$$

### 3.2.1.2. Assumptions

The theories assume that secondary nucleation along an otherwise flat lateral crystal surface is the rate-determining step in the growth of the crystal and proceed to show that this growth is maximum for one particular fold length  $l^*$ . In the first stages of the theories the nucleation of a surface strip itself (at a rate  $i$ ) determines the crystal growth rate  $G$ : once a strip is nucleated it will spread along the full face (or a specific portion of it) at a rate  $g$  where  $i \ll g$ , so that  $G \propto i$  (see Figure 3.10). (In later stages of the theory this mode of growth was denoted as Regime I, pertaining to low

supercoolings — see below.) Here the pertinent value of  $l$  is that for which  $G$  is fastest.

In the very first versions the spread of  $l$  values in the distribution calculated was regarded as corresponding to separate crystals with different  $l$ s, in each of which there was a maximum population with  $l^*$ . Subsequently it was assumed that there exists a distribution of  $l$ s within a given crystal, the value  $l^*$  pertaining to the maximum number. This implies that  $l$  can vary (within certain limits) as a strip deposits. Accordingly, such theories incorporate fluctuations in  $l$  during deposition. It was by no means obvious that fluctuations, once permitted, would converge, which is required if the theory is to explain the facts. Such a convergence could in fact be demonstrated within the framework of the theories [F. C. Frank and M. Tosi, *Proc. R. Soc. London, Ser. A* 263, 323 (1961); also the review by J. D. Hoffman, G. T. Davis and J. I. Lauritzen, in: *Treatise on Solid State Chemistry* (N. B. Hannay, ed.), Vol. 3, Chapter 6, Plenum Press, New York (1976)]. As a consequence it does not matter whether one starts from a thicker or thinner substrate layer:  $l$  will always converge to the same  $l^*$ , as required by the experimental findings.

### 3.2.1.3. Most Probable Fold Length

The main part of the theories is to find a steady-state expression for the flux  $S$  over the barrier of nucleation in terms of  $A_n$  (the rate constant for deposition of the first stem),  $B_1$  (that of the corresponding backward reaction),  $A$  (rate of deposition of all subsequent stems), and  $B$  (that of the corresponding backward steps). In the notation of Hoffman and Lauritzen (see review by Hoffman, Davis, and Lauritzen quoted above) we have (corresponding to the pathway in Figure 3.12; see also later):

$$A_n = \beta \exp \left( -\frac{2b\sigma}{kT} + \frac{4abl\Delta f}{kT} \right) \quad (3.6)$$

$$B_1 = \beta \exp \left[ -\frac{(1-\psi)abl\Delta f}{kT} \right] \quad (3.7)$$

$$A = \beta \exp \left( -\frac{2ab\sigma_e}{kT} + \frac{\psi abl\Delta f}{kT} \right) \quad (3.8)$$

$$B = \beta \exp \left[ -\frac{(1-\psi)abl\Delta f}{kT} \right] \quad (3.9)$$

Here  $\beta$  is essentially a retardation factor that contains the transport terms, incorporating effects like those resulting from viscosity and surface transport, geometric factors, etc.;  $\psi$  is an apportioning factor, which apportions the change in volume free energy  $\Delta f$  between the forward reactions ( $\psi$ )

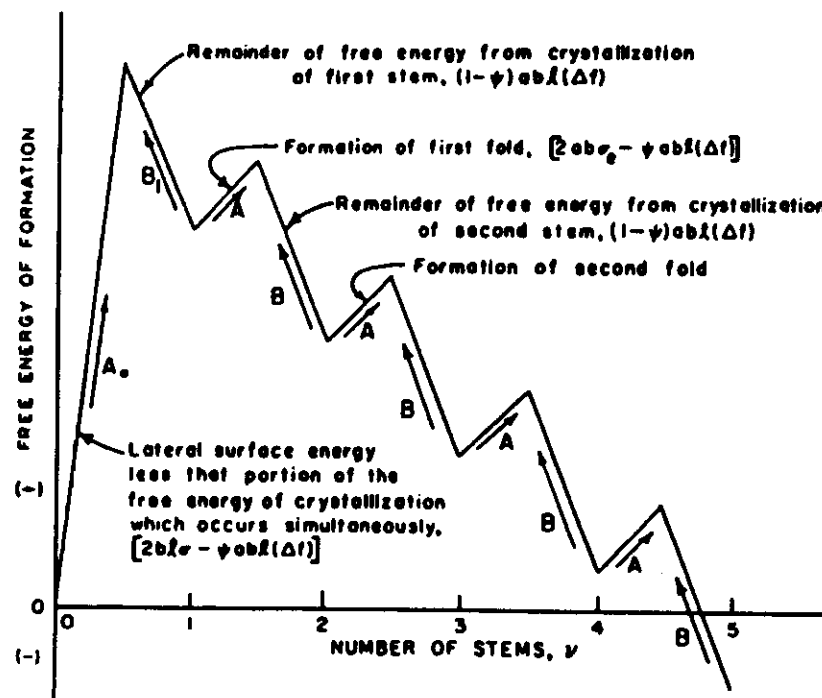


Figure 3.12. Free-energy pathway for chain deposition incorporating a factor  $\psi < 1$  (after Hoffman *et al.*<sup>20</sup>).

and backward reactions  $(1-\psi)$  (see Figure 3.12). (Thus the monotonic increase in  $\psi$  on depositing the first segment in Figure 3.9, i.e., along  $P-Q$ , corresponds to  $\psi = 1$ ; see later.)

Theory shows that for steady-state flux

$$S(l) = N_n A_n (A - B) / (A - B + B_1)$$

The total flux  $S_t$  is obtained by summing the fluxes over all  $l$ .

Of special interest is the mean lamellar thickness, which should be the observed  $l^*$ . In this case one forms the expression  $\int l S(l) dl / \int S(l) dl$ . The result of the calculation is

$$l^* = \frac{2\sigma_e}{\Delta f} + \delta l \quad (3.10)$$

which, on substitution for  $\Delta f$  [by equation (3.4)], becomes

$$l^* = \frac{2\sigma_e T_m}{\Delta H \cdot \Delta T} + \delta l \quad (3.11)$$

Here the first term on the right-hand side is  $l_{\min}$  [see equation (3.5)], the smallest  $l$  that is still stable, and  $\delta l$  is the additional term in  $l$  that enables the crystal to grow. At moderate supercoolings  $\delta l$  is a small fraction (10–15 %) of  $l^*$ , hence the detailed form of  $\delta l$  is of no tangible consequence. The different theories give different analytical expressions for  $\delta l$ .

The first Lauritzen–Hoffman theory gives

$$\delta l = \frac{kT}{2b\sigma} \quad (3.12)$$

According to a later version

$$\delta l = \frac{kT(4\sigma/a) - \Delta f}{2b\sigma(2\sigma a) - \Delta f} \quad (3.13)$$

The dominant term in equation (3.11) for  $l^*$ , namely  $2\delta, T_m^*/\Delta H \cdot \Delta T$ , provides the inverse  $\Delta T$  relationship, which had been the principal observation expressed by Figure 3.5 that the theories had originally set out to explain. The fit with experiment in this regime (where  $\delta l$  is small in any case) was found to be very satisfactory with reasonable values for the parameters  $\sigma$ ,  $\Delta H$ , and  $T_m^*$ . The values of  $\Delta H$  and  $T_m^*$  are known by extrapolation from other experiments ( $T_m^*$  corresponds to the melting or dissolution of crystals from infinitely long and infinitely extended chains, not the melting of the actual crystal). Quantity  $\sigma$ , contains the work to form a fold and can be estimated in a variety of ways: it is approximately 100 ergs/cm<sup>2</sup>, a value which agrees well with that emerging from the theories by applying the experimentally observed values of  $l$ .

The above agreement can be regarded as a major success of the kinetic theories and of their underlying models. As the model is currently under considerable criticism from certain circles [see below and also *Faraday Discussion* No. 68 (1979)] it is worth remembering that no alternative theory is being proposed by its critics. Without this model there would be no explanation why polymers crystallize as uniformly thick lamellae with lamellar thicknesses that correspond to basic observation and fact.

### 3.2.2. Further Developments and Problems

#### 3.2.2.1. Avoidance of the “ $\delta l$ Catastrophe”

The above theories predict that at high supercoolings  $\delta l$  in equation (3.13) will not remain small; actually, in a rather narrow range of  $\Delta T$ ,  $\delta l$  will increase abruptly and tend to infinity causing  $l^* \rightarrow \infty$  accordingly. This

predicted upswing (referred to as the “ $\delta l$  catastrophe”) at low  $T_c$  (i.e., high  $\Delta T$ ) has never been observed. Initially, the correspondingly high range of  $\Delta T$  was experimentally inaccessible with the much-studied polyethylene system and thus an explicit refutation of the “ $\delta l$  catastrophe” remained outside the scope of experimentation. Later, however, poorly crystallizable polymers enabled researchers to reach the  $\Delta T$  range where the “ $\delta l$  catastrophe” was expected. No upswing of  $l$  was found; on the contrary,  $l$  leveled off to a constant value as in Figure 3.6. Accounting for the absence of the “ $\delta l$  catastrophe” and of an  $l$  value independent of crystallization temperature at high  $\Delta T$  forms the next stage in the theoretical development currently in progress.

Let us begin with a few words on the origin of the upswing of  $l$ . In nonmathematical terms this upswing is due to the removal of the activation barrier for the deposition of the first stem. The path  $P$ – $Q$  in Figure 3.9 would lead to decreasing (not increasing)  $\phi$ , i.e., the line  $P$ – $Q$  will be inclined in the opposite sense. In other words, at very high supercoolings the depositing single-chain portion itself is capable of leading to a stable regime. Hence there would be no need to first form a secondary nucleus.

There are two approaches in any modification of the theory to make it fit experiment at high  $\Delta T$ .

1. Hoffman and Lauritzen (see review by Hoffman, Davis, and Lauritzen quoted above) make  $\psi$  in equations (3.6)–(3.9) sufficiently small (less than  $\frac{1}{2}$ , possibly close to 0). This will not remove the  $\delta l$  upswing altogether (except for  $\psi = 0$ ) but can keep it down to unrealistically high  $\Delta T$  values. Formally, this arises because making  $\psi$  small promotes the activation barrier to the forward step in the deposition of the first stem; in fact such a barrier can be created where, at the high supercoolings in question, it would otherwise not arise. This is readily seen from the representation in Figure 3.12. (Actually, the choice of reaction path in the form shown in Figure 3.12 was introduced in preference to that in Figure 3.9 so that this possibility became apparent!)

The above procedure acquired physical meaning by considering the possibility that a long-chain molecule would adsorb first prior to commencing its deposition according to the scheme in Figure 3.10, there being good reason to believe that such adsorption could take place. Here the activation barrier will correspond to this first step of the adsorption (pinning down of the chain with associated loss of entropy without gain in crystallization-free energy).

2. Irrespective of the possible effect of the adsorption, Point [J. J. Point, *Macromolecules* 12, 770 (1979)] has quite recently developed a deposition pathway that avoids the “ $\delta l$  catastrophe” and leads to the horizontal plateau (such as that in Figure 3.6) at high  $\Delta T$ , while correctly reproducing the  $l$  vs  $T_c$  curves at low values of  $\Delta T$  (Figure 3.5), similar to

the other kinetic theories with which the new theory merges at low values of  $\Delta T$ . The details are complicated. The essential point can perhaps be conveyed by stating that the pathway subdivides the stem deposition (represented as a single event, such as  $P-Q$ , by Figures 3.8 and 3.9) into a number of discrete subevents, the stem depositing in small increments each having its own activation barrier to surmount. The chain is then given the chance to fold back on itself at each substage. At very high  $\Delta T$ , where the overall path ( $P-Q$  in Figure 3.9) slopes downward, the chain available for deposition will gradually be "consumed," so to speak, by such a potential back-folding possibility at each step, thus limiting the final chain extension that can be attained. In this way the "blow-up" in  $l$  is avoided. In addition, and chiefly, it is shown that the mean length converges to a fixed value irrespective of further increase in  $\Delta T$ , thus accounting for the horizontal plateau in Figure 3.6.

3. A third, somewhat negative view may be added to the above two. In this approach, at such high supercoolings the quasi-equilibrium processes underlying all the kinetic theories are no longer pertinent and a totally new theoretical framework may be needed. No work in this direction has yet been carried out.

### 3.2.2.2. Existence of Different Growth Regimes

In all the above considerations the nucleation of a new strip (with rate  $i$  along a preexisting substrate) was taken as the growth-rate-determining step, this being much slower than the spreading rate ( $g$ ) of the strip along the substrate (see Figure 3.10). Subsequently this was termed Regime I pertaining to low  $\Delta T$ .

With increasing  $\Delta T$  (lowering of crystallization temperature) the nucleation rate becomes increasingly faster compared to the spreading rate. When  $i$  becomes comparable to  $g$ , there will be multiple nucleation along a given growth face, i.e.,  $i$  and  $g$  will compete. The  $\Delta T$  range when this occurs has been termed Regime II.

The criterion for Regimes I and II is that  $Z < 0.01$  and  $Z > 0.01$ , respectively, where

$$Z = iL^2/4g \quad (3.14)$$

$L$  being a spreading length along the substrate.

The expression for  $l^*$  in equation (3.10) remains unaffected by a change in regime, but the growth rate will be sharply affected, as revealed by kinetic studies on the melt (see also the next section). In a most recent theoretical treatise [J. D. Hoffman, *Polymer* 24, 3 (1983)] at still larger undercooling, a further growth regime (Regime III) has been postulated,

where nucleation along the growth face becomes so abundant that the stem deposition, constituting the formation of the closely spaced nuclei, itself represents most of the lateral growth of the crystals. This change from Regime II to Regime III should again lead to a sharp change in the temperature coefficient of the lateral growth rate (see below). Change in the growth regime is expected to affect the lateral habit type, Regime I giving rise to smooth prism faces, Regime II to less regular, possibly microfaceted prism faces, with further kinetic roughening of the growth face for Regime III.

### 3.2.3. Growth Rates

It has been observed directly that the linear growth rate of single crystals ( $G$  in Figure 3.10), like the radial growth rate of spherulites (see end of Chapter 2), is a constant at a given temperature [namely  $G(T) = K$ ]. By theory, if surface (i.e., secondary) nucleation is the rate-controlling step

$$G = G_0 e^{-\Delta F/kT} \cdot e^{-\Delta\phi/kT} \quad (3.15)$$

where  $G_0$  is a constant for the system,  $\Delta F$  is the activation to interfacial transport (related to  $\beta$  by the flux equations (3.6)–(3.9), while  $\Delta\phi$  is the work of forming a critical nucleus. In solutions, the effect of the first exponential should be small and hardly affected by temperature;  $\Delta\phi$  will depend inversely on  $\Delta T$  yielding an overall function  $G$  given by  $G \propto e^{-1/\Delta T}$ . Explicitly, by inserting  $\Delta\phi^*$  for the most probable  $l$  value one gets

$$G = G_0 \exp\left(\frac{-\Delta F}{kT}\right) \cdot \exp\left(\frac{-m\sigma_s \sigma T_m^2}{kT\Delta H \cdot \Delta T}\right) \quad (3.16)$$

where  $m$  is equal to 4 for Regime I and to 2 for Regime II (the effect of regime type on growth rate referred to above!). For the newly postulated Regime III  $m$  again becomes 4.

The  $G \propto e^{-1/\Delta T}$  relation has been verified both for solution-grown single crystals and for melt-grown spherulites by direct morphological measurement of their diameters as a function of time at different temperatures of growth. (See also equation (2.4) in the section on spherulites.) In the case of spherulites, a sudden transition was observed from Regime I to Regime II in accordance with  $m$  changing from 4 to 2 in equation (3.16). In fact, latest results in our own laboratory [P. J. Barham, J. Martinez-Salazar, and A. Keller, *J. Polym. Sci. Phys. Ed.*, in press] have quite unexpectedly identified a reversal from  $m = 2$  to  $m = 4$  with further increase in  $\Delta T$  in accord with the change from Regime II to the recently

postulated Regime III (see above). Values for  $\sigma\sigma_e$  could also be obtained from plots of  $\ln G$  vs  $\ln[1/(T\Delta T)]$ . Not only were these values consistent with values of  $\sigma$  and  $\sigma_e$  obtained by alternative ways, but in the few cases where the growth rates were measured on both single crystals and spherulites for the same material  $\sigma\sigma_e$ , assumed very close values for both (i.e., for solution and melt crystallization).

### 3.2.4. Melting Behavior as a Function of $l$

In very small crystals the melting temperature (like that of other phase transitions) will be lower than the value pertaining to crystals of macroscopic (in practice, infinitely large) size; more exactly, it depends on size and shape. For the crystal platelets under discussion, the corresponding melting-point depression is readily derived. It should be recalled that at the melting point of the actual crystal  $T_m$  the difference in free energy  $\Delta\phi$  between crystal and melt is zero. For a crystal of lateral dimensions  $p$  and  $q$  and thickness  $l$ , we have

$$\Delta\phi = 2pl\sigma + 2ql\sigma_e + 2pq\sigma_e - pql\Delta f \quad (3.17)$$

where again  $\sigma$  and  $\sigma_e$  are side- and end-surface (basal plane) energies, respectively, and  $\Delta f$  is the change in bulk free energy. The first three terms on the right-hand side correspond to the work required in the creation of the surfaces (the first two that of the sides, the third that of the basal surface), and the fourth corresponds to the free-energy change associated with the formation of the crystal lattice. As side surfaces are small compared to basal surfaces, terms involving  $\sigma$  can be neglected. On equating the rest of the right-hand side to zero and substituting for  $\Delta f$  from equation (3.4), we derive

$$T_m = T_m^0 \left( 1 - \frac{2\sigma_e}{l\Delta H} \right) \quad (3.18)$$

for the melting point of the crystal of thickness  $l$ . This is the reduced melting point compared to that of the infinite crystal  $T_m^0$ .

The value of  $l$  depends on the crystallization temperature in accordance with equation (3.11), so the above result means that the melting point will also depend on the crystallization temperature. Thus crystals formed at a higher temperature will also melt at a higher temperature, and vice versa.

At this point reference will be made to a long-standing observation of general validity according to which the melting point of a crystalline polymer is a function of its crystallization temperature in the above sense.

It is a rather satisfactory development that in equation (3.18) a long-known observation has found a natural explanation in terms of morphology in general and chain folding in particular.

The following additional consequences of equation (3.18) are noteworthy. Commercial polymeric objects do not usually melt sharply but have a melting range. Also, such samples are not crystallized isothermally but on cooling. The latter means that they crystallize over a range of temperatures and accordingly will have crystals with a range of  $l$  values. It follows that, by equation (3.18), melting will occur over a broad temperature range in agreement with experience.

In the absence of direct structural information on  $l$ , equation (3.18) can be used to determine this important parameter, a frequently adopted practice. Nevertheless, two important qualifications are involved in such a use of melting points:

1. The chains may refold during heating, hence affecting the melting-point measurement itself. The final melting point will then correspond to that of the refolded crystal, not to that of the original crystal. The occurrence of such a situation is usually apparent from the fact that the ultimate melting point is dependent on the rate of heating: the faster the heating the lower the melting point (there is less chance for chain refolding!).
2. The use of equation (3.18) for determining  $l$  assumes implicitly that the internal perfection of the crystals under comparison is identical; in fact, if the ideal  $\Delta H$  is used, the crystal is assumed to be defect-free, which may not always be the case.

Finally,  $T_m$  vs  $l^{-1}$  curves can serve both for extrapolating to  $T_m^0$  and for determining  $\sigma_e$ . It is a remarkable and reassuring fact that the values of  $\sigma_e$  obtained in this way usually agree well with the values of  $\sigma_e$  obtained by relating observed  $l$  values to the crystallization temperature according to the kinetic theories of crystallization via equation (3.11), and further, that this applies to crystallization both from solution and from the melt.

### 3.2.5. Comparison of Crystallization from Solution and Melt

When the derivation of the kinetic theories was first outlined above, it was stated that deposition of individual chains is assumed and that this process occurs singly, chain by chain, unimpeded by others. It follows that dilute systems were implied. Nevertheless, in the course of what followed crystallization both from solution and from the homophase melt was invoked. This inconsistency reflects fairly the present practice in the literature. In view of the numerous controversies (see below) it is important to understand this in the right light, hence the following comments.



Initially, the kinetic theories were formulated to account for folding and for the observed  $l$  values in the case of crystallization from solutions, where the assumption of isolated chain deposition is largely valid. In the meantime the lamellar nature of the melt-crystallized material has gained increasing support (see, e.g., Section 3.3.2.2 and Figure 3.19 below) hence the results of the theory, initially formulated for crystallization from solution, became gradually transferred also to the melt. The important point to appreciate is that in many respects this transfer was found to work and bear fruit. Some consequences have been mentioned above: for instance, equation (3.16) for growth rates and equation (3.18) for melting behavior were found to be equally valid for solution and melt crystallization; in fact, the distinction between Regimes I, II, and III crystallization was explicitly established in connection with the melt (there has been no corresponding attempt for solution crystallization). Further, the values for  $\sigma_s$  and  $\sigma_e$ , derived from equations (3.16) and (3.18), respectively, proved to be very similar for crystallizations from solutions and melts.

However, identification of the molecular mechanisms in the dilute and condensed systems is subject to much debate. In the melt the chains may be expected to impede each other on the assumption that they are entangled, and also because a given growing crystal along the crystal-melt interface is clearly in permanent contact with segments belonging to many different chains. In addition, an all-important difference in the available experimental material needs to be pointed out. In contrast to solution crystallization, material on melt crystallization is confined essentially to information concerning growth rates and not directly to the fold length. There are good reasons for this, because isothermal thickening (Section 3.1.3.3c) makes a direct assessment via equation (3.11) difficult if not impossible, and thus the  $l$  values recorded, by whatever method, correspond to already refolded crystals and not to the primary crystals in the case of melt crystallization. Even so equation (3.11) has provided the most direct test for the theories in the case of solutions. In the case of melt crystallization, however, in spite of all the satisfactory equating of the two systems regarding growth rates and melting behavior, no such direct test has been provided.

It will only be stated that at the time of writing, this last-mentioned handicap is in the process of being overcome. In a series of works the effect of isothermal thickening in melt crystallization is being gradually reduced and the initial fold length due to primary crystallization progressively approached [P. J. Barham *et al.*, *J. Polym. Sci. Lett. Ed.* 19, 539 (1981); *J. Polym. Sci. Phys. Ed.* 20, 1717 and 1733 (1982)]. In fact, in the latest work it appears to have been actually attained (P. J. Barham, R. A. Chivers, J. Martinez-Salazar, S. J. Organ, and A. Keller, unpublished). From the last results the satisfying conclusion is in the process of emerging that, for a given  $\Delta T$ ,  $l^*$  is always very similar, irrespective as to whether crystallized

from solution or melt. The full consequences of this result for all previous works and ideas on melt crystallization, which in the past have relied on growth rates alone, are waiting to be assessed. Whatever the outcome of such an assessment, a welcome unification of such widely disparate material comprising both melt and solution crystallization is hopefully anticipated. Even as matters stand at the stage of writing it appears as a firm trend that  $l^*$ , the primary fold length, is determined by the supercooling  $\Delta T$  and subsequent fold-length increase (whether on isothermal thickening or heat annealing) by the absolute temperature  $T$ .

### 3.2.6. Some New Perspectives in Crystallization Theories

It may be salutary to recall that crystal growth in general (not merely confined to polymers) can proceed by three mechanisms as described by the classical theories, in the first stages associated with the names of Kossel, Volmer, Stranski, and Kaishew and at a later stage with Frank, Burton, and Cabrera [for explicit references see general texts on crystal growth, such as J. J. Gilman (ed.), *The Art and Science of Growing Crystals*, John Wiley, New York-London (1963)]. These mechanisms are: (1) by secondary nucleation, (2) by dislocation, and (3) without either (1) or (2) but through the agency of equilibrium surface roughness of the growth face. Mechanism (2) through the familiar screw-dislocation mechanism is operational in the growth of the large majority of crystals and is manifest through the resulting spiral-terrace topography of the growth face. While such spiral terraces abound in polymer crystals (see Figures 3.1 and 3.17), the advance of the corresponding basal faces (with the Burgers vector of the corresponding screw dislocation being equal to the lamellar thickness) is not the rate-determining factor for the lateral growth of the crystal, nor is it responsible for chain folding. Both these latter factors are governed by chain deposition *along the lateral surfaces* (Figure 3.10). The kinetic theories outlined in the preceding sections rely on mechanism (1), i.e., on secondary nucleation as the ultimate cause, and thus rate-determining factor, of the lateral growth of the layer, hence in the ultimate analysis, of polymer crystal growth and associated chain folding. These theories have taken no serious account of the exact lateral habit type involved, e.g., whether it gives a pure lozenge (Figure 3.2) or a truncated lozenge (Figure 3.14), neither did they need to for the purposes in question.

Nevertheless, at increasing crystallization temperatures (absolute) qualitative changes in habit occur: the straight prism faces become gradually rounded; in fact, solution-grown crystals obtained at the highest temperatures become "leaf shaped." Further, such leaf-shaped crystals seem to be the rule for crystals grown from the melt, wherever lateral habits can be identified (just about distinguishable in Figure 3.19). Bearing

in mind that crystallization from the melt normally occurs at higher absolute temperatures than for solutions (even for comparable supercoolings), it is tempting to generalize that curved lateral habits are characteristic of crystals grown at high absolute temperatures. It was this trend that has directed attention to crystal-growth mechanism (3) [D. M. Sadler, *Polymer* 24, 1401 (1983)]. To recall, it is familiar among simple non-polymeric crystals that mechanism (3) can take over at sufficiently high temperatures where the *equilibrium* roughness of the crystal surface becomes appreciable and enables an advance of the growing surface as a result of a net gain in deposition, as opposed to detachment, of the atom or molecular entities constituting the crystal. It is well known that in contrast to mechanisms (1) and (2), the consequence of growth by mechanism (3) is the nonfaceted nature of the resulting crystal [H. L. Leamy, G. H. Gilmer, and K. A. Jackson, in: *Surface Physics of Materials* (J. M. Bameley, ed.), Vol. 1, Academic Press, New York (1975)] that manifests itself in curving crystal faces (possibly the clearest example being  $^4\text{He}$ ). As just cited, curving faces are being observed in polymer crystals grown at the highest temperatures where growth is still possible, which suggests the invoking of mechanism (3).

However, in view of the large bonding enthalpies involved when depositing a full fold stem to a growing face (Figure 3.10), the applicability of mechanism (3) to polymer crystal growth is by no means obvious *a priori*, and even less so that this will lead to lamellae with chain folding where, in addition, the fold length and the lateral growth rates of the crystals obey the experimentally observed supercooling dependence [equations (3.11) and (3.16)]. At the time of writing it has just been demonstrated that by considering the deposition of fractional fold stem lengths, one at a time, the application of mechanism (3) to polymer crystal growth could be justified. Moreover, it could be shown that the formation of lamellae of finite thickness (hence chain folding) and the appropriate functional relations involving lamellar thickness, as well as growth rates on the one hand and growth temperature on the other [as in equation (3.11) and (3.16)], can be upheld on the basis of mechanism (3) by treating it as an Ising model (D. M. Sadler and G. H. Gilman, in preparation). The impact of this new approach is too early to assess, in particular, whether it represents an extension to the usual secondary nucleation-based theories into growth temperature regimes where the former could not be applied previously, or whether the new approach will take over as the more appropriate one in at least some temperature ranges where the nucleation-based theories have been applied so far. (The problems arising as a result of applying the theories, such as that underlying Figure 3.10, to crystals with rounded surfaces will be immediately apparent.) Whatever the future reveals, the approach based on mechanism (3) has the merit of introducing lateral habit considerations

for the first time in theories of chain-folded crystal growth, and, more generally, it has expanded the conceptual framework of the whole subject, which was about to settle down to a more sedate course. However, viewed from the other side, the notable predictive power of the conventional theories along approach (1) must be kept in sight, in particular their verified prediction of the existence of growth regimes I, II, and III, and to a certain extent the temperatures of transition between the regimes. Finally, all theories will require an underlying molecular mechanism, which should be feasible, to say the least. The secondary nucleation-based theories have gone a long way to provide this, even if some aspects are being argued, and some of the most recently observed, astonishingly fast growth rates (approximately  $1 \text{ m s}^{-1}$  for polyethylene) are presenting them with new challenges. Mechanisms along route (3), being much more recent, have not yet been given the same chance.

### 3.3. Morphology of Chain-Folded Crystals

The basic unit is the single layer, although in "real life" crystals are mostly multilayer structures. The basic observations, however, have been made on individual monolayers, which will be reviewed first.

#### 3.3.1. Monolayer Crystals

##### 3.3.1.1. Sectorization — The Basic Idea

According to the foregoing sections chain-folded crystals grow by the deposition of folded ribbons along the prism faces of the lamellae (Figures 3.3 and 3.10). If this is so, it should give rise to a unique structural consequence, namely the fold-plane direction should be preserved by the structure after the growth front has passed, which means that the crystal should consist of structurally distinct sectors defined by the fold-plane direction, as indicated by Figure 3.3. It will be apparent that within a single crystal there should be as many distinct sectors as there are prism faces. In purely lozenge-shaped crystals (as in Figure 3.3) all prism faces are {110}, all four of which are structurally equivalent but differ in terms of the orientation of the plane of folding. A frequent habit in polyethylene is the truncated lozenge with six prism faces, which are {110} and {100} (Figure 3.13). It is apparent that such a crystal should consist of six sectors where {110} and {100} are not equivalent. In a first approximation the unit cell is identical within all sectors (some subtle distinctions have been observed but these will be disregarded for the present) and the sectors are distinct merely by virtue of the direction of folding.

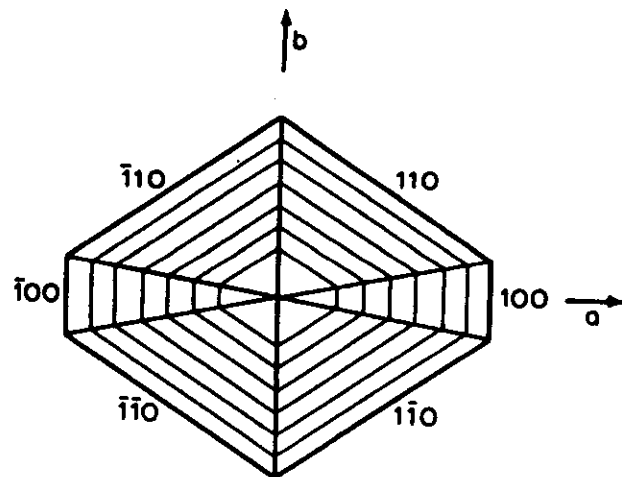


Figure 3.13. Principle of sectorization for a polyethylene crystal displaying  $\{110\}$  and  $\{100\}$  prism faces (truncated lizenge).

All the above was originally a surmise on the assumption that the chain-folding picture is correct. It was therefore most gratifying when these structurally unique predictions were verified experimentally.

### 3.3.1.2. Verification

The existence of sectorization was verified most dramatically and conclusively by a number of different approaches of which three will be mentioned here, as they can be simply described in brief.

*a. Morphological Evidence of Sectors.* The different sectors within a given layer can be distinct morphologically. This is most conspicuous in crystals that are hollow pyramids, rather like tents, where the different sectors form the different panels of the tents. During an ordinary examination in the dried state the nonplanarity is apparent through specific pleats in the collapsed structure and certain diffraction effects, but the fully three-dimensional tentlike object becomes evident when viewed (by dark-field optical microscopy) while suspended in the liquid (Figure 3.14). The straight-stem direction is always identical throughout all sectors and is parallel to the pyramid axis. The origin of this morphology lies in the fact that the folds do not all pack in a level manner but prefer to be staggered, which in turn must be related to the space requirement, hence possibly to the detailed shape of the fold itself.



Figure 3.14. Dark-field optical micrograph of morphological manifestation of sectorization. The crystal displays a hollow-pyramid habit while floating in its mother liquor (after Bassett *et al.*<sup>(2)</sup>).

*b. Thermodynamic Evidence of Sectors.* Sectors that are structurally different, such as  $\{110\}$  and  $\{100\}$  (see Figure 3.13), melt at different temperatures. This can be actually observed (see Figure 3.15). Such a striking visual observation is also supported by calorimetric evidence: crystals like that in Figure 3.15 display two endothermic melting peaks, one for each sector.

*c. Mechanical Evidence of Distinct Sectors.* The behavior of single-crystal fracture is clearly influenced by the fold-plane direction, e.g., there is ready cleavage parallel to a fold plane. Thus there will be a clean crack along a  $\{110\}$  direction within a  $\{110\}$  sector. However, when such a crack reaches a sector boundary and passes, say, from a  $110$  to a  $\bar{1}\bar{1}0$  sector, in the latter sector, the same  $\{110\}$  direction that was previously parallel will now lie at a large angle to the fold plane. A crack, if it continues into such a sector, will cut across fold planes and hence become bridged by threads. All this has, in fact, been observed (Figure 3.16).

## 3.3.2. Multilayer Crystals

### 3.3.2.1. Disposition of Consecutive Layers

This subject is essentially descriptive and the variety of pertinent observations will not all be enumerated now. The point to be made here will relate to some generalities concerning the relative disposition of consecutive layers within a multilayer structure, and mainly to the fact that



Figure 3.15. Thermal manifestation of sectorization. The  $\{100\}$  sectors melt at a lower temperature than the rest of the crystal. Electron micrograph.

consecutive layers in general are not strictly in crystallographic register. There are two classes of departure from perfect-layer register.

1. Rotational displacement of consecutive layers. Consecutive layers within a given crystal, when seen flat-on, are as a rule not in parallel orientation but rotated with respect to each other, usually by small amounts ( $1-3^\circ$ ) in an irregular manner. Under very exceptional circumstances such a rotation can be regular and always in the same sense, in

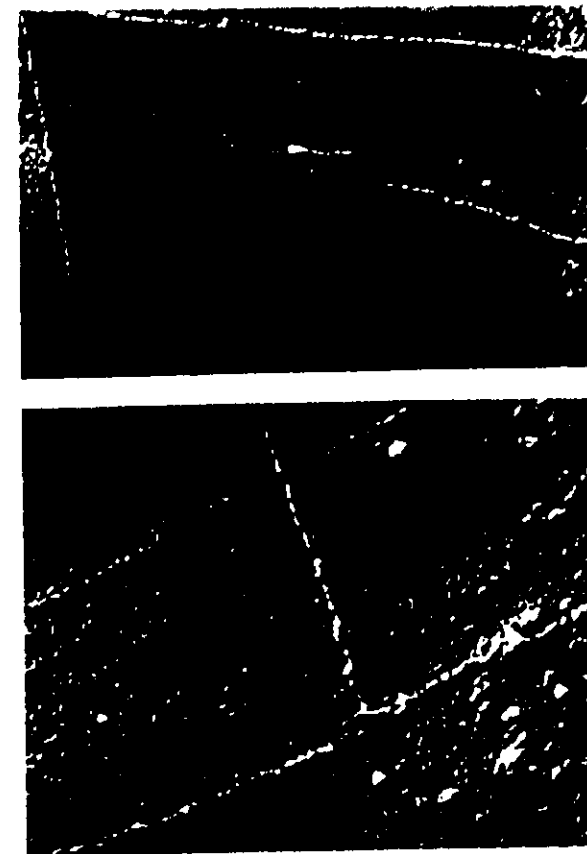


Figure 3.16. Fractographic manifestation of sectorization. The crystal cleaves cleanly parallel to the prism face within the corresponding sector where it runs along fold planes (top), but the crystallographically identical cleavage direction (along  $\{110\}$ ) pulls threads in a sector where it cuts across fold planes (bottom) (after Lindenmeyer<sup>(11)</sup>).

which case some striking appearances result. Such an example is illustrated in Figure 3.17 mainly for its aesthetic appeal. If rotationally displaced crystal layers are in close contact (often they are not — see below) interfacial dislocation networks may arise at the layer boundaries (twist boundaries).

2. Splay of consecutive layers. When multilayer crystals are viewed edgewise (only possible by optical microscopy while suspended in the

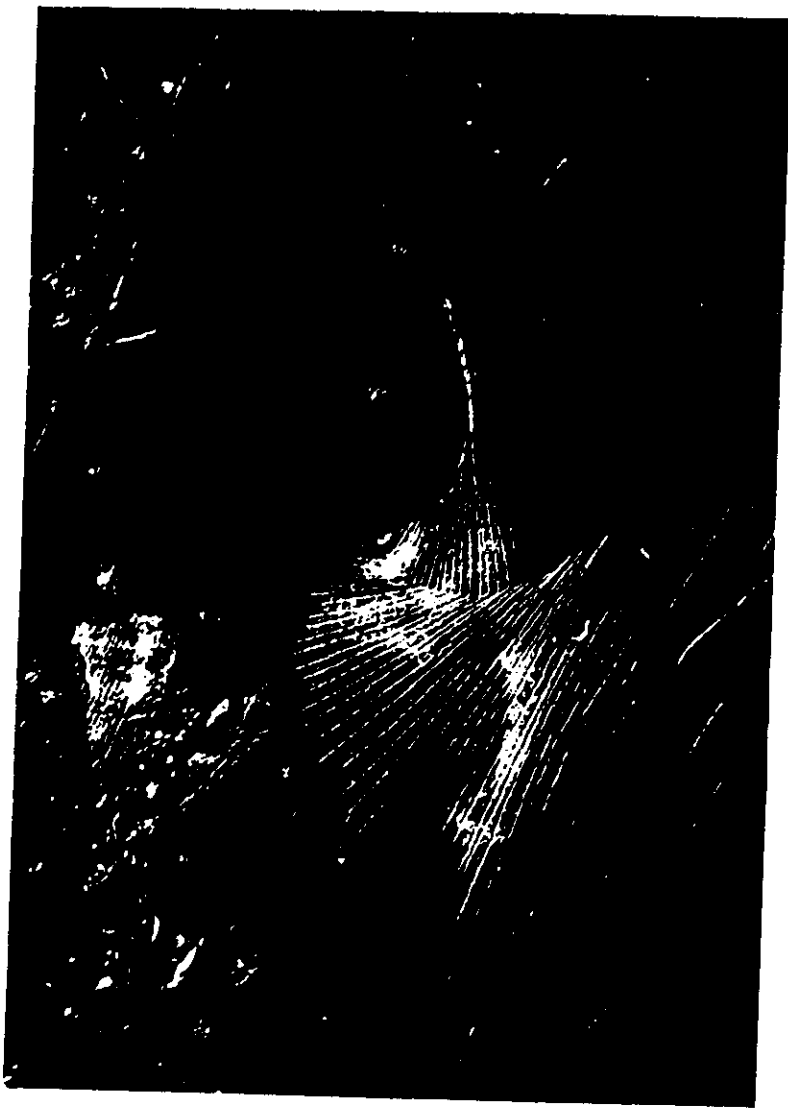


Figure 3.17. Electron micrograph of an exceptional example of a multilayer crystal of polyethylene displaying regular rotation of successive growth terraces (after Keller<sup>(12)</sup>).

liquid) the layers are often seen to splay apart. Figure 3.18 is such an edge-on view of a crystal shown in Figure 3.1.

Perhaps the most important physical consequence of (1) and (2) above is that a usual multilayer crystal, while a "single crystal" generically, is not a single crystal geometrically speaking. In other words, we cannot define a lattice vector that repeats throughout the whole object in view of the large discontinuities across the layer boundaries. This sets a natural limit to the growing of large chain-folded single crystals in the sense of conventional solid-state physics.

### 3.3.2.2. Approaching Spherulites

The splay in class (2) above can become increasingly irregular as the multilayer character of the crystal increases. This in turn is promoted by increasing the concentration of the solution in which the crystallization is conducted. Such crystals become increasingly "bushy," the layers curve, and in an edge-on view give the impression of sheaving fibrils. This leads naturally to the sheaf forms described previously as the precursors of spherulites (see Figure 2.22). Hence this splaying, sheaving multilayer development described so far in solution promises to be a natural bridge between solution-grown lamellar crystals and the melt-crystallized spherulites discussed in Chapter 2.

We previously alluded to the fact that lamellae have also been identified as the basic structure element in melt-crystallized spherulitic polymers. Now we shall illustrate this with an example (Figure 3.19). Here,

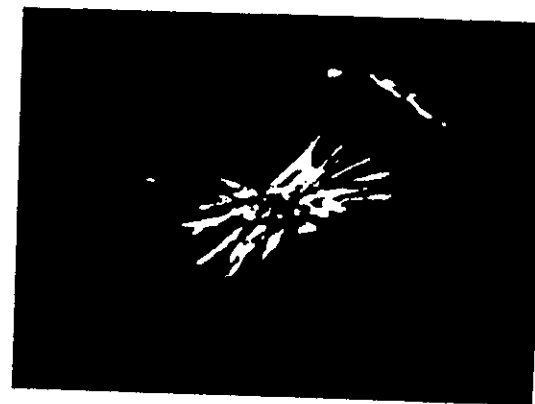


Figure 3.18. Optical micrograph of a multilayer crystal seen edgewise in its mother liquor revealing splaying of layers (after Mitsuhashi and Keller<sup>(11)</sup>).



Figure 3.19. Scanning electron micrograph illustrating the lamellar structure of a melt-crystallized spherulitic polyethylene. The cavernous texture enabling the lamellae to be seen in depth arises as follows: the lower-molecular-weight material segregates on crystallization in separate lamellar packets, which can be removed subsequently by selective dissolution treatment (after Winram *et al.*<sup>117</sup>).

as in many other examples, the lamellae are not obtainable in isolation and could be identified only as some etching or disintegration products, or in some cross-sectional view within microtome sections. Much less is therefore known about the detailed nature of such lamellae, even less about the way they fit together to build up the spherulite. Nevertheless, the common denominator of the basic lamellar unit invites some generalizations as regards the chain-folded structure (even with modifications — see later) that also pertain to crystallization from the melt. Further, the multilayer development of single crystals seems to provide continuity between the simplest crystal unit, the monolayer on the one hand, and the spherulite, the characteristic crystal element from the melt on the other.

### 3.4. Fold Structure — Nature of Amorphous Material

#### 3.4.1. The Issues

The subject of the present section is highly controversial and originates in two different, nevertheless interconnected, enquiries: What is the structure of the fold? How is the amorphous content of a single crystal to be visualized?

##### 3.4.1.1. Structure of the Fold

The fold is such an important part of the chain-folded crystal that its structure on the atomic level is of some consequence. Nevertheless, the problem remains outside the scope of traditional X-ray crystal-structure analysis because we cannot obtain a macroscopic chain-folded crystal. The nearest achievement is the structure determination of a cyclic paraffin. This is a closed ring-shaped paraffin of 34 C atoms. It crystallizes with the ring collapsed, so that most of the ring is in a close-packed form, such as that realized by linear paraffin chains (a slightly modified form of the structure is shown in Figure 2.3). Here adjacent straight portions are necessarily bridged by the rest of the ring, the bridge involving four C—C bonds. Such a bridge is clearly a close analogue of the fold. It does show that an adjacently reentrant sharp fold (a much contested issue nowadays) is clearly possible sterically when required by the constraint of the closed-ring shape of the molecule. Whether a long linear polyethylene chain will do the same on its own accord, however, is a more open question. On the assumption that it does, a number of conformational analyses were carried out to determine the exact fold conformation and have led to a variety of not grossly dissimilar fold conformations, involving three, four, or five C—C bonds. However, the whole problem has been, at least temporarily, superseded by an overriding issue: do chains fold in a specifiable regular manner? The latter question has its origin in the second enquiry posed above, to which we now turn.

##### 3.4.1.2. Amorphous Content of a Chain-Folded Single Crystal

It was noted earlier that a synthetic polymer is usually only partially crystalline, hence the existence of the whole subject of "degree of crystallinity" treated phenomenologically in Section 2.3 of Chapter 2. With the recognition of morphologically identifiable single crystals, the question has arisen whether such an entity possesses any "amorphous content" in the traditional sense. By applying the usual methods of crystallinity determination to such single crystals a not inappreciable crystallinity

deficiency was found; in the case of polyethylene this amounted to about 20%, which was then attributed to the existence of amorphous material. For a variety of reasons, which will not be enumerated here, this supposedly amorphous material was envisaged to be located along the lamellar surface and thus attributed to an irregularly, loosely looped structure of the folds (Figure 3.20). This was given more explicit form by Flory [P. J. Flory, *J. Am. Chem. Soc.* 84, 2857 (1962)], who envisaged the fold surface as a telephone switchboard (switchboard model). There is evidence for and against such a view. Accounting for the amorphous content is certainly a point in its favor. Nevertheless, the remarkably regular features observed in such crystals (sectorization and its consequences, for example) and, chiefly, the issue of how the overall fold length should be defined unambiguously by the crystallization temperature in the case of so much randomness at the fold surface (not to speak of how such a structure should form; there is no alternative class of theory other than the one outlined earlier, requiring a sequential deposition of fold stems) raises more questions (in the author's opinion) than the switchboard model can answer. In addition, there is an overriding geometrical problem, namely the prohibitive overcrowding that the switchboard model would create at the fold surface, where the density of the amorphous region would have to exceed that of the crystal (recognizable even in the sketch of Figure 3.20). The overcrowding can be relieved by making some of the chains fold back sharply in order to provide more room for other folds to form loose loops of an overall amorphous character. The necessity for such partially sharp

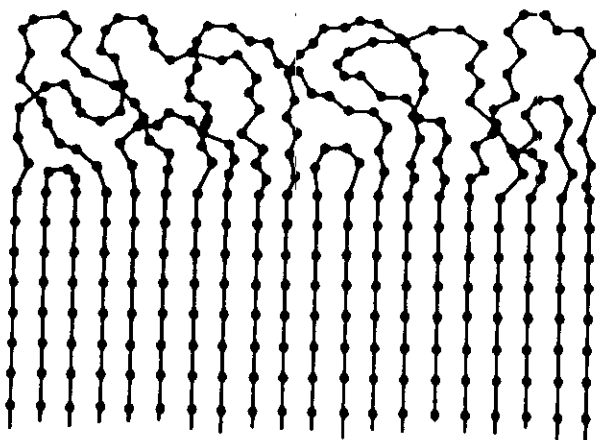


Figure 3.20. Sketch of a disordered fold surface: the switchboard model in a two-dimensional representation (after Fischer<sup>(10)</sup>).

refolding is nowadays more or less agreed on by all concerned. The issue about which the controversies are currently polarized turns around the question of how much such sharp refolding is required. On this, in turn, would depend whether the overall character of the fold surface is to be regarded as an essentially random or an essentially regular structure. In the present author's view, there is no *a priori* reason why the fold surface should always be the same in all crystals under all circumstances, hence that there is necessarily a unique answer to a question posed in the above way. Accordingly, it may make more sense to pose the question in the form as to whether or not a chain can fold in a regular manner, given the appropriate conditions. If the answer is "yes," there will be many reasons why departures from maximum regularity may occur in a given sample.

### 3.4.2. Experimentation in Aid of the Fold-Surface Problem

The fold-surface problem can be subdivided into two distinct structural issues, which are unfortunately often confused or inextricably telescoped together in much of the controversial literature:

1. Adjacent vs nonadjacent stem reentry (irrespective of the nature of the fold).
2. Regular vs irregular folds.

Only six of the experimental techniques employed in the arguments will be enumerated. A further one, the recent neutron scattering, will be dealt with in a separate section below.

1. Interchain interactions of isotopically labeled species in an isotopic mixture can be assessed by infrared spectroscopy. Thus one can mix a small amount of deuterated species of polyethylene into normal hydrogenated polyethylene and explore the nearest-neighbor environment of a given deuterated stem as reflected by the splitting of appropriate infrared bands. In this way adjacency and nonadjacency should in principle be distinguishable.

2. A chain-folded layer can be subdivided into fold surface and crystal core by small-angle X-ray scattering (SAX). This is done by detailed analysis of the intensity in the SAX pattern (in contrast to merely using Bragg's law to determine  $l$ , the overall periodicity, referred to so far).

3. Crystal-core thickness can be determined directly from line-profile analysis of suitable wide-angle X-ray reflections corresponding to a periodicity along the lamellar normal.

4. Raman LAM analysis could be used. In principle it should define the straight-stem length, hence the core thickness. (In fact, rather disappointingly it does not seem to do so but gives the same  $l$  value as SAX, at least by the simple analysis — see Section 3.1.3 on the LAM technique.)

5. Chemical methods can be used that rely on selective etching involving removal of the fold surface coupled with physical (SAX) and chemical (molecular weight) analysis of the residue.

6. Use can be made of detailed electron microscopy of effects relating to the fold surface.

Intentionally, no conclusions are drawn with respect to any of the above techniques since some of the interpretations are still being debated and no justice can be conveyed by a single statement pertaining to each. Some broad, overall statements will be made in what follows.

### 3.4.3. Outcome of the Enquiries

Certain evidence favors the switchboard model while other evidence requires the existence of regularity; the individual points will not be pursued here. Though there are obviously areas in which final conclusions cannot be drawn at the time of writing, nevertheless the material already presented, together with that of the following section on neutron scattering, occupies a considerable portion of the relevant literature. The present coverage should, at the very least, prepare the reader for approaching the original literature in the areas covered. However, in spite of uncertainties two specific outcomes will be mentioned in general terms.

The first pertains to the nature of the amorphous component. Instead of merely referring to the "amorphous fraction" as in the earlier chapter on crystallinity, arguments on the fold-surface structure have focused attention on the multitude of variants that would normally be covered collectively by the term "amorphous." This arises because disordered material, such as that in a chain-folded crystal, can now be classified in terms of its relation to the lamellar crystal core. Thus it can consist of loops that, even if not all regular, can correspond to different degrees of looseness. Alternatively, there can be loose hairs emanating from the layers that have failed to become incorporated at their other end, or they become incorporated into a different lamella, in which case they will not be loops but interlamellar ties. All this is not as purely qualitative as it may appear, because the different ways of incorporating loose "amorphous" portions into the crystal can be quantified in terms of loss of configurational entropy due to the loose chain or portion being confined at one or both ends with a specific distance between the ends.

The second outcome is that these modes of constraints can significantly affect the behavior of such chains, hence the macroscopic properties. In particular, tie molecules will be load-bearing (all important for mechanical behavior) while loops, at least on their own, will not; this again is relevant to mechanical properties (relaxation behavior). Further, when the effect of the constraints, and the associated entropy changes, are

considered in combination with the crystals, they will potentially influence the melting behavior of the crystals themselves (premelting, superheating — see later).

An awareness of all the above factors provides a more explicit molecular basis on which to define and treat the so-called amorphous component of a semicrystalline polymer.

It also follows that the generalization of an "amorphous content" or "amorphous-crystalline ratio" is an oversimplification. The experimental methods listed above are leading increasingly to the overall conclusion that what at first sight had been termed "amorphous" component really corresponds to a state of intermediate order, which in the broadest generality expresses the fact that a spectrum of material with different constraints is involved.

## 3.5. Neutron Scattering Experiments: The Chain Trajectory

In recent years the subject has received a major boost by the application of neutron scattering, made possible by the availability of new high-flux neutron sources. The results have extended the scope of the enquiries, but have also further aggravated existing controversies. For an impression of the subject and an in-depth study involving all aspects of the controversies, the most up-to-date and comprehensive reference is *Faraday Discussion* No. 68 (1979).

### 3.5.1. Technique and Potential

The technique in question involves coherent elastic scattering of neutrons at small angles. The idea is to use scattering data to obtain information on the overall dimensions of, and the path described (trajectory) by, a chain molecule in an environment of its own kind. In such an approach a minority of the molecular population needs to be distinguishable from the rest as regards scattering, i.e., there must be contrast, which is achieved by isotopic doping. Hence a small fraction of the molecules must be isotopically different in a way that makes them distinct as regards scattering of neutrons, but not otherwise. For the present issue this is achieved by mixing deuterated guests to the normal proton-containing host, the scattering power of the two isotopes of hydrogen being significantly different. Thus individual molecules of the guest species become amenable for studies in the condensed phase, as in the dilute phase (solutions), by light scattering.

The obtainable information depends on the angular range of the scattering: the smallest angles provide information on the large-scale



features, the global dimensions of the molecule as a whole, while increasingly larger angles yield information on increasingly smaller features of the molecular trajectory. While there is no intrinsic discontinuity in terms of angles, nevertheless some distinctions arise in actual working practice due to the technicalities of the experiment and the various convenient approximations used in the interpretation.

### 3.5.2. Angular Ranges

1. Smallest angles ("Guinier" range). For the present type of polymer problem this range is given by

$$10^{-1} < q < 5 \cdot 10^{-2} \text{ \AA}^{-1}$$

where  $q = (4\pi \sin \theta)/\lambda$ ; here  $\theta$  is the scattering angle and  $\lambda$  the wavelength.

This range provides a measure of the radius of gyration  $R_g$  of the molecule

$$I/I_0 = 1 + q^2 R_g^2/3 \quad (3.19)$$

or its approximation by the Guinier law

$$I = I_0 \exp(-R_g^2 q^2/3) \quad (3.20)$$

where  $I$  is the intensity scattered at a particular  $q$  and  $I_0$  at  $q = 0$ , respectively.

2. Intermediate (but still small) angles. The range here is

$$5 \cdot 10^{-2} < q < 5 \cdot 10^{-1} \text{ \AA}^{-1}$$

Scattering in this range gives a certain amount of information on the details of the chain trajectory, particularly pertinent to the chain-folding problem.

Results are most informatively expressed in terms of  $Iq^2$  vs  $q^2$  plots (so-called Kratky plots).

3. Larger angles. The range is given by

$$5 \cdot 10^{-1} < q \rightarrow 1 \text{ \AA}^{-1} \text{ and beyond.}$$

Scattering in this range gradually approaches the usual crystallographic information on chain conformation and (in the case of crystalline polymers) interplanar dimensions.

### 3.5.3. Some Results

The first studies were carried out on amorphous polymers, melts, and glasses. Perhaps the most significant result was obtained in the region of smallest angles. Here  $R_g$  was found to correspond to the value for an unperturbed random coil (as in  $\Theta$  solvent) with  $R_g \propto M^{1/2}$  as expected from a random coil, a result quoted earlier in connection with the amorphous state (Section 1.6.1).

The next stage was to follow what happens to the molecular dimensions and trajectory on crystallization. Here a significant complication was encountered in the form of isotopic segregation, at least in the best-examined, and in other respects best-explored system of polyethylene. This means that the isotopic guest molecules do not quite behave as their hosts with respect to crystallization, as initially expected, but form isotopically enriched regions or clusters (there are different views as to which of the two are formed). Hence the neutron-scattering technique will not see a given guest molecule in isolation, and so can no longer provide the information required, at least at sufficiently low angles that enable  $R_g$  to be identified. (This became apparent from excess intensity at the extrapolated zero angle, excess in regard to the expectation from a single molecule of known  $M$ .) To avoid this segregation, crystallization must be carried out rapidly, i.e., at high supercooling. This is a very serious limitation as it restricts the technique to samples where the chains have not been given a chance to sort themselves out. Apparently this disturbing segregation effect is absent with isotactic polystyrene and polypropylene, where measurements can and have been carried out at (from the crystallization standpoint, most fundamental) low supercoolings. Nevertheless, these latter polymers are less crystalline and their morphologies are less understood. Consequently the information from neutron scattering does not yet carry the same weight as regards the abstract basic question of the chain trajectory in crystalline polymers, the issue over which existing controversies have now centered.

The actual results will only be very briefly mentioned (see *Faraday Discussion* No. 68 for details). In melt-crystallized polyethylene, at any rate,  $R_g$  did not change on crystallization (at the high supercoolings to which experiments were restricted), hence the much publicized notion that globally nothing happens to the molecule: it merely "freezes in" with some local order representing crystallization. This, however, disregards all the morphology, i.e., the question as to why lamellae form with well-defined thickness, not to speak of why the chains fold with the uniformity and supercooling dependence observed. However, in solution-grown crystals  $R_g$  is certainly observed to change on crystallization; in fact it gets smaller with some interesting additional effects not to be detailed here.

In the angular range given in (2) Section 3.5.2, the results seem to be

most clear-cut with solution-grown crystals: they are consistent with the scattering object having the form of a sheet with dimensions corresponding to a chain-folded ribbon deposited along a crystal face (see, e.g., Figure 3.10). This is in agreement with morphological studies; nevertheless there is much argument as to what extent the stems belonging to a given molecule are arranged adjacently. It appears at present as if there were numerous gaps in the ribbon formed by a given chain, and the point being argued is whether the basic picture of adjacent folding (with some defects) can still be retained, or whether the description of a more random folding pattern is appropriate. In melt-crystallized (rapidly cooled by necessity) samples, the stems scatter neutrons more like individual isolated rods (by some claims), or as very short rows of at least partially adjacent stems (by other, most recent claims!).

I have no intention of exploring the arguments further; I shall merely indicate their scope. Clearly this all leads back to the fold-surface problem of the previous chapter. A few general questions will be posed for the sake of perspective when trying to evaluate individual claims:

1. In any particular sample examined, have the chains been given adequate opportunity to realize a sufficiently representative mode of deposition to serve as a model for crystallization behavior?
2. Is the interpretation of a particular scattering pattern sufficiently unique for a far-reaching generalization?
3. In a given model are elementary space-occupation problems being adequately dealt with? (See the issue of overcrowding at a lamellar surface in the preceding chapter.)

### 3.6. Alternative Morphologies

The morphologies to be listed here are still part of the general class C (Section 2.1.3), i.e., they correspond to the crystallization of random chain molecules in the quiescent state.

#### 3.6.1. Extended-Chain-Type Crystals

In the cases of several polymers, crystallization from the melt under elevated pressures ( $3 \cdot 10^3$ – $9 \cdot 10^4$  atm) leads to brittle solids (as opposed to the usual pliable solids, such as a normal polyethylene type) with near-100% crystallinity [Wunderlich, Bassett. For specific references see textbooks by above authors: N. Wunderlich, *Macromolecular Physics*, Vol. 1, Academic Press, New York (1973); D. C. Bassett, *Principles of Polymer Morphology*, Cambridge University Press, Cambridge (1981)]. Fracture surfaces reveal that they consist of very thick lamellae with the chains

normal to the lamellar planes (Figure 3.21). The lamellar thickness can extend up to several  $\mu\text{m}$  and become comparable to the chain length. For molecular weights  $M$  of about 15,000 (for polyethylene), the lamellar thickness corresponds to the chain length and the spread of lamellar thicknesses over a given sample to the actual molecular weight distribution of the material, indicating among other points surprisingly accurate fractionation during crystallization by molecular weight. (This gives rise to the unanswered question as to how accurately the chains group themselves into fractions and how they can achieve this.)

It follows that the chains in the above crystal type are fully extended within the crystal, hence the term "extended-chain" crystals. (It is noteworthy that *these* extended-chain crystals formed from unoriented melts are lamellae, not fibers; see later.) With higher molecular weights ( $M = 10^4$ – $10^5$  for polyethylene) there is no longer an exact correspondence between  $M$  and lamellar thickness: the lamellae can be thinner by factors of 2–3 X. Hence in such cases there must be *some* folding. Nevertheless, such samples remain distinctly different from those crystallized at atmospheric pressure in the normal manner. Hence the term "extended-chain-type" crystals.

The full story of the reasons for such crystallization is only partially understood. It has been observed that such samples, at least with

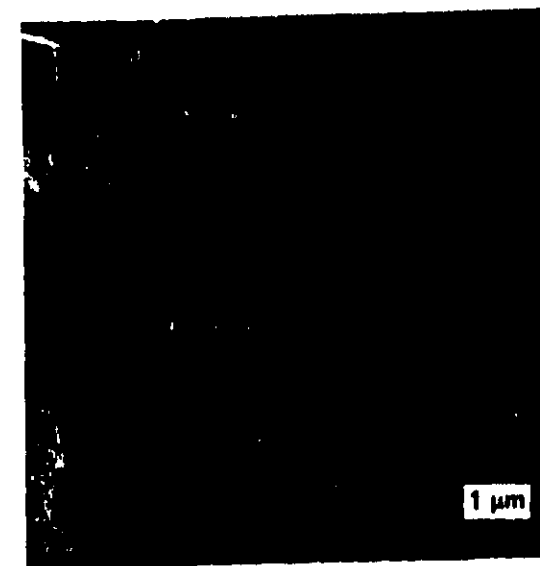


Figure 3.21. Electron micrograph of extended-chain-type crystal of polyethylene crystallized under 4800 atm pressure. (By courtesy of Wunderlich based on Wunderlich *et al.*<sup>(10)</sup>.)

polyethylene, crystallize first in a hexagonal phase while under high pressure (as opposed to the usual orthorhombic phase to which it transforms on cooling and pressure removal). It is claimed that this is a general requirement for extended-chain-type crystallization [D. C. Bassett, in: *Developments in Crystalline Polymers* (D. C. Bassett, ed.), Vol. 1, p. 115, Applied Science Publ., London (1982)]. Further, it was observed that the lamellae forming under pressure are thin to begin with, but subsequently thicken following initial growth. Accordingly, this is a case of fold-length increase corresponding to an extreme case of isothermal thickening (see Section 3.1.3.3c), which here proceeds to *full* or *nearly full* chain extension. Accordingly, it is this extreme chain refolding that seems to be promoted by the high hydrostatic pressure. Among possible reasons are the conformational changes in the melt induced by the pressure and/or the changed properties of the crystals actually formed. In any event we know that the crystal, when formed, is not the usual one, namely that the chains within it pack in a hexagonal lattice. It is known that hexagonal phases are more mobile than the usual orthorhombic ones (see Section 2.2.3), hence refolding will be facilitated. Also, the possibility that a liquid-crystal-type phase intervenes has been suggested.

Whatever the reasons for its formation, the properties of the resulting product are quite exceptional for a polymer. As stated earlier, they are virtually fully crystalline and thus contain no amorphous component. Their melting point is very high, and can attain values beyond the theoretical value for fully extended chains because of superheating. For all these reasons samples with this extended-chain-type texture can serve as models of the corresponding infinite polymer crystal as regards several properties, often quoted in theoretical works.

### 3.6.2. Micellar Crystals (Crystal Gels)

The fringed micelle (Figure 3.22) was the traditional model for crystallization before being superseded by the chain-folded lamellae. It is now having a comeback under the very special circumstance of crystallization at very high supercooling in systems capable of such supercooling. This class of effects is currently becoming apparent through the phenomenon of thermoreversible gelation from solutions.

As an example, we consider a very highly supercoolable polymer, such as isotactic polystyrene. When an appropriate solution of it is being cooled, the normal crystal suspension of chain-folded platelets forms first. At very high supercooling, however, such solutions display a very conspicuous effect: they may set as a gel. X-ray diffraction indicates that such gels consist of crystals. On heating the gel dissolves, hence it is thermoreversible.

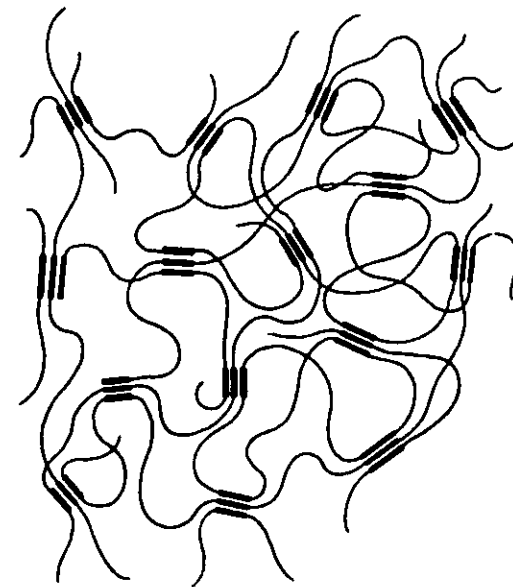


Figure 3.22. Model of fringed, micellar gel-forming crystallization (after Keller<sup>17,18</sup>).

Gelation is due to connectedness. Structurally, a gel is a swollen network. In the network under discussion the junctions are the crystals. For them to be junctions, several chains have to come together, hence they must be largely of micellar character as in Figure 3.22.

The above type of micellar crystals are very small, possibly approximately 100 Å linear dimensions, and melt at much lower temperatures than lamellae. The smallness of the micelles is a structural necessity for this type of crystal form. Greater lateral extension creates the overcrowding problem at the interface where the chains emerge from the lattice (mentioned in Section 3.4.1.2). This problem can only be relieved if some of the chains fold back, which in turn would bring us back to chain-folded lamellae. The above argument suggests a connection between micelles, hence gel formation, and the high supercooling: at very high supercooling the critical crystal nucleus is only required to be very small — thus it would be sufficient for only a very few chains to come together, which then “stick,” — so to speak — forming a stable nucleus with lateral dimensions still too small to create cumulative strain at the interface where the chains emerge.

There is evidence that in an appropriate  $T_c$  range, micelles and lamellae can compete and form simultaneously. To mention one charac-

teristic, such samples display the properties of a composite morphology and accordingly possess two distinct melting points.

Gelation is a direct result of connectedness. Accordingly, such connectedness can only be diagnosed by this straightforward test in crystallization from solution. If the same network generating crystallization were to occur also from the melt, it would remain undetectable by such a simple test for connectivity (because here gelation would not apply). There is evidence that crystals formed from the melt at very high supercooling (e.g., close to  $T_g$  (see Figure 2.12) as opposed to those at low supercooling close to  $T_m^0$ ) are very different (e.g., they possess a very much lower melting point), which suggests that they may not merely be smaller but may have a qualitatively different character compared to those formed at low supercoolings, i.e., the lamellae, the main subjects of study in crystallization behavior so far. There is therefore a likelihood that they have a micellar character without substantial amounts of chain folding.

We shall now revert to the other classes of crystallization listed in Section 2.1.3, where we stated that they have no counterparts, not even conceptually, among nonpolymeric substances.

# Other Classes of Crystallization

A. Keller

## 4.1. Crystallization Concurrent with Polymerization (Nascent Polymers)

Most polymers, including technologically important ones (such as polyethylene, polypropylene, and polyoxymethylene), are crystalline when polymerized. So are most natural polymers (cellulose, wool, etc. — biosynthesis!). They crystallize concurrently with the polymerization reaction itself. The significance of this lies in the fact that here the polymerization reaction and crystallization may interact with each other: the polymerization reaction influences the crystal morphology, while crystallization affects the reaction, molecular weight, and its distribution in particular. For instance, chains grow up to a certain length and then crystallize (precipitate from solution), or the monomers add to the polymer, which is already in the crystalline state. Little is known about this area. The "nascent" crystal morphology itself is in general little explored (e.g., that arising in a reaction vessel), but it is known that such morphology can be very specific with special properties, which the polymer will lose on customary reprocessing.

In some instances, when the polymer cannot be processed at all (infusible, insoluble), this nascent morphology is the final one. To make such a polymer useful, the actual nascent morphology has to be controlled. (Normally the morphology is determined by the subsequent processing operation.)

A recent important example of the above situation is polyacetylene (see Section 1.5.2.3). As stated there, after suitable doping this polymer

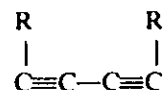
---

A. Keller · Department of Physics, University of Bristol, England.

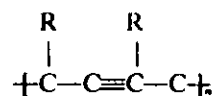
conducts electricity, raising the possibility of becoming a commercially viable conductor, optimistically replacing copper. However, currently its usefulness is limited by the uncontrolled polycrystalline, randomly oriented nascent morphology, which cannot be altered subsequently, at least at present.

In general, nascent polymers are polycrystalline. This usually applies also to the case of *solid-state polymerization*. Here one usually starts with a macroscopic monomer single crystal and induces polymerization of the monomer while within the crystal (e.g., by heat or radiation). The monomers then join up into chains, when usually the crystal falls apart into submicroscopic polymer crystals. In a few exceptional cases, however, the monomer crystal converts into a macroscopic polymer single crystal with the polymer chains running through the whole crystal, apparently without interruption. Very special geometric conditions must be satisfied for this to happen. The first such instance was the formation of polyoxymethylene from tetroxane, the cyclic tetramer of formaldehyde.

Of greater significance are the polydiacetylenes [G. Wegner, see, e.g., Faraday Discussion, No. 68, *Organization of Macromolecules in the Condensed Phase*, p. 494 (1979)]. These are polymers of the monomer of type



where R stands for a variety of chemical groups. The polymer is



and provides practically perfect macroscopic crystals. Such crystals have special macroscopic properties (Figure 4.1): first, because they have a one-dimensional character with valence bonds all along a given direction in a continuous sequence; second, because of the alternating triple-double bonds along the chain. The latter gives rise to many unusual optical and electrical properties, which form the subject of many physical studies.

Another example is  $(\text{SN})_n$  forming from  $\text{S}_2\text{N}_2$ . (The monomer is a  $\text{S}_2\text{N}_2$  ring that opens up to form chains.)

The  $\text{S}_2\text{N}_2$  crystal forms first by sublimation, but polymerization

50 hr at 60 °C

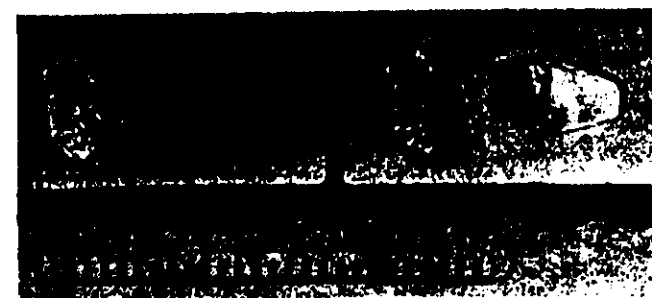


Figure 4.1. Macroscopic single crystals of a polydiacetylene obtained by solid-state polymerization (displaying anisotropic optical properties in different orientation with relation to plane-polarized light) (by courtesy of D. Bloor, unpublished).

immediately starts to produce the  $-\text{S}=\text{N}-\text{S}=\text{N}-$  chain. Macroscopic crystals of a variety of shapes (prisms, needles) up to 1 cm in size can be obtained. As already stated in Section 1.5.2.3, they are quasi-one-dimensional metals with strong metallic conductivity along the chain direction and are superconducting below 0.3 K. It is an important substance for the study of one-dimensional systems. However, it is likely to be a unique "one-off" compound and not a member of a family as originally hoped.

All macroscopic single-crystal polymers are very special cases. Nevertheless, they form the closest link between traditional solid-state physics and polymer science and are potential models for theoreticians. They have found no practical application so far, nonetheless they have the potential for specialty devices due to their special electronic behavior (optical and electric).

## 4.2. Orientation-Induced Crystallization

### 4.2.1. General

This is the second, specifically polymeric mode of crystallization (Section 2.1.3.2). Historically this was one of the first observations of polymer crystallization, when a stretched rubber was examined for X-rays in 1925 [M. Katz, *Naturwissenschaften* 13, 410 (1925)].

Orientation reduces the entropy of the random chain, hence on crystallization  $\Delta S$  is also reduced. Accordingly the melting point is raised, because  $T_m = \Delta H/\Delta S$ . This means that for given  $T$  the supercooling is increased, hence so is the driving force for crystallization. It is even possible to produce crystallization in this way when  $T$  is above the melting point in the unstretched state; here the crystals melt on stress removal.

#### 4.2.1.2. Kinetic Considerations

A chain in its fully, or partially stretched out, oriented state is closer to the configuration it will adopt in the crystalline state. Entropy considerations apart, this means that less conformational rearrangement is needed for a chain to fit into a crystal lattice, hence it can proceed faster, less hindered by retarding factors such as viscosity.

#### 4.2.2. Morphological Background

We have seen above that a random chain will form chain-folded platelets if allowed to crystallize. If the chains are being stretched while in the amorphous state, they will crystallize as fibers (Figure 4.2). It will be reinvoiced that before the recognition of lamellar crystallization, fibers were the products expected from crystallization of long chains *a priori*. It is for this reason that lamellar crystals were so unexpected. We now see that

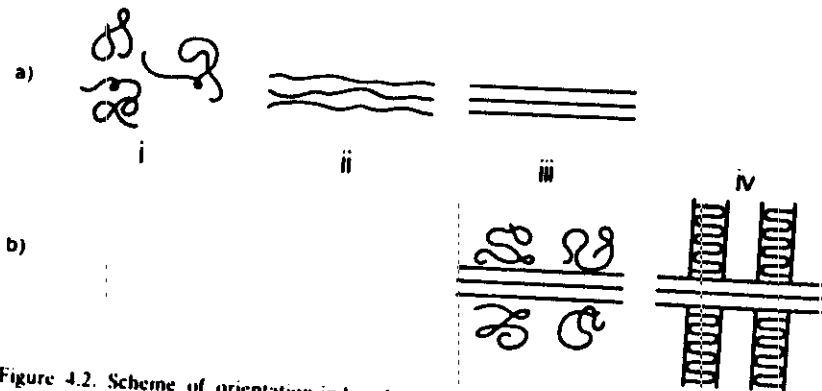


Figure 4.2. Scheme of orientation-induced crystallization. (a) Formation of smooth, extended chain fibers: (i) random coil, (ii) chains become oriented by external influence, (iii) preoriented chains have crystallized. (b) Formation of fiber-platelet composites ("shish-kebabs"). Here not all the chains have been aligned and at stage (iii) only the oriented chains crystallize. The remaining random chains use the already-formed fibers as nuclei for the formation of chain-folded platelets (iv) (after Keller<sup>10</sup>).

fibers are indeed obtained during oriented crystallization, nevertheless it should be noted that to obtain fibrous crystals the chains need to be oriented first, otherwise chain-folded platelets will result.

However, this is not the full story. Usually it is not possible to orient all the chains within and assembly. Some chains will become stretched out while others will be left more or less random. The stretched-out chains will form the fibrous crystals as above. The unoriented chains will use these fibers as nuclei and deposit onto them epitaxially as chain-folded platelets, as shown by the sketch of Figure 4.2 and observed experimentally (Figure 4.3). This composite fiber-platelet structure is the usual product of orientation-induced crystallization and is termed "shish-kebab" for obvious reasons.

The above fiber-platelet morphology illustrates the principle expressed in Section 3.1.3.3a of Chapter 3 in a rather extreme way: namely even when presented with an infinite substrate the newly depositing, unaligned chains will crystallize onto them by folding, with a fold length that corresponds to the prevailing supercooling. We recall that this behavior has featured prominently in the formulation of the kinetic theories.

The subject will now be subdivided into the following four aspects: (1) mode of chain extension, (2) structure of shish-kebabs, (3) properties of shish-kebabs, and (4) practical consequences.

#### 4.2.3. Mode of Chain Extension

##### 4.2.3.1. Static Chain Extension: Networks

Amorphous melts can be stretched, and held stretched, until crystallization sets in, provided the chains remain stretched and do not meanwhile relax. This is only possible on a sufficiently extended time scale if the polymer is cross-linked so as to form a network. The classical example is vulcanized rubber. In fact it is known that the crystallization of rubber on stretching (contrary to historical models) occurs along the shish-kebab route. In the case of such networks, chains can also be stretched out while in the form of a solution (which will then correspond to a swollen gel).

##### 4.2.3.2. Dynamic Chain Extension: Flow

The chains in a flowing solution or melt may become stretched out, which brings us into the realm of hydrodynamics. To achieve such a situation the flow must be of a special kind where the extensional component dominates over the rotational component. Such flow is termed "extensional." In the usual kind of flow, such as capillary flow, which is



Figure 4.3. Electron micrograph of a shish-kebab-type crystal of polyethylene grown by oriented crystallization from solution (after Hill *et al.*<sup>(10)</sup>).

simple shear flow, the rotation and extension rates are of equal magnitude. In such a case the fluid element, and the chain contained by it, cannot attain a high degree of extension. The extensional component will dominate, hence flow becomes extensional if, e.g., the flow accelerates or decelerates. Mathematically

$$[S/(\omega)]^2 > [\sigma]^2 > 0$$

where  $S$  is the extensional and  $\omega$  the rotational strain rates. Only if  $[\sigma]^2 > 0$  will there be persistent extension, where  $\sigma$  is the persistent extension rate. The simplest extensional flow (to quote an example) is pure uniaxial stretching flow defined by the velocity gradient tensor

$$\dot{\gamma} = \begin{bmatrix} 1 & 0 & 0 \\ 0 & -\frac{1}{2} & 0 \\ 0 & 0 & -\frac{1}{2} \end{bmatrix}$$

Chain extension in elongational flow is an increasing function of molecular weight; for a given strain rate, the longest chains stretch out most. In fact, for a given strain rate beyond a certain critical chain length the chains will all be practically fully extended, and below this strain rate virtually unextended. Thus in the case of a distribution of molecular weights we have fully extended and unextended chains in a system undergoing elongational flow. This in itself should suffice to account for the situation outlined in Figures 4.2 and 4.3, and hence for the composite fiber-platelet structure of shish-kebabs arising when such a system crystallizes.

The above molecular-weight dependence implies that each chain is isolated, as it would be in a sufficiently dilute solution. If chains become entangled or associated in any other way (e.g., by localized micellar or fibrous crystallization) then it is the relaxation time of the whole aggregate entity, which in turn depends on its molecular weight, that will determine the chain extension. If the association/entanglement is beyond a critical value, and hence extends over the whole system, this will then become a network (a gel in solution) and the effect of the orientational influence will essentially amount to the stretching of a network, i.e., correspond to Section 4.2.3.1 above. According to current developments, many structures that were believed in the literature to arise through the stretching of individual chains have their origin in the aforementioned gel stretching. It follows that the boundary between the stretching modes dealt with in Sections 4.2.3.1 and 4.2.3.2 has become blurred. This whole subject is therefore in a very fluid state at the time of writing.



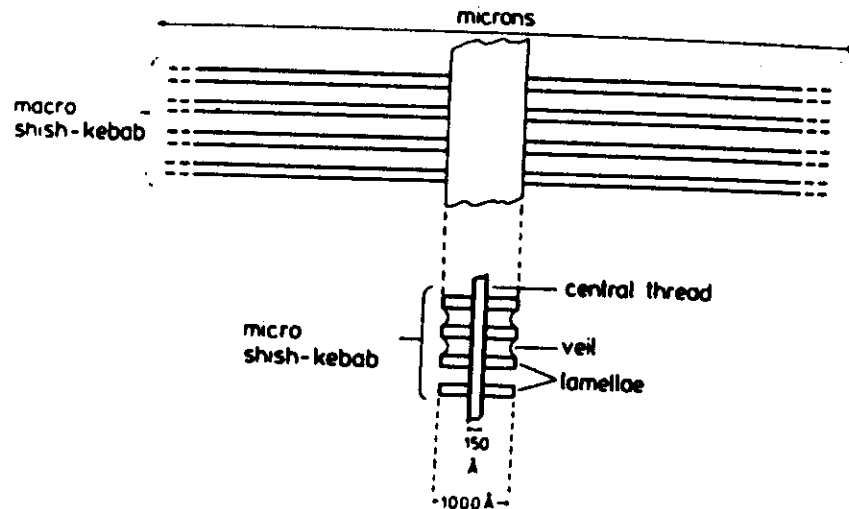


Figure 4.4. Schematic representation of the relation between macro- and micro-shish-kebabs (after Keller and Barham<sup>(10)</sup>).

#### 4.2.4. Structure of Shish-Kebabs

According to the foregoing a shish-kebab is a two-component structure consisting of a central fiber and a platelet overgrowth.

##### 4.2.4.1. The Platelet Overgrowth

The platelets can be of two types.

1. *Large-scale removable platelets.* These platelets correspond to epitaxial overgrowth of separate molecules, usually formed when a partially crystallized melt or solution, already containing the fibrous backbone, is being cooled to room temperature. They can be removed by selective dissolution achieved by reheating the suspension, or prevented from forming altogether by exchanging the hot solvent at the original temperature of fiber formation. It is helpful to term this whole shish-kebab entity a macro-shish-kebab (Figure 4.4).

2. *Small, molecularly attached platelets.* The fiber core of the above macro-shish-kebab is, however, not a smooth fibrous crystal but, contrary to all expectations, was found to display a shish-kebab character itself on a much smaller scale (sketched in Figure 4.4 and termed micro-shish-kebabs). Such micro-shish-kebabs cannot be denuded of their platelet population, which accordingly must be molecularly connected to the

central fiber core. An "artists impression" of this connectedness, due to Pennings (who developed so much of our current knowledge on shish-kebabs), is presented in Figure 4.5. According to recent works the origin of the attached platelets is as follows: The fibers as formed are "hairy" to begin with, the "hairs" loose, but attached molecules dangling freely in solution. It is these hairs that crystallize by forming the attached chain-folded platelets on further storage or on subsequent cooling. Proof for this model is provided by the fact that the scale and separation of platelets, in fact the entire external appearance of micro-shish-kebabs, can be reversibly altered by heating and cooling the whole assembly while in the solvent. Here the platelets dissolve, reverting to loose but attached hairs, which then renucleate and reform according to the condition prevailing under the conditions of this subsequent storage or cooling. Thus the appearance of a micro-shish-kebab can be affected and controlled by what we term a "hairedressing" procedure.

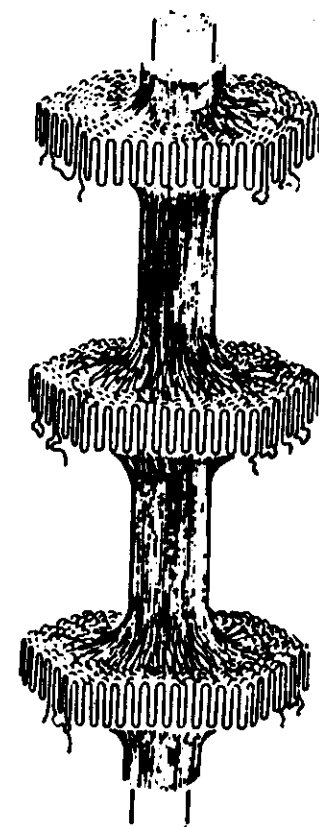


Figure 4.5. Diagram of a micro-shish-kebab showing molecular connections between chain-folded platelets and central core (after Pennings<sup>(12)</sup>).

In the last paragraph we consistently referred to solution crystallization only, because only in this case can micro-shish-kebabs be obtained in isolation. In practice, melt crystallization always yields macro-shish-kebabs as in Figure 4.4, where the large platelets cannot be removed by ready methods.

#### 4.2.4.2. The Backbone Fiber

These are essentially of the chain-extended type as implied by Figure 4.2. Nevertheless the latest electron-microscope (and some thermal-shrinkage) evidence implies that the crystals in such backbones are not continuous throughout. In fact the backbones are rather segmented into amorphous and crystalline, or rather, perfectly and less perfectly crystalline regions connected in series. Current theoretical attempts regard these structures as resulting from multiple crystal nucleation occurring in series along several localities of the chains that are already aligned by the flow.

#### 4.2.5. Properties of Shish-Kebabs

##### 4.2.5.1. Thermal Properties

Shish-kebabs are a composite texture and therefore display a correspondingly complex melting behavior. The main features are as follows:

1. Shish-kebabs possess a multiple melting behavior, the platelet component melting at a lower temperature than the core fiber.
2. The core fibers not only melt at higher temperatures than the platelets, but in fact may do so at temperatures beyond the equilibrium melting temperature of the infinitely extended chain crystal (as denoted earlier by  $T_m^0$ ), i.e., such fibers are prone to superheat.

##### 4.2.5.2. Mechanical Properties

For an appreciation of the issues the following preamble, significant in its own right, is deemed necessary. Ideally fibrous material consisting of stretched-out and aligned long chains should be very stiff and strong along the chain direction, because here the external force acts against primary valence forces. However, most disappointingly in practice, the maximum achievable stiffness and strength with the usual technological fibers are not even being approached (for figures see below). The reason is the presence of chain folding. In the usual technological fibers the chain may be highly oriented by appropriate tests (X-ray diffraction, birefringence), which does

not mean, however, that it is also fully stretched out (see also later, Figure 5.2), because a parallel stack of chain-folded platelets would produce the symptoms of a high degree of chain orientation, as in fact it does in the technological fibers, without realizing the full potential of the fully extended chain.

Achievement of full chain extension is more than a trivial matter. One approach is through oriented crystallization that leads to shish-kebabs. Here the platelets detract from the final properties. Hence the objective is to produce backbones that are as platelet-free as possible, a target of many recent endeavors. To this condition must be added the further, most recently realized objective, that the structure of the backbone be as defect-free as possible, i.e., the segmented nature of the crystal sequences (referred to above) must be reduced. Recently special preparation conditions have enabled the theoretical values for modulus and strength to be approached. For example, in the case of polyethylene the theoretical stiffness is 250–400 GPa (according to the mode of estimate). The conventional technologically drawn fiber or film has a modulus of approximately 5–10 GPa. Good solution-grown shish-kebab fibers have moduli of approximately 100 GPa. In one special case 280 GPa has already been achieved. To appreciate this achievement it suffices to say that the typical modulus of a steel wire is of the order of 200 GPa.

#### 4.2.6 Some Practical Consequences

The modulus and strength issue has already been mentioned. At present, industrially oriented research is endeavoring to create elongational flow fields or to stretch networks in order to achieve ultrastiff, ultra-strong fibers. This is purposeful utilization of fundamental knowledge.

The consequences of what has been described above are manifest, even if unintentionally so, in practically all processed materials where melts or solutions are at some stage in a state of flow. In the preparation of injection-molded articles the melt passes through constrictions and orifices and meets obstacles where the flow, even if only locally, will accelerate or decelerate, and hence will assume an elongational character and correspondingly undergo chain stretching. This in turn will give rise to shish-kebabs. Such shish-kebabs, occurring only in the appropriate localities, will represent heterogeneities within the final molded object. This will influence the properties of the technological products, usually in a deleterious manner. It will also affect test samples such as those prepared for scientific purposes. An awareness of such possibilities is thus clearly required also in academic studies.

The traditional spinning processes always involve a certain amount of elongational flow (melts or solutions passing through spinnerets!), hence a

certain amount of, often uncontrolled, fibrous crystallization will occur and affect the final structure, and correspondingly the properties.

An important manufactured product is the melt-extruded film (often obtained by blowing large cylindrical bubbles from the melt in a continuous manner). The usual polyethylene or polypropylene wrapping sheet is a familiar example. Here crystallization occurs while the expanding melt solidifies. This creates shish-kebab structures of the macro kind — see Figure 4.3 — with the following, further important variant.

In such films the stresses during solidification are low. This means that the elongational strain rate characterizing the flow, the degree of network stretching, and hence all extensional influences will be correspondingly moderate. As a consequence, the resulting concentration of fibrous crystals will be low and the fibers will lie far apart, but still parallel to the orienting influence. Under the low stress the overgrowth platelets will tend to crystallize, as they do in the unoriented melt, hence they will tend to form spherulites, where the ribbon-type overgrowth crystals will twist (see Figure 2.22c). With nucleation centers close together along the core fiber the spherulite growth will be confined to essentially two dimensions, the resulting spherulitic “disks” being stacked parallel while strung along the central core (Figure 4.6), the whole assembly forming a columnar structure.

The usual melt-extruded film indeed consists of an assembly of such parallel columns with some explicit consequences as regards structure and properties. This example is not only a very widespread and important one in practice, but is also an instructive illustration of the hierarchical nature of the morphology of a crystalline polymer. The complex and intricate interrelation of the different morphological entities (fibers, platelets — the latter with twists, columns) should be noted.

In the next chapter the material already presented will be summarized, however, not in the manner of a conventional summary but by utilizing the previous material in connection with some enquiries pertinent to the field of polymers. The enquiries in question are important in their own right, but at the same time offer an opportunity to reiterate the multitude of structural information invoked in the preceding chapters within several different contexts.

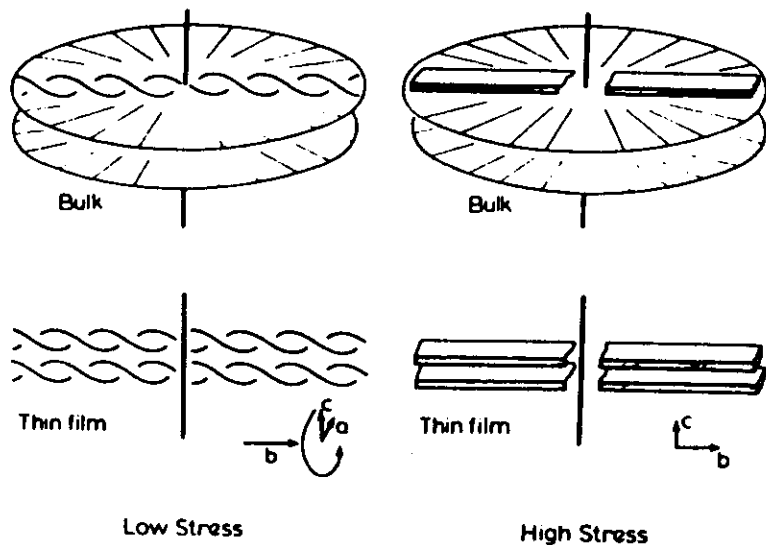


Figure 4.6. Diagram of columnar structures arising during crystallization of flowing melts. Left: under low stress, with columns far apart, when the overgrowth platelets twist as they do in spherulites. Right: under high stress when the overgrowth platelets are all aligned parallel with chains along the stress direction (vertical) (after Keller and Machin<sup>(11)</sup>).



# Hierarchical Nature of Macromolecular Structure

A. Keller

## 5.1. Introduction

One of the most important themes throughout this subject has been the hierarchical nature of macromolecular structure. Explanation or interpretation of any property must take cognizance of the existence of this hierarchy, which forms the main topic of the present summarizing survey. First, the members of the hierarchies will be briefly recapitulated.

The basic building unit is, of course, the chain molecule. In amorphous material this will assume a more or less random configuration.

### 5.1.1. Crystalline Constituents

In the crystal the molecule will be the constituent of a *lattice*. The crystal lattice will then be the building block of the higher-level *morphological hierarchies*.

The basic morphological elements are *lamellae*, the as yet only diffusely identified *micelles*, and the *fibers*.

The lamellae build up a variety of lamellar aggregates culminating ultimately in the spherulites.

The fibers form the central core of a range of platelet-fiber composite structures which range from the fibrous shish-kebabs, as obtained in solutions, to the columnar entities in melt-crystallized material.

---

A. Keller · Department of Physics, University of Bristol, England.

### 5.1.2. Amorphous Constituents

As mentioned earlier, an awareness of the hierarchical nature of the crystalline architecture of a crystallizable polymer also enriches our conception of the amorphous component within a semicrystalline polymer. In other words, the relation of amorphous chains with respect to the crystal entities creates a finer distinction between what otherwise would be termed collectively amorphous material.

Let us recapitulate. First we have the pure amorphous component unconnected to any crystal entity, e.g., the matrix material not yet pervaded by spherulites.

All other forms of amorphous chains are constrained in some way by being molecularly connected to crystals. One example comprises amorphous chains associated with lamellae: in an isolated layer the noncrystalline chain portions are confined to a given lamella constituting the fold surface. The chains may be attached at both ends (loose loops) or at one end only with the other end free (cilium). In the case of amorphous material lying between two lamellae there will be chains with two ends confined to each. These are the interlamellar ties.

A second example consists of amorphous chains associated with fibers. They include two classes: first, those within the central core that interrupt crystal continuity (the source of the segmental nature of the core), and second, the chain portions tying the platelet overgrowth to the central core (originally loose hairs when the core had formed; see Section 4.2.4.1).

The absence or presence of constraints, or the detailed nature of the constraints arising from its relation to the crystal hierarchy, influences the mobility of such chains and can affect macroscopic behavior.

In what follows the consequences of the hierarchical nature of a crystalline polymer will be traced through three subject areas: (1) crystal defects, (2) thermal behavior, and (3) deformation behavior.

## 5.2. Crystal Defects

Defects have a prominent role to play in the physics of simple solids. This applies equally to polymers but, with the greater variety of structural elements, they span a much wider range of effects.

### 5.2.1. Defects Within the Crystal Lattice

Polymeric sources of defects arise specifically through the lack of perfect chemical, including stereochemical, regularity of the chain molecule itself. As discussed in Section 2.1.2 these include occasional

branches, comonomers, cross-links, tactic inhomogeneities, etc. Only when these are taken into account do we come to the level of defects familiar from the physics of more conventional solids, such as point defects, dislocations and stacking faults. These latter can be of significance, nevertheless they are usually overshadowed by the much more prominent consequences of the imperfections in the molecular architecture referred to above, and by the much larger-scale disturbances on the higher hierarchical levels of the structure.

### 5.2.2. Defects Beyond the Level of the Lattice

#### 5.2.2.1. Lamellar Structures

Let us first consider the single lamella. Here we have the fold surface in its various representations. From whichever way it is viewed, it represents an interruption of the lattice continuity and in addition, dependent on the kind of sample (and opinions held), it embodies various elements of disorder, or may even display features characteristic of amorphous material.

Next let us consider the multiple lamella. Here we have a natural discontinuity when passing from one lamella to the next. In addition to the possibility of interlamellar material there arises the question of imperfect layer register. These can be of two kinds: rotational mismatch, and splay of consecutive layers.

Finally we consider spherulites. These complex lamellar aggregates, in addition to all the sources of defects arising in multilayer crystals, embody new sources of structural imperfections of their own. Most prominent is the central discontinuity, next the unexplained twisting of the lamellae within spherulites, and all the discontinuities that must arise from the way the space is filled (not understood even in a descriptive sense). The overall, radially arranged fibrous texture is known to be a potential source of radial discontinuities and, of course, the junctions of different spherulites represent major fault lines in a melt-crystallized polymeric object.

#### 5.2.2.2. Molecular Segregation during Crystallization

Molecular segregation during crystallization can be a major source of inhomogeneity, which can manifest itself in different forms.

1. Lower-molecular-weight but crystallizable species have lower melting points. They become ejected during the crystallization of the rest of the material and crystallize in isolated pockets, later on cooling with correspondingly thinner lamellae.

2. Noncrystallizable portions are ejected (such as atactic chains or chain portions) and form amorphous pockets of various size and disposition in the final material.

The principal accumulation sites of ejected material of either kind can be situated within spherulites along radial discontinuities and/or at the spherulite boundaries.

#### 5.2.2.3. Defects in Fibrous Crystallization

These possibilities follow directly from what was said about fibrous structures. It was stated that the central fibrous core, while of extended-chain character, is not continuous crystallographically but contains interruptions.

There are a variety of defect structures relating to the overgrowth platelets of shish-kebabs, some of which are common to those associated with chain-folded crystals while others arise from the mode of their connection to the central core (e.g., "veils" between platelets and between platelet and fiber).

On a still larger scale are the discontinuities associated with the columnar boundaries in melt-crystallized material that have much in common with the spherulitic interfaces.

It is clear from this brief recapitulation that there are many sources of departure from ideal crystal properties and, chiefly, that these will not be easily attributable to a single cause but to the entire hierarchical nature of the morphology. Thus fracture, to take one example, may arise in structural terms from weakness at any level of the hierarchy, ranging from chemical weaknesses along the chain to those along the boundaries where spherulites meet.

### 5.3. Thermal Behavior

Let us consider what may happen when a semicrystalline polymer is being gradually heated up. Here again, the changes that take place will involve all elements of the structure hierarchy.

#### 5.3.1. Amorphous Material

The amorphous components in all their variety will pass through the stages expressed by Figure 1.4. In particular, they will pass from glassy to rubbery behavior when going through  $T_g$  with correspondingly profound effects on the properties.

#### 5.3.2. Crystal Lattice

As in any other crystalline material, polymorphic transitions can take place with change of temperature while still below the melting point. These will not be itemized here. We only make the general statement that in the case of chain molecules, increase in thermal vibrations leads to increased amplitudes in vibration corresponding to rotations around bonds, both of the main chain and the side group. The former in particular can lead to the so-called "rotary phase," which in appropriate polymers may correspond to a transition from an orthorhombic (or triclinic) to a hexagonal phase (see Section 2.2.3 in Chapter 2).

#### 5.3.3. Melting Range

Crystalline polymers usually possess a broad melting range. The reason for this is best appreciated in terms of the molecular inhomogeneity and the morphological hierarchy usually present in polymeric materials, the two often being intricately interlinked.

##### 5.3.3.1. Molecular Inhomogeneity

This factor arises through the existence of a distribution in molecular weights and perfections. The mere existence of such distributions, even in the case of complete, homogeneous mixing, would lead to a depression of the melting point. In addition, we have seen that the different species may segregate during crystallization leading to regions of different melting points. Even without the intervention of any other factor this will broaden the temperature interval within which the sample as a whole melts.

##### 5.3.3.2. Morphological Factors

We can distinguish between the effect of premelting and partial melting.

**Premelting.** We stated above that the amorphous chains and/or chain portions can exist in different relations to the underlying crystals according to the morphology. This creates a variety of possible constraints on the amorphous chain with related effects on the configurational entropy, which in turn will affect the melting point of the whole crystal with which such constrained amorphous chain portions are associated. This can lead to premelting and under special circumstances, superheating phenomena [H. G. Zachman., *Kolloid-Z. Z. Polym.* 231, 504 (1969); E. W. Fischer, *Kolloid-Z. Z. Polym.* 231, 458 (1969)].

Let us consider, e.g., the fold surface of a lamella. Loose loops, which may be present, are constrained at both ends, consequently their entropy will be reduced compared to the totally unrestricted chain. If now the crystal starts to melt from the fold surface downward, the loops will become longer (with end separation unaffected) and hence the effect of the constraint on the entropy (entropy tension) will be reduced. Without entering into details here, it will merely be stated that as a result of such considerations the overall entropic component (i.e., crystal plus amorphous) associated with such melting will be increased beyond that due to melting of the crystal lattice alone, giving credence to the uniquely polymeric process of interfacial premelting of lamellae.

Similar situations could be quoted in the case of fibrous crystals due to loosening up of the constrained tie chains during the gradual melting of crystals.

**Partial Melting.** The main point here is that small crystals melt at lower temperatures. Here we reinvoké what was stated in connection with equation (3.18), namely that crystals with small  $l$  have lower melting points. In the case of a range of  $l$  values, the existence of a melting range will follow. The origin of a range of crystal thicknesses may be manifold. The most self-evident case is where crystallization takes place during cooling, when different  $l$  values result at the different crystallization temperatures. Another source is the phenomenon of isothermal thickening during crystallization in the melt (see page 80), which will result in a range of crystal thicknesses in the final crystal product. And finally, as already stated in Section 3.2.4 of Chapter 3, as a crystalline sample is being heated in the course of melting-point determination, it may re-fold in the process to higher  $l$  values than present in the original crystal. This frequently takes the form of a multiple population of crystal thicknesses with corresponding multiplicity of melting points.

### 5.3.3.3. Superheating Phenomena

Superheating effects arise under a variety of circumstances, mostly in extended-chain-type morphologies. The essential reasons are due to two classes of effects. (1) The chains cannot transform into their random form in any other way than to peel off one by one from the outside, as in the case of morphologies shown in Figure 3.21. This takes time during which, under practicable heating rates, the crystals superheat. (2) The chain in the melt does not relax instantaneously, as in the case of the central cores of the shish-kebab crystals. As for the unrelaxed stretched chains  $\Delta S$  (for melting) is smaller, thus  $T_m$  will be higher, with reference to the random melt. Hence the system (on a limited time scale) will superheat.

In summary, it is apparent that in a polymer there exists an intricate

multistranded connection between the thermal behavior and the presence, detailed characteristics, and interconnectedness of the various structural entities that constitute it.

## 5.4. Deformation

This is the last example chosen to illustrate the role of hierarchies, even if only in the briefest terms. Deformation is particularly important for polymers, as most thermoplastics are deformed in the course of fabrication (drawing, rolling) in a plastic manner, while long-range elastic deformation is, of course, the characteristic feature of elastomers. Changes occur during deformation in all the regimes of the structural hierarchy, which in turn also influences the resulting properties (stiffness, fracture, etc.).

### 5.4.1. Polymers as Self-Structured Composites

#### 5.4.1.1. Generalities

As a generalization, it may be useful to visualize a partially crystalline polymer as a kind of composite where the individual constituents are the amorphous and the crystalline components. Some overriding consequences follow from this viewpoint.

Above  $T_g$  the amorphous material is a rubber (particularly if and when the crystals act as cross-links) with the following characteristics: the modulus is low, but the deformation remains elastic up to very high strains (several 100%). In contrast, the crystal portions (like any crystal) have high moduli but remain elastic only up to very low strains (1% or less). In the composite treated here we have a combination of both. For instance, we can have a situation in which, for a given macroscopic strain, the crystals deform plastically while the deformation of the amorphous component, even if very substantial, is still within the elastic range. Suppose, e.g., the load is removed in such a case, then the amorphous portions will retract but not the crystals, which will remain in their plastically deformed state. In addition, the elastic retraction force due to the former can induce further plastic-deformation modes in the crystal.

The above serves to illustrate that a semicrystalline polymer is a composite with components of mechanically, grossly disparate properties where, in addition, the components may interact in a unique fashion. The exact mode of interaction will depend on the mode of coupling of the constituents, which in turn depends on the detailed morphology of the system under consideration. As a broad, phenomenological generalization



1. Series coupling where the stresses, but not the strains, are equal in both components (Figure 5.1a).
2. Parallel coupling where the strains, but not the stresses, are equal (Figure 5.1b).

Of course in "real systems," there will be a whole spectrum of cases intermediate between modes (1) and (2) as regards gradation of components (e.g., we have seen that there can be ranges of behavior even within what we grossly termed "amorphous"), and many intermediate states in the coupling pattern between modes (1) and (2). Further, if the different phases are not macroscopically separate blocks (as in Figure 5.1) but the components in question are mutually dispersed or interleaved in an intricate fashion, there will be mutual constraints influencing each other's behavior. (For example, a layer of rubber sandwiched between wide plates made from some stiff material to which it closely adheres — a close analogue to crystal lamellae in polymers — will not be able to extend according to the Young modulus it would possess were it on its own in response to tension being applied to the stiff plates, because of its inability to contract laterally owing to the constraints created by the plates.) In brief, we have a composite where the deformation behavior will be affected both by the nature of the components of the structure hierarchy at all levels, and by the way they are coupled mechanically.

We shall now briefly survey the hierarchy from the above point of view.

#### 5.4.1.2. Amorphous Component and Crystal Lattice

Let us first consider the random amorphous chain. The essentials of its behavior, particularly above  $T_g$ , has been repeatedly defined: it is the seat of the long-range elastic or viscoelastic behavior of the system. If coupled in series with the crystal it will support nearly all of the strain (Figure 5.1a); if coupled parallel it will "dilute" the effect of the crystals as regards supporting stress (Figure 5.1b).

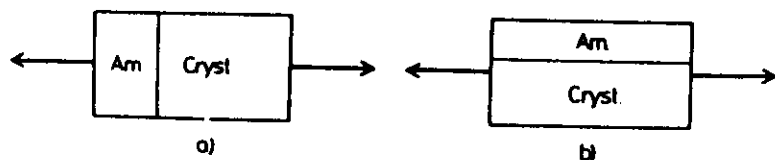


Figure 5.1. Simplest representation of (a) series and (b) parallel couplings of amorphous and crystalline components of a partially crystalline polymer for the interpretation of response to external loading (arrows).

As regards the crystal lattice, here the usual elements of crystal plasticity apply as in any other crystal and comprise slip, twinning, and phase transformation (martensitic type). There exist explicit works demonstrating the existence and consequences of each. Nevertheless, one may state in broad generality (and that is all I can do at this juncture) that these crystal-plasticity effects are not as important for polymer deformation as in the case of other crystalline substances. The reason for this has already been implied by the foregoing, namely that the main source of deformation in a polymeric solid lies elsewhere: it is the stretching-out of the amorphous random chain, or, as far as the crystal is concerned, the pulling-out of the fold (see below). Thus, just as lattice defects *per se* make only a small contribution to the total defect structure of a usual polymeric solid (see Section 5.2), so the generation and propagation of lattice defects play only a subordinate role in the deformation of the average semicrystalline polymer. In any event they are associated with small strains, and *vice versa*, while the most conspicuous characteristics of polymers are due to their capability of undergoing large extensions.

Nevertheless one feature of the polymer crystal lattice is of major importance, namely its extreme mechanical anisotropy, associated with the existence of valence bonds along the chain direction, as compared to the much weaker interchain forces perpendicular to it. This will favor chain slip over other slip modes and ultimately lead to the alignment of the chains (e.g., during uniaxial tensile deformation) even within the crystal. This is in addition to the stretching-out of chains from the random conformation within the amorphous portions. More will be said below about this chain alignment and chain stretching, which fall within the realm of large-scale deformation.

#### 5.4.1.3. Larger-Scale Crystal Entities

The description of polymer deformation abounds with the mention of "anomalous orientations" by which is meant that the overall chain direction as assessed by, e.g., X-ray diffraction, is different from what one would expect *a priori*, namely chain alignment along the direction of the orienting influence. All such "anomalous" effects can be traced back to the influence of morphological factors. Accordingly, appropriate stress systems may not necessarily always tend to align the chain as such, but orient some larger morphological entity, the resulting chain orientation then conforming to this orientation of the morphological unit in question. While this principle is general, we shall invoke it specifically in connection with the lamellae.

c. *The Lamellar Element.* The lamellar entity has a role of its own to play in the deformation of a semicrystalline polymer. The lamellar surfaces

themselves may act as slip planes, which in a suitable stress system can produce *interlamellar slip*. Thus it is possible to demonstrate that lamellar surfaces may align parallel and perpendicular to extensional or compressive stresses, respectively, even if this may lead to chain orientations that are grossly different from what one would expect if chain slip or chain extension were acting alone.

Rotation of otherwise unaffected crystal lamellae is being envisaged in the aforementioned interlamellar slip. Instead, or in addition, the lamellae themselves may undergo plastic deformation by chain slip within them. In the case of such *intralamellar slip* the chain direction (the direction of the straight chain traverse — fold stem) will be altered with respect to the lamellar surface.

Finally, the separation of the lamellae themselves can be affected. For example, a tensile component normal to the lamellar surface can pull the lamellae further apart (increasing the lamellar periodicity, by which such an effect is assessed) presumably by acting on the interlamellar tie molecules.

In a polycrystalline lamellar system all three of the above effects, namely interlamellar slip, intralamellar slip, and change in interlamellar separation, contribute to the total deformation up to small or moderate strains, where the latter may amount to 50%. Such deformation effects are fully or partially reversible.

*b. The Spherulite.* Everything mentioned earlier about lamellae applies to spherulites, composed of such lamellae. Here we take a micro- and a macrostructural approach.

First we examine the microstructural aspect. Let us consider a spherulite (as in Figure 2.22c) acted on by a tensile force that is, e.g., vertical. The first point to note is that the different spherulite radii will be situated at different angles to the direction of the deforming influence. As far as these radii have a structural existence of their own, the vertical radius will be stretched along the radial (ribbon) direction and the horizontal radius in a perpendicular direction, and correspondingly for the intermediate cases. It is readily seen that the resulting deformation along these different radii is expected to be very different.

The second point is the periodically varying orientation of the ribbon-shaped lamellae along each radius. This means that along, e.g., the horizontal radius in Figure 2.22c, consecutive portions of a twisting lamella will be stressed alternately parallel and perpendicular to the ribbon plane (which, in view of the fact that the chains are approximately perpendicular to the lamellar surface, means that the stress will be perpendicular and parallel to the chain direction, respectively). It follows that all three lamellar deformation modes invoked in the preceding section will become operative, but each to a different extent within the different spherulite

localities, depending on the resolved shear stress in a given locality with respect to a particular deformation mode. Of course the spherulite itself is a contiguous body, so the locally different deformations will be correspondingly constrained by what happens in the other portion of the spherulite, an issue that has not yet been properly solved.

Now we consider the macrostructural aspect. Here it suffices to say that the deformation of the spherulite can and needs to be considered also at the level of what happens to it as a microscopic inclusion or grain. In the simplest case it deforms in affine relation to the macroscopic sample, i.e., a sphere converts into an appropriate ellipsoid. Frequently, however, this affine relation does not hold, and according to circumstances the spherulite may, e.g., on uniaxial tension, become contracted at its "waist" — as if it yields along radii perpendicular to the direction of the tension — or may stretch out more at its apex (radius parallel to the extension).

In conclusion, it should be apparent from the above examples that the deformation of each hierarchical entity must be treated at its own level first, while taking note of the fact that there will be interactions with the levels below and above in the morphological hierarchy. The orientation effects observed, say by diffraction, will represent the resultant, which however would be difficult to interpret, if at all overall possible, without an awareness of the underlying hierarchical structure.

#### 5.4.1.4. Full Chain Extension

All the above cases referred to moderate extensions that may extend up to say 50%. The ultimate objective in deforming a macromolecular substance is to stretch the chains. This of course takes place at high strains, 100% or more (up to 3000%). At such high strains the random chain portions stretch out, and chain folds become aligned and pulled out to varying extents. In fact, the morphological entities discussed above become irreversibly disrupted in its course. The lamellae themselves break up into small chain-folded blocks and remain strung together to form beaded fibers. The whole oriented structure becomes an assembly of microfibrils [A. Peterlin, *J. Mater. Sci.* 6, 490 (1971)].

At this point it is essential to distinguish between chain orientation and chain extension, as already alluded to in Section 4.2.5. A parallel array of chain-folded blocks, the remnants of the original chain-folded lamellae, such as those forming continuous microfibrils (Figure 5.2a), may be registered by diffraction methods as a highly oriented structure with the chains all parallel even if they are far from being fully extended (Figure 5.2a). The usual technological fiber drawing (cold-drawing) process only leads to the stage in Figure 5.2a, and very special, only comparatively recently adopted methods are required to approach the full extension in

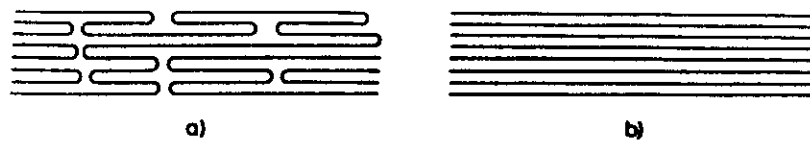


Figure 5.2. Oriented fibers (a) without full chain alignment and (b) with chains fully stretched. Usual tests for orientation cannot distinguish between cases (a) and (b), nevertheless the mechanical properties can be significantly different.

Figure 5.2b, currently referred to as *ultradrawing*. The implication of full chain extension (or the lack of it) for the modulus and strength was mentioned in Section 4.2.5.2, where the alternate method for achieving high chain extension by oriented crystallization (as opposed to deforming structures that are initially crystalline) was described.

Clearly, even within the restricted sphere of deformation behavior many of the morphological constituents of the structure hierarchy were left unmentioned. Nevertheless those that were mentioned should hopefully help one appreciate how intricately the response of polymeric materials to stress depends on its microstructure at different levels. And beyond deformation, in fact beyond the issues covered in the present summarizing survey, it should now be apparent that an understanding of polymeric matter requires an awareness of the whole fabric of structures constituting it, and an awareness of the multitudinous ways in which they are connected.

Before turning to the final chapter on polymers, concerned with the influence of processing on polymeric materials, it is worth reiterating that the objective of these five chapters has been to cover most, even if not all, of the elements that constitute a solid polymeric structure, from the molecules to the various multilevel organizations. It is hoped that the bewildering multitude of structural organizations will not discourage the theorist who may have expected more derivations from a few fundamentals. If the above chapters do not provide deepened understanding, in the sense meant by the theoretician, they at least indicate causal connections and interrelations that will doubtless serve to establish a theoretical framework in the future.

